

Final Design Report

"Smart Pick" for Rock Cutting – Team 85

Client Name:

Dr. Jamal Rostami



Team Members:

Ben Bergeron

Milos Jankovic

Sophia Mimplitz

Kobe Prior

Jared Richel

Graham Walter

April 26th, 2026

Executive Summary

This report presents the design, development, and validation of a Smart Pick for Rock mining applications, a system developed to, in real time, characterize the wear status of a rock pick and the rock that it is mining into. The project integrates hardware and software components that deliver actionable data to an intuitive command and control graphical user interface, including raw capacitance values that track trends in force acceleration magnitude, and acceleration frequency spectrum.

The design process followed a structured engineering methodology beginning with the identification of project constraints and client requirements, which guided all subsequent decisions. Multiple design concepts were evaluated using decision matrices, leading to a solution that balances performance, cost, and feasibility.

The most prominent technical contributions to the Smart Pick for rock mining include the design and assembly of a custom printed circuit board, the development of a capacitive load cell, and a modular software architecture that ensures future scalability and maintainability. Additionally, computational analysis such as finite element analysis and careful material modelling was performed to optimize system performance for load cell sensitivity and durability under mining conditions.

The system architecture is organized using a block diagram, which exemplifies the modularity of the solution and enables efficient integration of future subsystems such as wireless communication, distributed power management, and a real-time graphical user interface.

Verification and validation procedures were conducted to ensure that the system meets all functional and performance requirements described. Testing results demonstrate the efficacy of the final design against ground truth calibrated load data from a linear cutting machine (LCM).

Final system deliverables, including testing procedure, the graphical user interface as a means for data acquisition and display, qualitative data analysis, and preliminary machine learning analysis, are discussed.

A summary of the systems used, the work breakdown structure, next steps for future teams, budget documentation, and overall project management techniques are discussed.

Throughout the project, there were several lessons learned regarding working in a team effectively, balancing design tradeoffs, and several technical challenges that helped to reinforce the importance of structured engineering practice. Overall, the project successfully delivers all goals described above.

I.	Project Review.....	5
II.	Application of Design Methodology	10
A.	Project Constraints and Client Needs	10
B.	Design Options and Decision Matrices.....	11
C.	Computational Driven Design Decisions.....	15
D.	Load Cell Design	17
E.	Printed Circuit Board Design.....	20
F.	Modular Software Structure.....	27
G.	System Block Diagram	29
III.	Verification and Validation.....	30
A.	Verification (Analytical).....	30
B.	Experimental Verification (Compression Testing):.....	30
C.	Validation (Field-Representative Testing):.....	31
IV.	Final Deliverables	33
A.	Testing Procedure	33
B.	Graphical User Interface	38
C.	Qualitative Data Analysis	39
D.	Preliminary Machine Learning Implementation.....	41
V.	Project Management	51
A.	Overview.....	51
B.	Work Breakdown Structure	51
C.	Management with Scrum	52
D.	Next Steps.....	52
E.	Budget Management	53
VI.	Lessons Learned.....	54
VII.	References.....	54
VIII.	Appendix.....	57
A.	Printed Circuit Board Design.....	64
B.	Team Schedule.....	Error! Bookmark not defined.
C.	Team Budget.....	Error! Bookmark not defined.
D.	Code and Documentation.....	Error! Bookmark not defined.

E. Technical Drawings	Error! Bookmark not defined.
F. Operational/Service Manual	Error! Bookmark not defined.
G. LED Interface Guide.....	Error! Bookmark not defined.
H. LMC & Smartpick Data.....	72
I. Machine Learning Graphs.....	90
J. Team Members	96

I. Project Review

Rock pick assemblies (Figure 1), like those used on Continuous Miners, Longwall Shearers, and Road headers (Figure 2), are used around the clock in various mining applications. In this process, a “pick” with (usually) a tungsten end chips into the rock at an angle, breaking the rock apart. Generally, a rock pick lasts anywhere from a few hours in hard, abrasive rock to several weeks in softer materials such as coal [1].

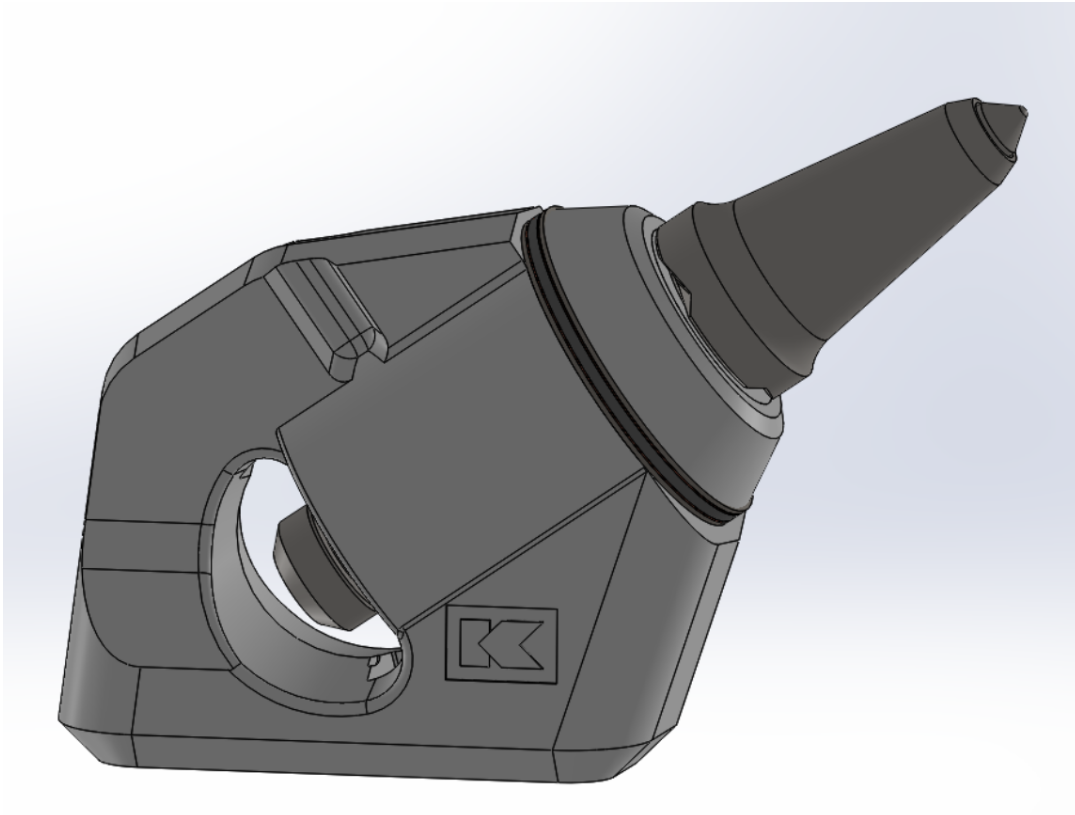


Figure 1: A Rock Pick, Sleeve, and Block



Figure 2: (Top to Bottom and Left to Right) Continuous Miner[2], A Longwall Shearer [3], Road Header [4].

Changing these picks is a labor-intensive process that requires downtime of these machines, cutting into the profit margins of mining operations. Further, knowing when these rock picks are worn and need to be changed is usually a guessing game, leading to unnecessary downtime. Interestingly, if a single bit is worn on a drum-type miner, cascading damage can occur due to uneven loading on adjacent picks and even on the drum itself. Currently, there are no products on the market that help identify the wear on rock picks, nor real-time rock type characterization in the mining industry. Real-time rock characterization is so important because, as Prokopenko mentions, "...the life of picks ranges from a few weeks (in coal) to a few hours (in sandstone)," which highlights the importance of rock identification because if you can avoid abrasive hard rock, you can significantly lengthen the uptime of a mining operation. B. Tiryaki writes that downtime associated with replacing picks and repairing drums in underground mines makes up a high cost as much as "one thousand dollars per minute," further qualifying that a "1 per cent improvement in productivity... causes an improvement of about 3 per cent profit" [5].

The “Smart Pick” team was tasked with designing a load cell to be implemented on mining machines that can sense cutting forces to determine pick wear and rock types while cutting. After discussing different types of load cells the team could build, we chose to design a capacitance load cell. The team worked with material engineers to help determine what materials we should use for our load cell. The initial design to indicate the plausibility of the solution for the load cell used reinforced rubber and copper foil to build a prototype (shown in Figure 3).



Figure 3 First Load Cell Used for Concept Exploration.

A complementary multi-board sensor, breadboarded design consisting of an ESP32 Dev module and CN0052 capacitive-to-digital converter evaluation kit (shown in Figure 4), allowed the team to collect load data under quasi-static load using a hydraulic press (See Figure 5).

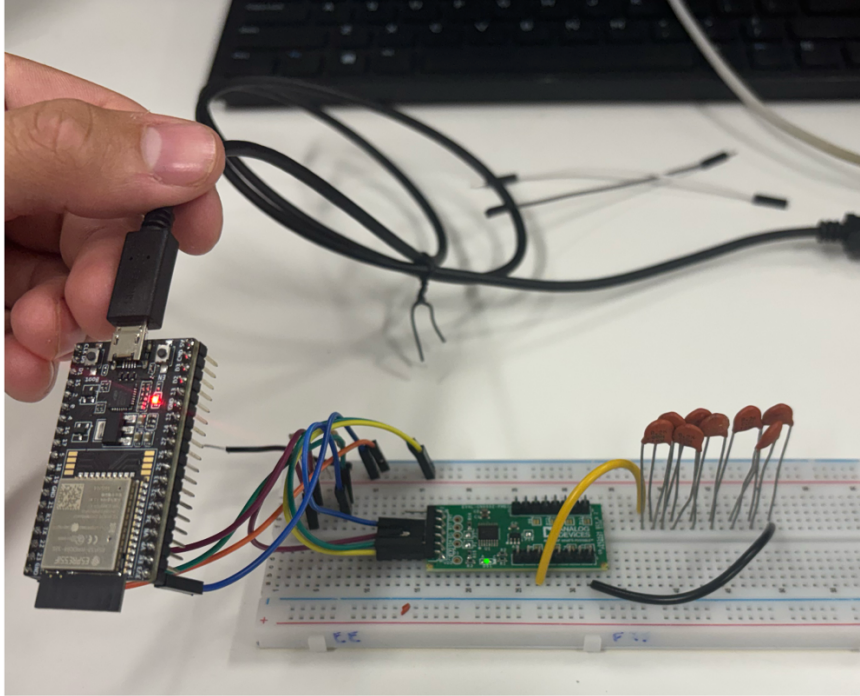


Figure 4 Capacitance to Digital Converter Concept Exploration.



Figure 5 Hydraulic Press Experiment with Capacitive Load Cell.

The test confirmed our idea would work since we were able to generate a linear curve between raw capacitance value and input force, as seen in Figure 6 but needed refinement.

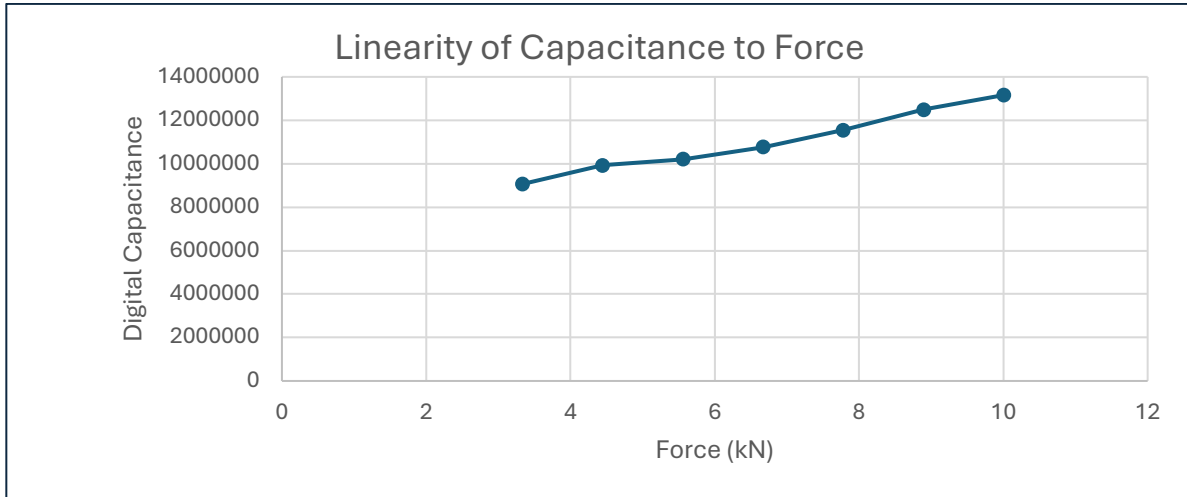


Figure 6 Raw Digital Capacitance Vs Force in kN.

In order to modularize the design, the design and assembly of a custom printed circuit board with an on-board accelerometer and flash memory solution was incorporated. Furthermore, a more resilient load cell was developed with sensitivity optimized for load standards in mining operations. Specifically, layers of high-density polyethylene (HDPE) were laminated with an epoxy resin to hold the layers together and add strength to the assembly.

The solution that is presented in detail in the following sections effectively gathers data about loads exerted on the capacitive load cell and several acceleration metrics in order to make actionable predictions about the wear status of a conical-type rock pick and real-time characterization of certain rock types with accuracy as good as 86 percent.

II. Application of Design Methodology

A. Project Constraints and Client Needs

Below are tables of design requirements for the Smart Pick load cell. Table 1: Design Requirements illustrates the capabilities required of the load cell. Table 2: Additional Specifications provides requirements on the size of the load cell based on the dimensions of the sleeve and block from the Kennametal U92 rock pick model, required service life, load, and operating conditions.

Table 1: Design Requirements

Type	Req #	Requirement	Verification Method	Want(w) or Need(N)	Application	Description
High Level	1	Load Cell that Senses Normal Force in the bit.	Demonstration	N	Universal	Device that can measure the load applied to the longwall bit. Specifically, looking at the normal force in the bit.
	2	Capable of Data Transfer	Demonstration	N	Universal	A load cell sends data to a CPU that <i>can</i> be sent to an antenna.
Functional	3	Gather and send data for at least 6 months in Mine conditions	Demonstration	N	Universal	The device needs to work for at least 6 months, so it does not need to be replaced until the drums are replaced.
	4	Powered by $\leq 5V$ to bypass MSHA[6] compliance regulations.	Demonstration	W	Universal	If the device is powered by less than 5V then it does not need to be permissible by MSHA standards
	5	Data Processing	Demonstration	W	Universal	Data can be processed to determine bit wear and rock type being cut.
Non-Functional	6	Target cost of \$100/unit	Quantitative	W	Universal	The goal is to make the device cost around \$100/ unit

Table 2: Additional Specifications












Load Range	1kN-100kN	Inner Diameter	2.75 in
Resolution	400 N	Outer Diameter	3.75 in
Temperature Range	-30C to 40C	Thickness	Optimized
Material Yield Safety Factor	2.0	Service Life	6 months
Sampling Rate Accelerometer	800 Hz	Sample Rate CDC	90 Hz

Together, these requirements define a load cell that must fit within the existing U92 sleeve geometry while surviving 6 months of underground operation while taking on forces of 1kN to 42kN. The under 5V power ceiling and the \$100 per unit cost targets, although classified as wants to enable creativity in the ideation process, significantly constrain the final design viability in the mining market and are treated as effective design drivers in the concept evaluation that follows. Ultimately, the final product needs to be low cost to not deter operators from implementing the technology due to cost restrictions, it needs to be durable to not add extra maintenance to the mining operation than already exists, and it must collect the correct data to be able to predict bit wear and rock layer classification.

B. Design Options and Decision Matrices

Concept selection was done very carefully for the critical design elements of the project. First, there are numerous ways to measure and characterize the loads exerted on a conical rock pick; namely, a piezoelectric sensor, an inductive proximeter approach, strain gauges, hydraulic, pneumatic, Magnetostrictive, or the design that we landed on, a capacitive load cell.

Table 3 Decision Matrix for Load Cell Type

DECISION MATRIX						
Scoring Key: 0 = Worst 5 = Best						
CATEGORY (0 WORST - 5 BEST)	 CAPACITIVE	 INDUCTIVE PROXIMETER	 STAIN GAUGE	 MAGNETOSTRICTIVE	 PNEUMATIC/ HYDRAULIC	 PIEZOELECTRIC
 COST	5	3	3	1	2	4
 COMPLEXITY	5	3	4	1	2	5
 DURABILITY	4	5	2	2	4	3
 REPLACEABILITY	5	3	3	1	2	5
 TOTAL SCORE	19	14	12	5	10	17

The capacitive load cell scored the highest in three of the four categories, due to its minimal part count consisting of two conductive plates separated by a dielectric, its straightforward fabrication within the existing U92 sleeve geometry, and the low material cost of its constituent components. Piezoelectric was the closest competitor at 17 points, tying or beating the capacitive load cell on complexity and replaceability, but lost ground on durability due to being prone to charge leakage and temperature dependent drift as well as being too brittle to survive the full service life without structural damage.

When discussing what kind of microcontroller to use a spider plot shown in Figure 7 was used to compare 3 types of microcontrollers that were suitable for the applications. Across the categories that were essential for the project, we determined that the ESP32 was the ideal platform for development of a smart pick because of its superior sampling rate, small form factor, good documentation, acceptable cost, and large analog to digital converter range for the possible usage of non-digital sensors.

Comparison of Microcontrollers for Smart Pick

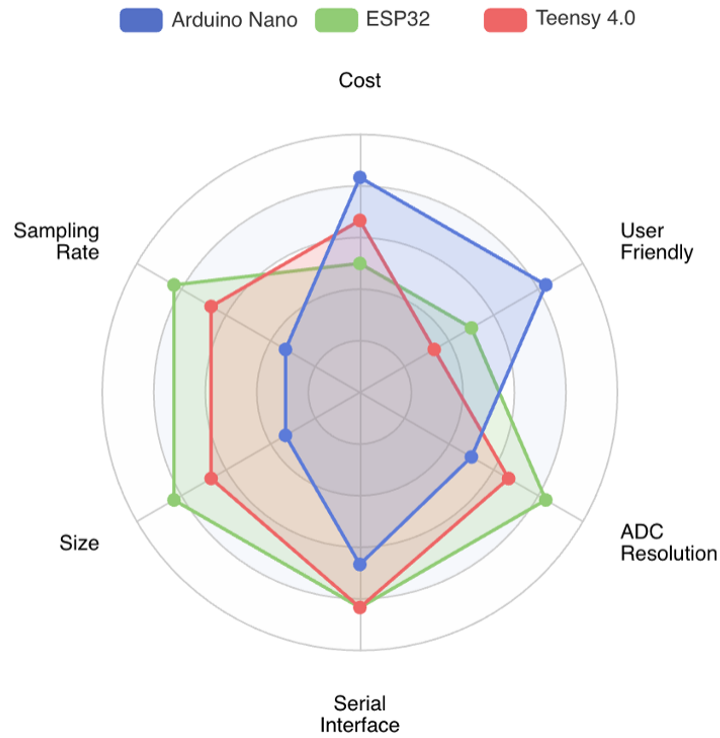


Figure 7 Spider Plot for Deciding on a Microcontroller for the System

It is not mentioned directly in the spider plot, but the ESP32 has the added benefit of low-power wireless communication. Although wireless communication falls outside of the Rock Solid Solution’s scope, including it as a feature is for the benefit of the team that continues this project.

The system that was finally implemented was a capacitive load cell accelerometer combination, with a summary of pros and cons described in Table 4 below.

Table 4 Pros & Cons Table: Annular Capacitive Load Cell + Accelerometer System

Feature/Attribute	Pros	Cons/Risks	Customer Needs Addressed	Notes on Cost/Environment
Annular Capacitive Load Cell	<ul style="list-style-type: none"> -High sensitivity to changes in force -Smooth analog response -compact design 	<ul style="list-style-type: none"> -Requires careful shielding -mechanical fabrication requires precision 	Accurate measurement of static and dynamic forces	<ul style="list-style-type: none"> -Medium cost -HDPE dielectric is environmentally harmless

Accelerometer Integration	-Measures vibration and harmonics directly	-Adds sensor cost and complexity -Requires good mounting	Capture high frequency dynamics and harmonic content	-Low cost -minimal environmental impact
Capacitive to digital conversion	-Direct digital output simplifies data acquisition -reduction in analog noise	-ADC resolution limits force accuracy -Force calibration required	Reliable, highly linear, low-noise digital data for force vs time visualization	ADC cost moderate; Electronic footprint small
Dual-Core Microcontroller (ESP32)	-Can handle simultaneous data acquisition for efficient real-time processing - Bluetooth/WIFI enabled	-Software complexity -Potential timing issues between cores	Real time force vs time and FFT spectrum	Low cost, energy efficient, small environmental footprint
Serial Data Interface	-Simple, robust communication -Lots of documentation	-Limited bandwidth at high sampling rates -potential latency issues	Ease of integration into user display and logging system	Negligible cost; no environmental impact
Force vs Time Visualization	-Intuitive to understand mechanical response -easy verification	-complex software involved to filter and analyze force vs time data	Direct feedback for operator or analyst	Software-only

FFT/ Harmonic Analysis	-Identifies vibrational harmonics -supports predictive maintenance	Requires sufficient sampling rate	Detect harmonic peaks for rock identification	Software-only
-------------------------------	---	-----------------------------------	---	---------------

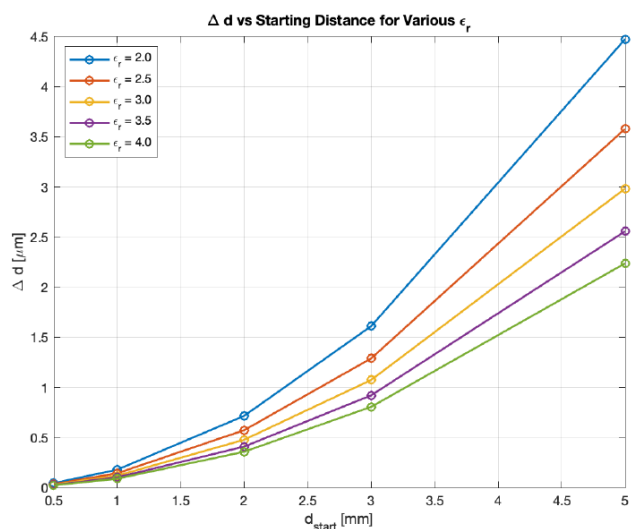
It was determined that for the identified problem, this solution sufficiently addresses all components.

C. Computational Driven Design Decisions

The fundamental equation governing the capacitance of a capacitor is:

$$C = \frac{\epsilon_0 \epsilon_r A}{d}$$

Where C is capacitance ϵ_0 is the permittivity of vacuum, ϵ_r is the relative permittivity of a dielectric material, A is the total area of the conductor, and d is the distance between conductors. In the case of an annular-shaped (donut) capacitive load cell, the capacitance becomes a function of the distance between the plates. We can design an equation that takes ΔC as the minimum readable change in capacitance and, for a wide variety of dielectric materials and starting dielectric heights, determine the types of capacitance changes we can expect for different deformations of the material. Figure 8 generates a family of curves illustrating how important material selection is for generating a load cell that operates within the range of the sensor and has enough variation in capacitance when a load is applied, while maintaining other structural qualities that are important for mining applications.



$$C = \frac{\epsilon_0 \epsilon_r A}{d_{start}}$$

$$\Delta C = \epsilon_0 \epsilon_r A \left(\frac{1}{d_{start} - \Delta d} - \frac{1}{d_{start}} \right)$$

$$\Delta d = d_{start} - \frac{1}{\left(\frac{\Delta C}{\epsilon_0 \epsilon_r A} + \frac{1}{d_{start}} \right)}$$

Figure 8 Minimum Deflection Required to Produce Measurable Capacitance.

The primary computational method applied was finite element analysis. For several donuts, we applied loads and computed expected deflection (See Figure 9 and Figure 10), which narrowed down the material, its height, and dielectric constant.

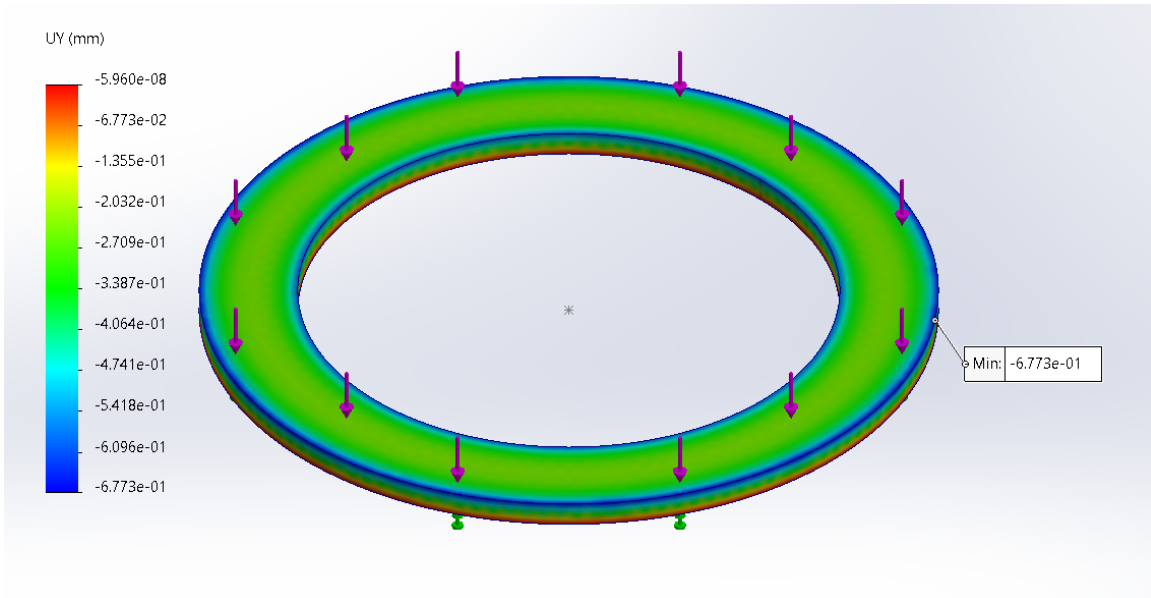


Figure 9: 1/8" Rubber Core with 5 kN applied.

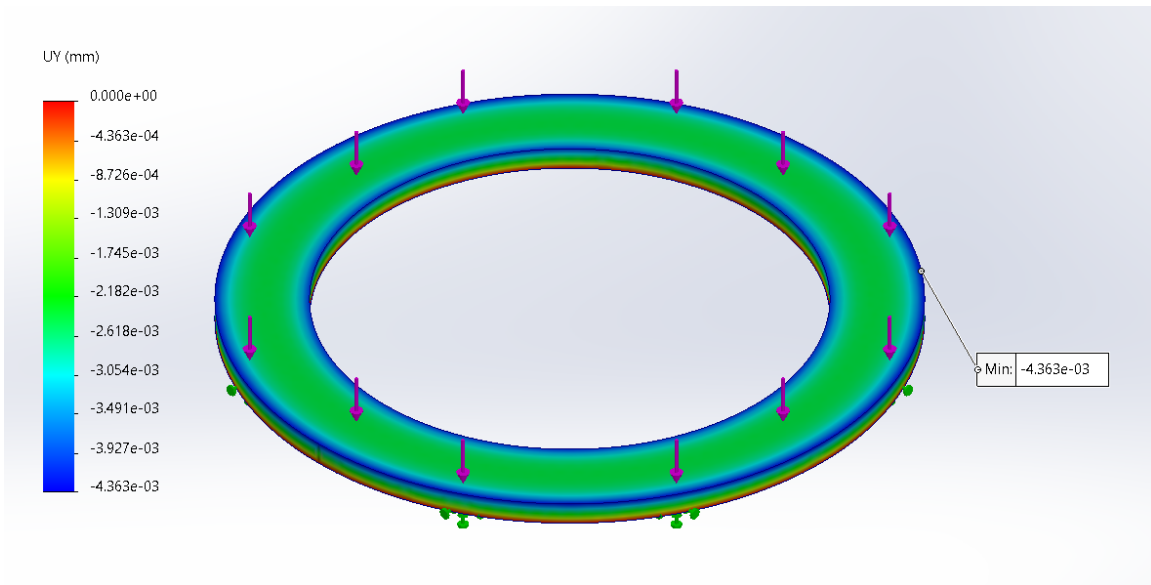


Figure 10: 1/8" HDPE Core with 5kN Applied.

The height of the compressible material for the load cell is directly related to the baseline capacitance and sensitivity to different loads; that being said, thinner materials are generally less compressible. To optimize for the ideal height substrate, Newton's optometric methods were applied and determined that 1/32" HDPE core responds the best and conservatively bounds

nominal and overload forces within the range of the capacitive to digital converter while presenting meaningful changes in capacitance for meaningful changes in forces applied. While this method was mostly theoretical, testing confirmed the results well, as our highest performing load cell was 1/32'' HDPE. The technical drawings can be found in *Appendix A*. Dielectric thickness optimization calculations were performed and the resulting optimization curves are presented in *Appendix B*.

D. Load Cell Design

1. Overview

The Smart Pick system involves two main components: a capacitive load cell to gather an electrical signal, and a printed circuit board (PCB) to process that signal into data. As seen in *Section II.A* above, the client and project overview provided many constraints for the design of this load cell. Ultimately, the team landed on a capacitive design for the load cell side of the Smart Pick system. This includes two layers of thin copper surrounded by three layers of another material (See Figure 11 and Figure 12).

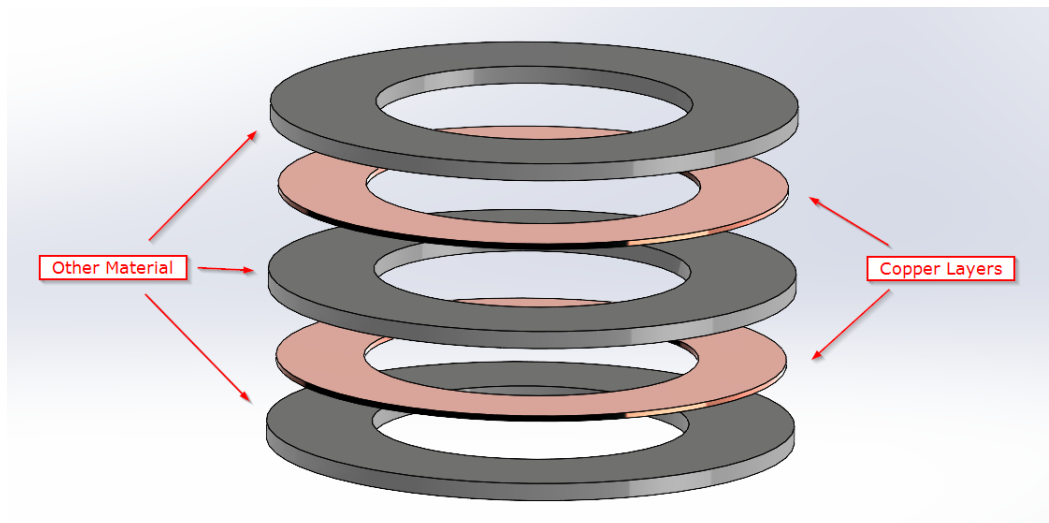


Figure 11: Exploded View of Load Cell Layers

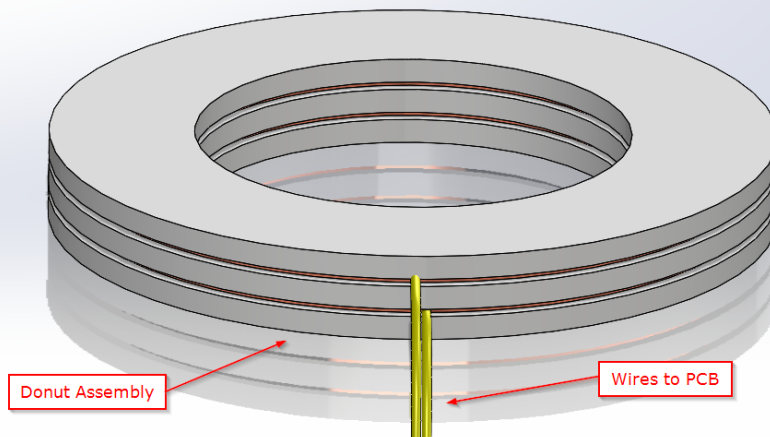


Figure 12: Load Cell Layered Design

This “donut” shape cell is designed to fit between the block and sleeve of an existing rock pick (See Figure 13). When the rock pick contacts a surface, forces will be transferred through the pick to the sleeve and then the block, causing the load cell to compress and thus changing its capacitance. From here, it is the job of the PCB to analyze the changes in measured capacitance on the load cell.

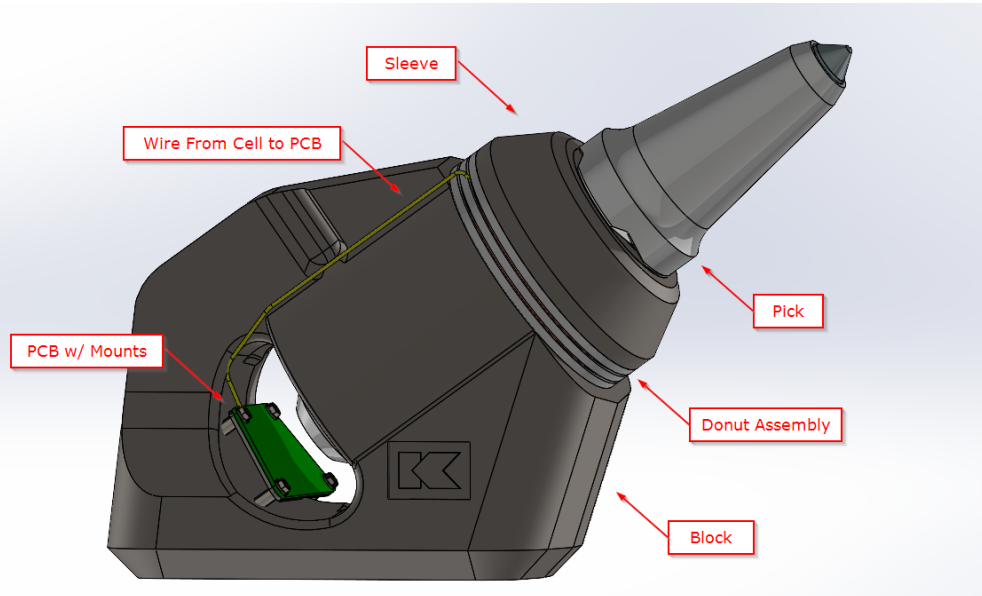


Figure 13: Overview of Load Cell and PCB Locations

2. Material Selection

The material used in the load cell design had several constraints summarized in Table 5 below:

Table 5: Material Selection Criteria

No.	Constraint	Criteria
1	Minimum Deformation	Determined by minimum change in capacitance required. (See <i>Section II.C</i>)
2	Dielectric Constant, ϵ	Must be > 2.0
3	Forces Applied	Does not yield under 40 kN force
4	Working Environment – Temperature	Must maintain mechanical and electrical properties between 40 – 110 F
5	Total Height	Cannot Exceed 3/4” Total
6	Cost	Cannot Exceed \$5 / cell

Based on the criteria list in Table 5 and data available from the Granta Materials Database, the team determined **High-Density Polyethylene (HD4PE)** at a thickness of 1/8” per layer (~3/8” total thickness) as ideal for prototyping. This thickness was further refined through prototype validation and verification.

3. Predicting Deformation and Required Thicknesses

To meet the first requirement, the team determined the range of capacitance values desired from the Load Cell. Then, the team determined the stresses the cell would experience based on the pre-determined cross-sectional area of the cell and forces applied. The team used these stresses and minimum deformation requirements to determine a target modulus of rigidity (E) and minimum yielding stress (F_y) values for the material. See *Section III.A: Verification (Analytical)* for further information.

4. Prototype Assembly

The team ordered copper and HDPE sheets online through sources such as McMaster Carr (See *Appendix Error! Reference source not found.: Team Budget*). The team cut ‘donut’ shapes out of these blanks. The copper rings were designed to be recessed 1/8” from the edges of the HDPE. Wires were then soldered onto the copper rings before the layers were glued together with epoxy (Figure 14).



Figure 14: Prototype Assembly. Left: Soldering wires to copper. Right: Gluing layers together.

E. Printed Circuit Board Design

1. Schematic

Rock Solid Solutions used Altium Designer as its circuit design tool of choice. This software supports hierarchical schematic design, which is critical to the maintainability and scalability of a circuit design project. Similar to the idea of object-oriented programming presented in *Section II.F.1*, hierarchical circuit design allows the team to define circuit subsystems and overarching circuit designs with appropriate dependencies. The advantage of this setup is the ability to add subsystems at will or change things about existing subsystems without reworking the entire setup. *Appendix D* shows the schematics for each subsystem and the top hierarchy, but the details of each will be discussed thoroughly here.

ESP32 Microcontroller: The advantage of using the ESP32 microcontroller for our design is the incredible amount of online resources, including online guides[7-8], manufacturer schematic examples[9], and accessible data sheets[10]. This allowed us to mimic the components used on the development module that Espressif created, but tailor it to our specific purpose. The biggest change is to the schematic presented in [9] for the ESP32 sub module, is excluding the USB UART interface since USB OTG is sufficient for serial communication and flashing code to the board. Furthermore, not all GPIO ports are used, so we can selectively choose which to use for each of our sensors. We use 2 separate I2C channels, a SPI channel, and 4 general-purpose GPIO pins for illuminating the LEDs. Figure 15 illustrates which modules were excluded from the Espressif development modules for our specific design.

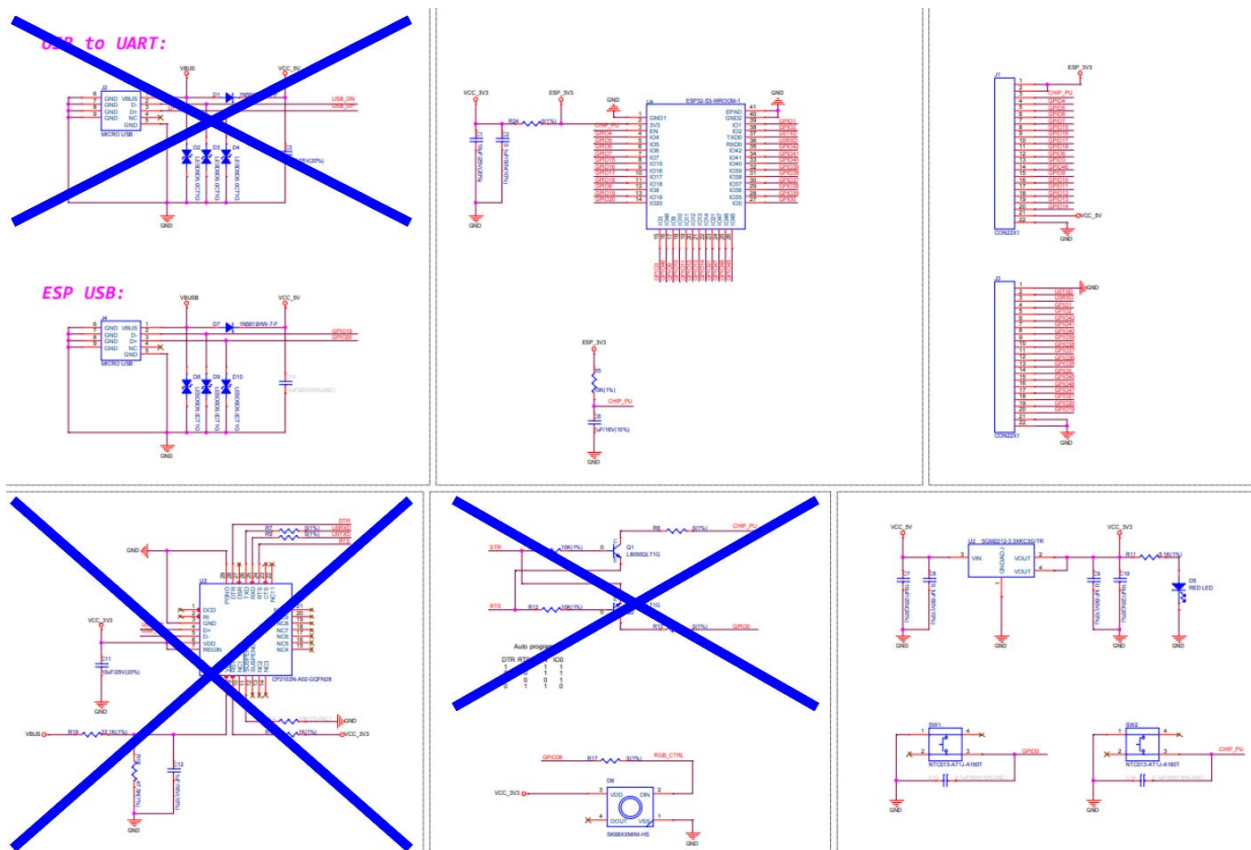


Figure 15 ESP32 Essential Module Selection[x]

Capacitive to digital converter: The capacitive to digital converter used is the AD7746 integrated circuit designed by Analog Devices [11]. The submodule we created by referencing

the provided block diagram (See Figure 16) of the CN-0552 [12] extended range capacitive to digital converter evaluation kit.

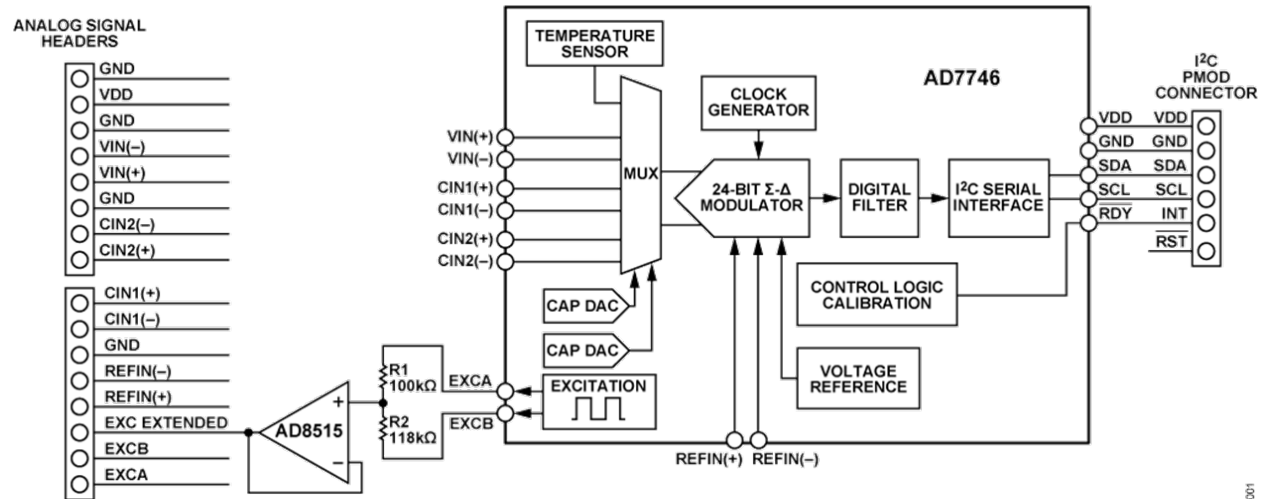


Figure 16 Block Diagram of CN-0552 [x]

Again, only essential components were kept as to reduce the overall complexity of the system

Accelerometer: Similar to the capacitive to digital converter circuit, note recommendations ADXL375datasheet [13] provided insight into what components needed to be paired with the device to ensure that it worked properly. Furthermore, the data sheet recommended placing the accelerometer close to mounting points on the board, which informed the location in our final design presented in Figure 19 in *Section II.E.2*.

Battery Management: The battery management system is designed to allow the USB port to power the board and charge the battery while it is plugged in, then switch to battery power when no USB port is present. Several considerations had to be made for this design, including the charge rate [14], which is determined by the ratio of resistors on Pins Prog1 and Prog3. For the system, we chose a charge rate optimized for Li Batteries with 3.7V 500 mAh capacity.

Flash Memory: The flash memory module [15] was likely the easiest to wire since there are only a handful of pins, and they are labeled standard SPI names such as MOSI, MISO, SCK, and CS. These were wired directly to an available SPI port on the ESP32 module.

Note that decoupling capacitors were placed at virtually every supply pin for all integrated circuits to maintain stable power delivery.

2. Layout

As shown in Figure 13 from *Section II.D.1* they physical shape of the printed circuit board is designed to fit inside the block behind the conical rock pick. The main considerations when designing this printed circuit board were signal integrity and resilience against electromagnetic interference (EMI). The area surrounding mining equipment is highly subject to EMI because of variable frequency drives on machines, so careful signal integrity steps are taken to minimize the

effects of EMI on signals essential to data acquisition. One method of signal integrity that was applied was common-mode noise filtering using a differential pair with 90-ohm effective impedance and picosecond length matching [16]. The purpose of a differential pair is to send two copies of the same signal, but the second is inverted. When these are fed into an inverting-summing amplifier, all common-mode noise is canceled, and only the true signal passes through. On the board, a differential pair is used for USB. To control the impedance, the Altium Designer Impedance Manager was utilized. Specifically, Figure 17 shows a coplanar differential pair with several dimensions that govern the effective impedance of the pair. For the specific circuit board material used, the dielectric constant and height inform these dimensions, and they can be established as rules applied to all differential pairs on the board.

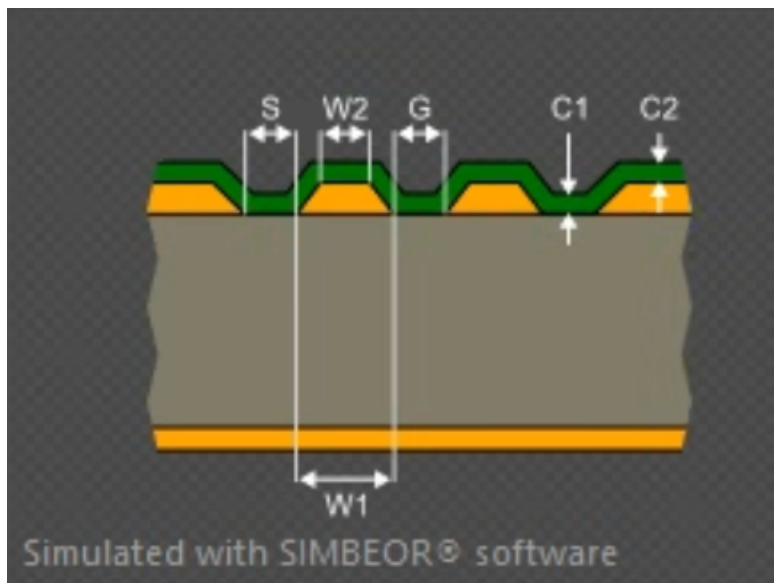


Figure 17 Co-Planar Differential Pair Graphic.

Next, the chosen layer stackup is shown in Figure 18 below, which includes four copper layers where power layers are located in the center and routing layers are located on the top and bottom. Although it was possible to entirely top route the board and utilize only two layers, four-layer boards are superior for signal integrity because inner layers can be dedicated to uninterrupted ground and power planes, which provide low-impedance return paths, controlled impedance, decoupling capacitance, crosstalk reduction, and power distribution integrity. Next, to maintain continuity between ground layers, vias are used throughout the board to connect all ground layers.

Layer Stack Legend		Material	Layer	Thickness	Dielectric Material	Type	Gerber
			Top Overlay			Legend	GTO
		Surface Material	Board Layer Stack Top Solder	0.010mm	SM-001	Solder Mask	GTS
		CF-004	Top	0.035mm		Signal	GTL
		Prepreg		0.185mm	PP-006	Dielectric	
		CF-004	GND	0.035mm		Internal Plane	GP1
				1.030mm	FR-4	Dielectric	
		CF-004	VCC	0.035mm		Internal Plane	GP2
		Prepreg		0.185mm	PP-006	Dielectric	
		CF-004	Bottom	0.035mm		Signal	GBL
		Surface Material	Board Layer Stack Bottom Solder	0.010mm	SM-001	Solder Mask	GBS
			Bottom Overlay			Legend	GBO
Total thickness: 1.561mm							

Figure 18 Printed Circuit Board Layer Stackup.

One last consideration is the risk of static shock damaging components. To prevent this, the main power input, and most susceptible to static shock, the USB, has TVS bi-directional diodes attached to allow transient voltage spikes to be shunted to ground before damaging critical components.

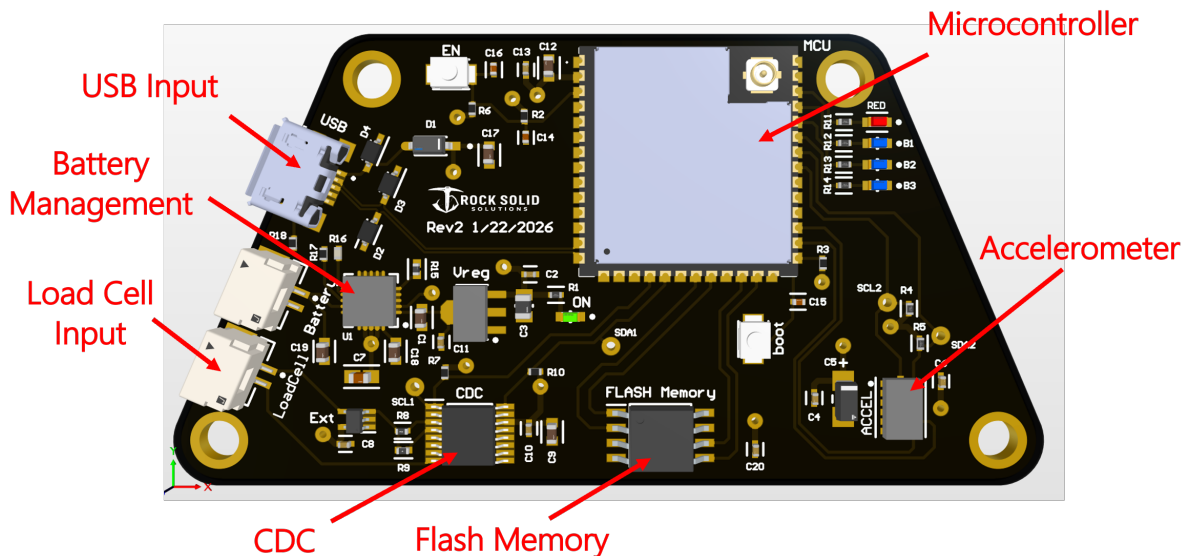


Figure 19 Description of Components on Layout.

3. Assembly and Verification

The printed circuit board could be fabricated within the budget and timeline, but assembly relied on our teams' engineering and soldering capabilities. The team used 0402 components all over the board, which can be very difficult to place by hand because they are very small. Figure 20

below shows the board without any components on it.

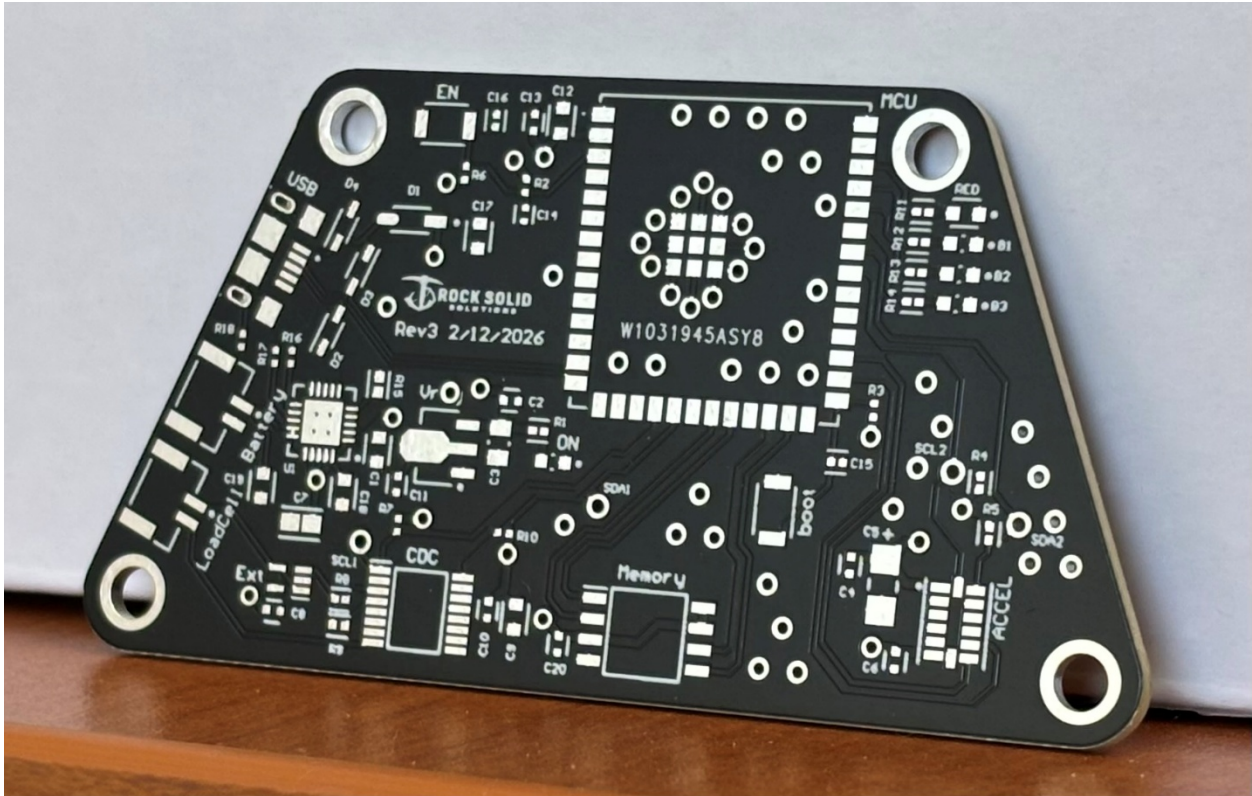


Figure 20 Fabricated Printed Circuit Board Without Components.

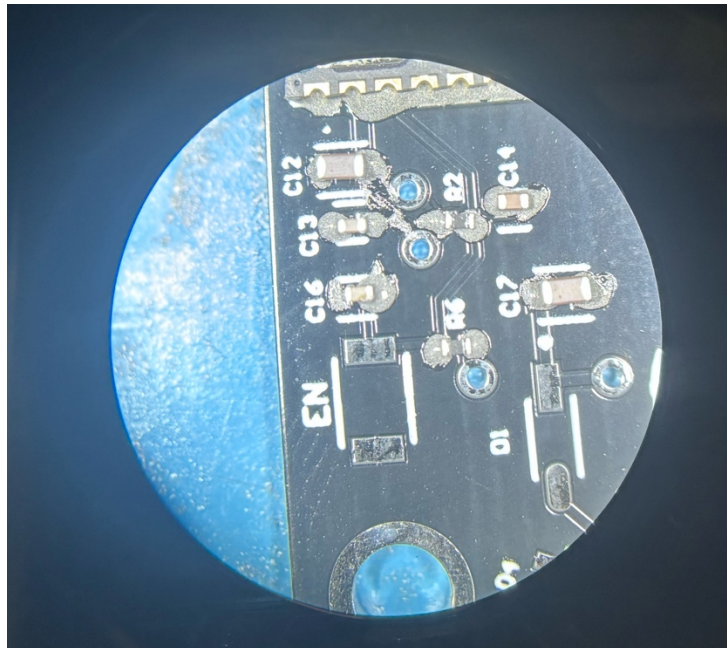


Figure 21 Solder Paste and Component Placement Under Microscope.

After all components were placed with solder paste, the next step was to reflow the solder paste and solidify the connections. This was done using the reflow oven (shown in Figure 22) in the Electronics Discover Center in the Electrical Engineering Department.



Figure 22 Circuit Board Placed into Reflow Oven.

After the solder was reflowed each connection was examined under the microscope. Figure 23 below shows a good connection with no visible bridges for a handful of components.

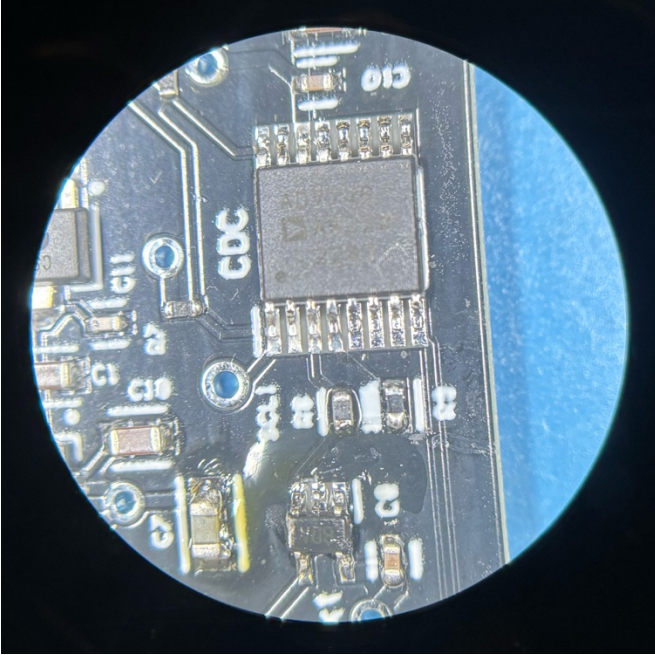


Figure 23 Inspecting Component Placement.

Before plugging in the board, testing for potential shorts is necessary, to do so the digital multi meter was used in continuity mode to check if there were any short circuits between

ground and 5V or ground and 3.3V. When a short was identified, reworking of the board was required. After getting the board to a point where no shorts were occurring, testing the data integrity of sensors was next. The T command described in *Section II.F.2* allows testing of all SPI and I2C modules. After approximately 5 adjustments to soldering, spanning 35 hours of debugging, the board was fully functional. Figure 24 below shows the battery and load cell attached, capable of making steady-state capacitance measurements.

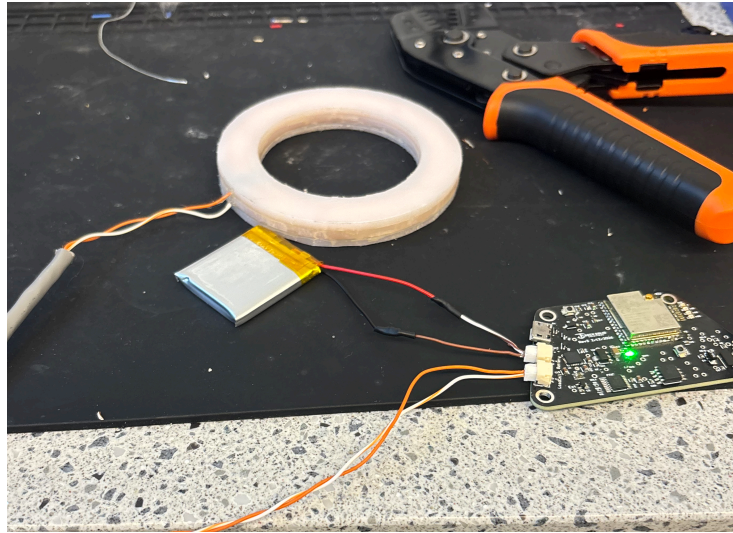


Figure 24 Preliminary Board Validation.

F. Modular Software Structure

1. Object-Oriented Programming

Rock Solid Solutions followed an object-oriented programming [17] design structure to maintain code that is scalable and maintainable. Just as hierarchical circuit design was employed to create subsystems, classes were used to define different subsystems; namely, the capacitive to digital converter, the accelerometer, the flash memory, and the LEDs. A summary of the functionality of each subsystem is described briefly in the following list:

Capacitive to digital converter: The AD7746 CDC (part of the CN0552 platform) measures capacitance changes from the sensing element over I2C, producing 24-bit raw readings at rates between 10–90 Hz. It supports a standard measurement range of ± 4.096 pF with resolution down to ~ 4 aF and can be extended to ~ 50 pF through excitation configuration (EXCA/EXCB). An internal offset DAC (CAPDAC) shifts the measurement window to accommodate large static common-mode capacitance. Readings are polled via a data-ready status flag before being packaged and forwarded to flash storage.

Accelerometer: The ADXL375 high-g accelerometer communicates over I2C and provides 3-axis raw acceleration data, which is converted to magnitude using a scale factor of approximately 49 mg/LSB. The device is configured for activity detection via two hardware interrupt lines, allowing the system to respond to impact or motion events without continuous polling. This data

is logged alongside capacitance readings in each flash packet to provide a complete picture of the physical conditions at the moment of a sensing event.

Flash memory: An external SPI flash device serves as the primary non-volatile data store for all logged sensor measurements. A double-buffered (Red/Blue) architecture in RAM allows continuous high-speed data capture while completed buffers are written to flash in the background via a service routine, minimizing disruption to real-time acquisition. Each 16-byte FlashPacket stores a timestamp, accelerometer magnitude, capacitance reading, and a reserved field. The logging region is user-configurable, and overflow detection is enforced to prevent data corruption. Flash must be erased before any write operation.

LED subsystem: Four onboard LEDs provide real-time visual feedback on system state. The red LED illuminates during active data recording and extinguishes when recording has stopped. The B1 LED indicates an ongoing data read operation. B2 and B3 flash to signal Threshold A and Threshold B events, respectively. On power-up, all four LEDs execute a sequential startup flash (RED → B1 → B2 → B3, repeated twice) to confirm correct GPIO initialization. Complete details on what illumination pattern signifies what can be found both in the operational manual in *Appendix E* and in *Appendix Error! Reference source not found.*

2. Overall Software Architecture Flow Diagram

The overall system architecture is described in detail based on the flow diagram shown in Figure 25 below.

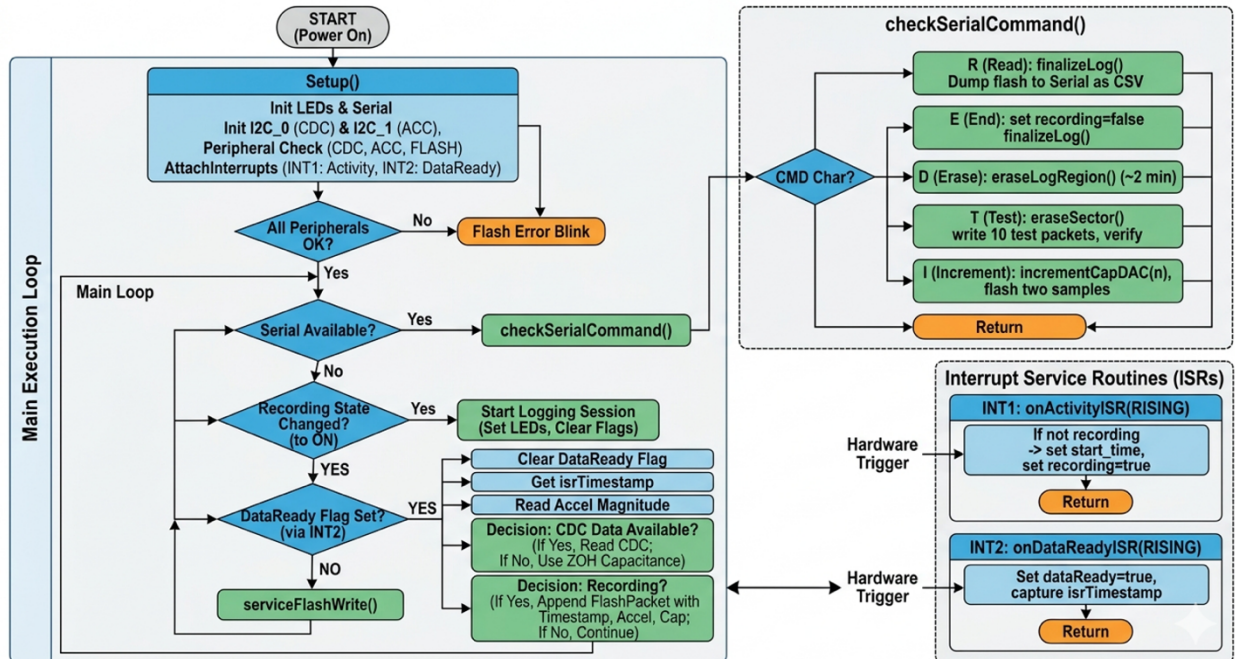


Figure 25 Flow Diagram for Smart Pick Code.

The left block includes everything that happens in the hardware “super loop.” At startup, several setup steps are performed, and depending on the sensors’ status responses, different LED

illumination patterns are sent to inform the user of the sensor. More details about the LED Human interface are defined in *Appendix Error! Reference source not found.* During each execution of the super loop, a check is made to see if any serial commands have been made. These are the commands supplied by the graphical user interface to end data collection, read data to a CSV, erase data, test sensor packet integrity, or increment the capacitance CAPDAC, which allows for calibration of the capacitance range to maximize the available loads that can be measured. There are two sensor-driven interrupts described above that allow for the software to collect data only when it is available, and service writes to memory between sample intervals. One sensor interrupt checks if data is ready from the capacitive to digital converter.

G. System Block Diagram

The system block diagram defining the system in its entirety is shown below in Figure 26.

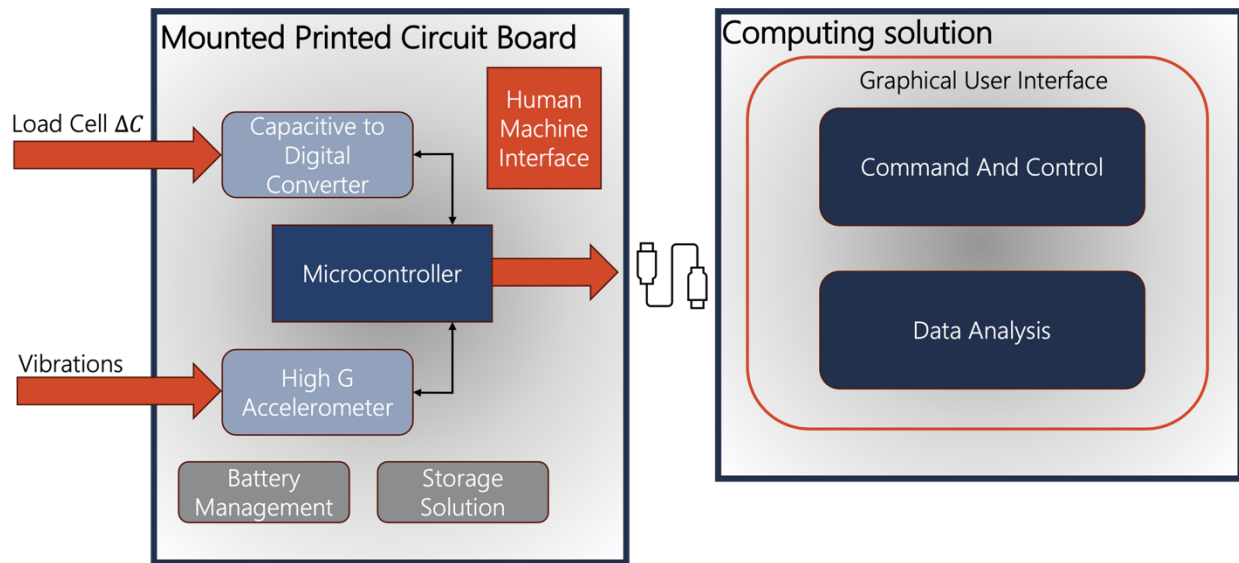


Figure 26 Electrical System Block Diagram

There are two inputs to the system: vibrations and a change in capacitance from a load cell coupled to the normal force acting on a conical rock pick. Each sensor connects to a microcontroller for processing. A battery management system is applied to energize the circuit, and a flash memory storage solution is used to save data from the microcontroller. This idea could be changed so that the system can stream data to a central hub instead of logging it to a storage solution; in fact, this would greatly simplify the current complexity and timing of servicing the flash buffer between samples. Finally, on the mounted printed circuit board is an LED Human Machine Interface (HMI) to allow the user to understand program flow during operations when serial monitoring is unavailable. The current solution utilizes a USB connection to a computer hosting a web-based graphical user interface to command and control the printed circuit board and also perform data analytics.

III. Verification and Validation

Verification and validation of the load cell consisted of confirming the expected behavior of the solution as well as demonstrating its functional use in a scale mining environment. With the scope of the project being to show proof of concept, testing had an emphasis on qualitative validation rather than precise quantitative validation.

A. Verification (Analytical)

Early verification consisted of calculations using known material properties to determine a relationship between applied force, structural deformation, and change in capacitance. Calculations shown in the Excel spreadsheet included in the project submission display verification calculations of load cell deformation at minimum and maximum forces experienced as well as the associated change in capacitance. This model was created to confirm that the range of forces experienced by the load cell would lead to the deformation required to produce a readable and reasonable increase in capacitance. A link to the Excel spreadsheet can be found here: [Verification Calculations.xlsx](#)

A model of the load cell was created in SolidWorks and FEA was performed to further evaluate its deformation under applied loads. Refer to Figure 9 and Figure 10 for FEA analysis results. The results confirmed that the deformation of the load cell is uniform and in the intended direction of measurement. The FEA also verified that the load cell remained below the mechanical yield point.

B. Experimental Verification (Compression Testing):

Compression testing was performed on the load cell using a hydraulic press to apply known static forces. Seven forces ranging from 3.5 to 10 kN were applied to the load cell with capacitances being recorded at each step. This verified the load cell's expected linear relationship between force and capacitance. Shown below in Figure 27 is the result of this test.

Linearity of Capacitance to Force

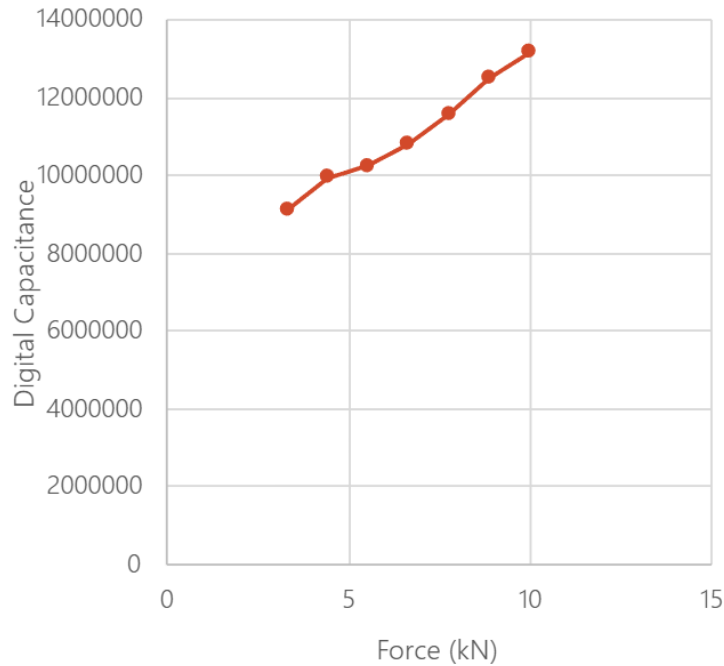


Figure 27 Finite Element Analysis of Load Cell

C. Validation (Field-Representative Testing):

Validation was performed by integrating the load cell with the linear cutting machine (LCM), shown below in Figure 28. The LCM is a full-scale rock cutting device that moves a conical pick through a rock sample, creating accurate field simulation. Additionally, the LCM is outfitted with a secondary calibrated load cell to monitor cutting forces allowing for validation of the smart pick. Validation focused on showing similar force trends between the two load cells which was successfully shown in testing. The figures shown in *Appendix G* show a comparison of the force graphs of the smart pick and reference load cell. This qualitative agreement shows that the smart pick is able to capture meaningful force variations in realistic conditions.



Figure 28 LCM With Integrated Load Cell

Limitations and Future Work

The validation and verification process was limited by the lack of precise load cell calibration. No specific force vs capacitance relationship was established with the final load cell design, only qualitative trends were shown. Additionally, the accuracy and sensitivity of the load cell were not determined.

Future work will include a precise and scientific calibration of the final load cell under known forces on a hydraulic press. A conversion from capacitance to force must be determined by comparing the smart pick's data to that of the LCM's onboard load cell. LCM tests will be performed many more times to determine the repeatability and durability of the smart pick.

IV. Final Deliverables

A. Testing Procedure

To qualify the effectiveness of the solution, a testing procedure is implemented that allows the simulation of cutting several different rock types in a single continuous pass. The Linear Cutting Machine (LCM) is a rock mining measurement tool that has been used by the Earth Mechanics Institute (EMI) for many years to describe rock mechanics. Rock Solid Solutions poured 3 types of concrete with variable PSI ratings to simulate cutting into different rock types with different hardness. Figure 29 below shows three types of rocks:



Figure 29 Rock Pour for variable strength Rock Simulant.

The middle is meant to simulate coal and has an estimated strength of 800 psi and incorporates biochar and Hydrostone to best imitate coal. At the front is 1200 psi concrete, and at the back is 4000 psi concrete. This layering is chosen to simulate what may occur in the mine where the cutting head transitions from cutting in hard sandstone or lime stone to engaging the target coal layer and then veering past again and hitting the hard rock mine ceiling above the coal layer. These transitions are the main focus of the experimental setup because it is important to be able to sense when the miner has veered out of the target production layer in order to notify the operator and return the cutter head to the target layer. Figure 30 below shows how the smart rock pick is applied for testing. From the figure, there is a battery that energizes the board, and the load cell is also connected with two wires to the load cell placed between the block and the

sleeve of the pick assembly.



Figure 30 Experimental Setup for Smart Pick Testing.

The procedure of testing is outlined in detail below:

Purpose: The procedures cover the end-to-end process for conducting a controlled linear cutting test with the Smart Pick Module, including device priming, test execution at 10 m/s, and post-test data retrieval and review.

Scope: Applies to all personnel operating the linear cutting machine with Smart Pick data logging equipment in the Earth Mechanics Institute (EMI)

Put on Personal Protective Equipment (PPE)

- Safety goggles (full seal, impact rated)
- Long-sleeve shirt (must cover entire arm and wrist)
- Long pants (must cover entire leg to the ankle)
- Inspect all PPE for damage before use. Replace compromised items.

Hardware connection

- Bring the linear cutting machine to a complete stop and verify all motion has ceased.
- Connect the load cell to the smart pick module
- Connect the battery to the smart pick module
- Press the EN (enable/reset) button to reset the onboard microcontroller
- Connect the computer to the smart pick module via USB
- Open the Smart Pick Graphical User Interface (GUI)
- Check the recording status indicator LED
 - If on -> click the stop recording button in the GUI before proceeding
 - If off -> proceed to the next step
- Click the erase flash button in the GUI and confirm (be patient, this can take up to 5 minutes)
- Monitor the LED indicating the erase command in progress
 - LED on during erase -> wait.
 - LED turns off, flash erase is complete, continue to the next step
- Disconnect the USB cable from the smart pick module.

Cutting Test Execution

- Adjust the linear cutting machine path to align with a new, unused section of rock sample (there are indicators on the jog for predetermined locations)
- Open LabVIEW on the computer near the linear cutting machine control panel
- Navigate and open the project file named Linear cutter.
- Review all settings in the LabVIEW interface and confirm cutting parameters are correct before starting the trial
- When all personal and equipment give verbal confirmation of readiness, start the linear cutting machine by pressing the 10m button
- Observe the LED on the smart pick module; it should illuminate as soon as the pick makes contact with the rock (if it doesn't you may need to restart the trial)
 - Reference the troubleshooting guide in the operational manual if issues persist

Post-Test Shutdown

- Once the cutting pass is complete, back up the linear cutting machine carriage to the starting position (or a safe parked position)
- Power down the linear cutting machine system completely.
- Confirm all machine motion has fully ceased before approaching the work area

Data Retrieval

- Reconnect the USB cable from the computer to the Smart pick Module
- In the Smart Pick GUI, send the Stop Recording command

- Send the read data command to transfer the recorded data from the module to your computer
- When prompted, save the retrieved data to a CSV file using an appropriate file description

File Naming Convention	Recommended format: <code>YYYYMMDD_SampleID_WearStatus_CutPass#.csv</code> Example: 20260426_Rock01_Good_Pass3.csv
-------------------------------	--

Figure 31 File Naming Convention for LCM Testing

Data review and verification

- In the smart pick GUI, click the Simulate Miner Experience button.
- Navigate to the playback settings within the simulation view
- Set playback position to 3,200 samples. Viewing 3,200 samples provides a complete view of the cutting stage, allowing you to quickly confirm whether or not the data was recorded correctly
- Review data traces
- Save all CSV files to an appropriate project data directory, preferably one with the same name as the sample ID from the naming convention above.

Procedure summary checklist

Table 6 Procedure Summary Checklist.

✓	Stage	Item
<input type="checkbox"/>	PPE	Safety goggles, long-sleeve shirt, and long pants donned
<input type="checkbox"/>	PPE	PPE inspected and confirmed undamaged
<input type="checkbox"/>	Setup	Machine fully stopped before connecting equipment
<input type="checkbox"/>	Setup	Load cell and battery connected to Smart Pick Module
<input type="checkbox"/>	Setup	EN button pressed to reset the board
<input type="checkbox"/>	Setup	USB connected to computer; GUI opened
<input type="checkbox"/>	Setup	Recording light checked; Stop Recording clicked if active
<input type="checkbox"/>	Setup	Erase Flash executed; waited ~2 min for LED to turn off
<input type="checkbox"/>	Setup	USB disconnected from Smart Pick Module
<input type="checkbox"/>	Pre-Test	Machine path adjusted to new, unused rock sample area
<input type="checkbox"/>	Pre-Test	LabView opened and Linear Cutter project file loaded
<input type="checkbox"/>	Execution	All personnel clear before starting machine
<input type="checkbox"/>	Execution	Machine run at 10 m/s; blue LED confirmed on rock contact
<input type="checkbox"/>	Shutdown	Machine backed up and powered down after trial
<input type="checkbox"/>	Data	USB reconnected; Stop Recording command sent
<input type="checkbox"/>	Data	Read Data command sent and CSV saved with descriptive name
<input type="checkbox"/>	Review	Simulate Miner Experience opened; playback set to 3,200 samples
<input type="checkbox"/>	Review	Data trace reviewed and confirmed complete and valid
<input type="checkbox"/>	Review	Test log updated and CSV filed in project directory

After many passes, the rock specimen is shown in Figure 32 below.



Figure 32 Rock Specimen After Several Passes.

B. Graphical User Interface

The graphical user interface is shown in Figure 33 below, and each button is described. At the top left of the graphical user interface, there is a drop-down menu that reports all current ports available to the computer. When the Smart Pick Module is plugged into the computer, it will be clear which one to click as the device has a unique device identifier “Smart_Pick_Module.” No button will work, and user notifications will be sent if a button is clicked without a port being selected. The stop recording button sends the appropriate serial command to stop recording. The read data command prompts the user for a CSV file name, then records all data on the flash into the csv data in the format timestamp in microseconds, acceleration, and digital capacitance. The Simulate Miner Experience allows the user to select from any CSV file recorded and view acceleration magnitude vs time, acceleration frequency spectrum, and zero-order hold capacitance and associated moving average with a user-defined window. Finally, the Increment CAPDAC is a button that allows for real-time calibration of the load cell range.

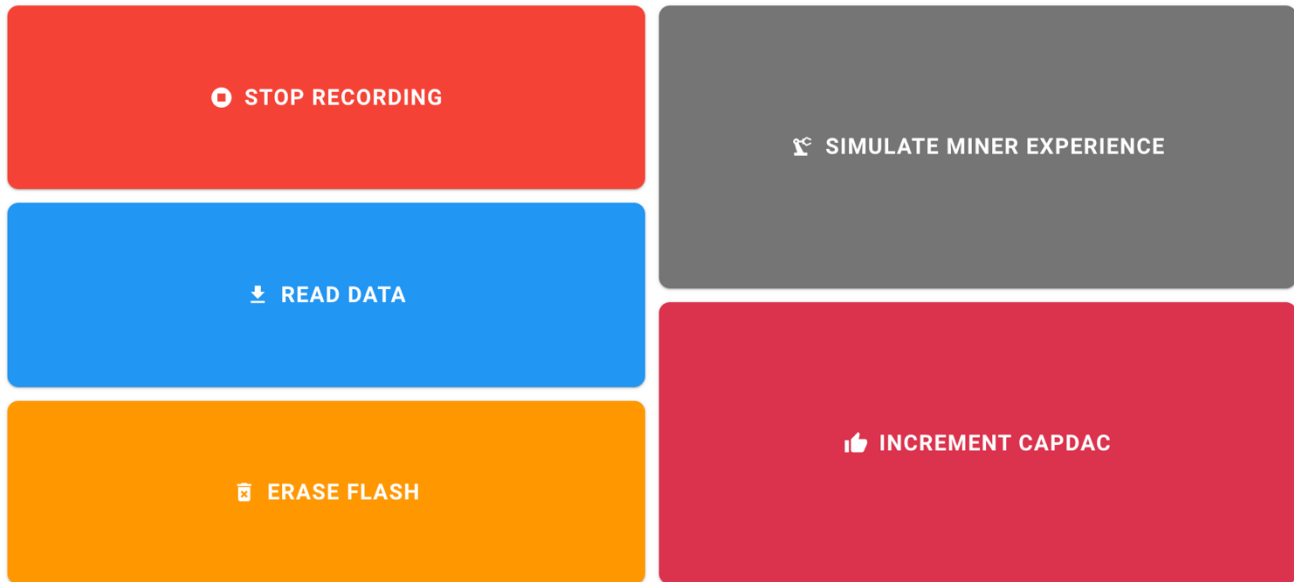


Figure 33 Graphical User Interface.

The CAPDAC can be thought of as a negative capacitance applied so that the baseline capacitance of the load cell can be accounted for and the range of possible, measurable loads can be maximized.

C. Qualitative Data Analysis

Without applying machine learning, we can get qualitative insights into the effectiveness of this solution to measuring loads on the rock pick and characterizing the rock wear status and material being cut. Figure 34 shows a characteristic loading profile which aligns well with the rock types being cut in sequence first medium concrete (1200 PSI), then coal simulate (800 PSI), then hard concrete (4000 PSI).

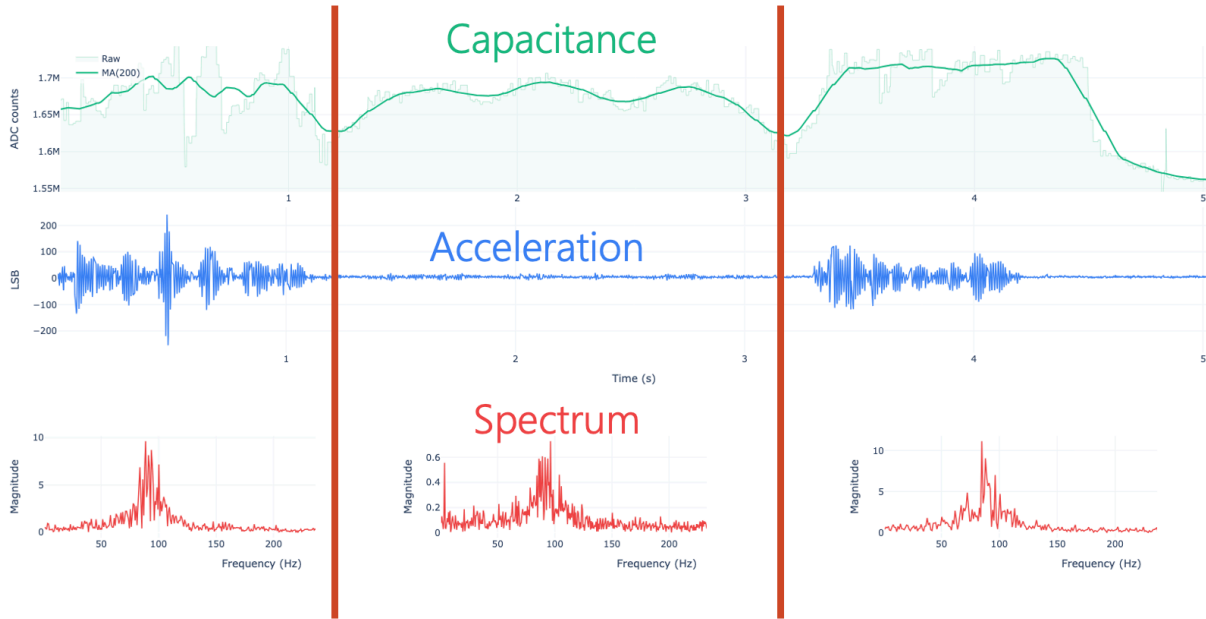


Figure 34 Capacitance and Acceleration vs Time, and Acceleration Spectrum.

From the data with a 200-sample moving average, we can clearly see trends in forces that correspond directly with the hardness of the rock being cut. The coal and medium concrete are very close in magnitude, but there is a clear jump in force when cutting hard 4000 PSI concrete. We also notice at the interface of each rock type, there is a significant drop in loading, i.e., the smart pick load cell disengages when there is no pressure on it. The acceleration magnitude is a great differentiator between coal simulant and the two concretes, as much higher vibrations are observed when cutting more abrasive, harder rock. To further justify the feasibility of the solution, 7 trials of acceleration magnitude are overlaid along with a mean capacitance over time with a 1 standard deviation confidence interval in Figure 35, indicating trends in cuts across similar specimens. Note that the concrete pours were not uniform, which accounts for the deviation in data.

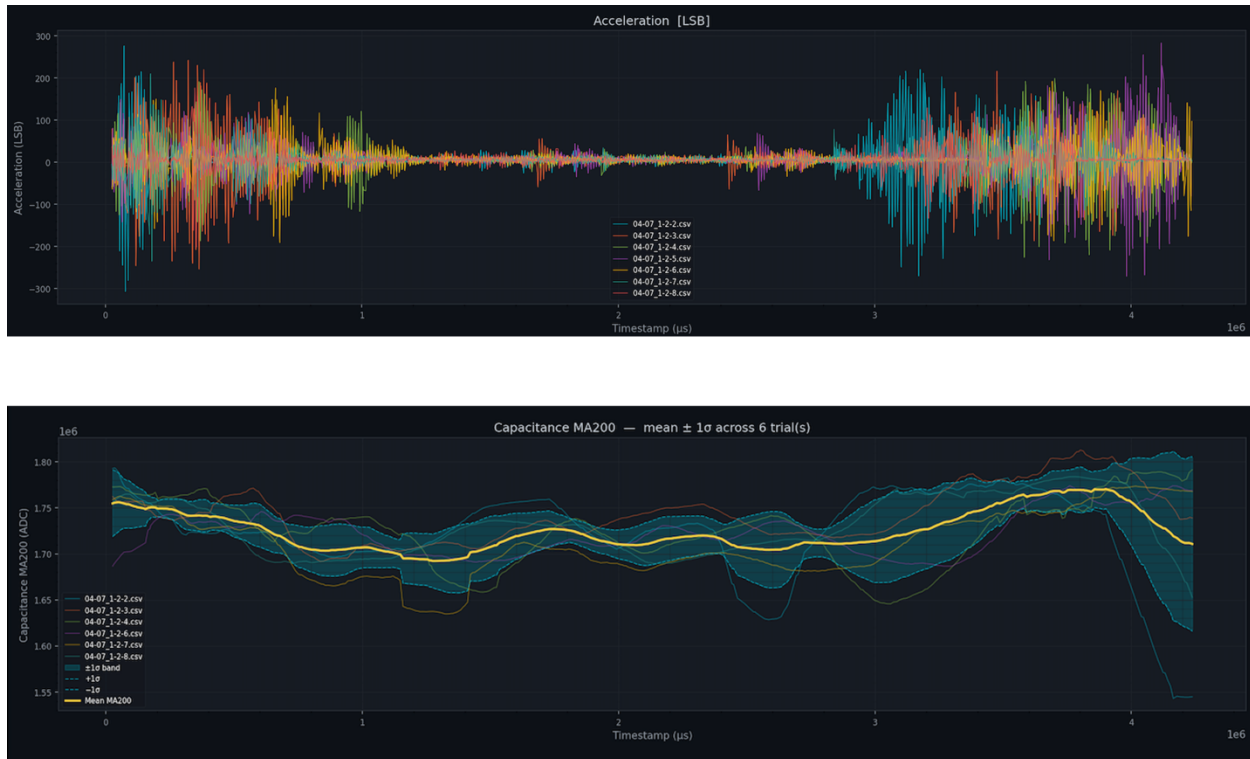


Figure 35 Multi-trial Overlay of data.

D. Preliminary Machine Learning Implementation


1. Motivation and Approach

The qualitative analysis above demonstrates that the Smart Pick captures clear, rock-dependent trends in capacitance and acceleration, but reading those signals by eye is not a viable strategy for an operating mining environment. The analysis must occur in real time and alert the operator to which rock is being cut so action can be taken immediately if the cutter head veers out of the target layer. To turn the raw sensor stream into actionable measurements, a multi-task neural network was trained to predict three quantities of immediate interest to the operator: the normal cutting force on the pick, the rock layer currently being cut, and the wear state of the bit. The neural network was trained on Smart Pick data collected simultaneously with ground-truth force readings from the LCM load cell. This way, the machine learning program can calibrate capacitance implicitly through the regression and comparison to the LCM data rather than a separate bench fit. The outcome is an end-to-end pipeline that converts raw sensor data into force readings, rock classification, and bit wear in real time. The software architecture is designed to be forward compatible with larger datasets and more capable pipelines that future data collection will enable.

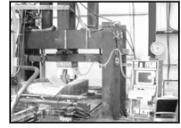
2. Data Reduction and Packaging

Before the data can be utilized in the neural network, it must be reduced to eliminate noise data that was collected before and after running the test (bit not in contact with rock) as well as to pair up the Smart Pick data with the LCM data in a matching sample rate. To do this, a macro-

enabled Excel reduction spreadsheet was created to intake LCM and Smart Pick data files and produce a clean machine learning file ready to feed into the neural network for training and testing the model. The spreadsheet has an intuitive user interface with buttons that run complex Visual Basic code in Excel VBA to perform various data functions. The user interface is shown below in Figure 36.



Earth Mechanics Institute
Mining Engineering Department, CSM
LCM Reduction Program (V 3.1)



Client : EMI
Project : Smart Pick
Project Location : Colorado School of Mines
Calibration File : Manual Reduction_01_1/7/2021

Date Tested : 04/07/2026
Date Reduced : 04/12/2026
Tested by : MJ,BB,JR,GW,KP,SM
Reduced by : MJ

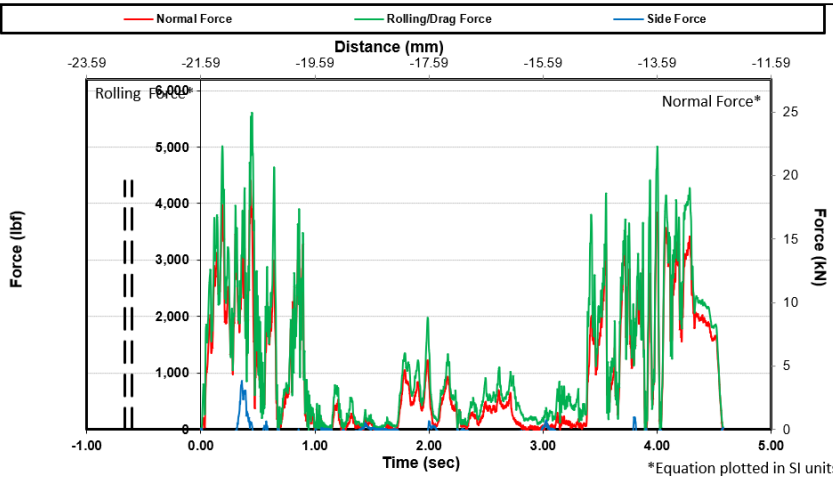
Test Series : A15
Book No : 1
File Name : 04-07_1-2-7_lm
Rock Sample : Conc-Biochar-Conc
Rock Source : CSM
Cutting Tool : U92
Cutting Tool Source : Kenametal

Saddle : Red Radial
Target Cutting Speed : 10.0 in/sec
Actual Cutting Speed : 0.0 in/sec
Line Spacing : 4.00 in 102 mm
Penetration : 1.000 25.40
S/P Ratio : 4.0

Force Angle: 0
Cutting Coefficient: 1.253
Specific: 0.592 hp-hr/yd³
Energy: 0.581 kWh/m³

	US System (in lbf)	Average	Std. Dev.	Minimum	Maximum
Normal	963	1110	-67.2	4410	
Rolling / Drag	1210	1320	-69	5610	
Side	-290	517	-1900	851	

	SI System (in kN)	Average	Std. Dev.	Minimum	Maximum
Normal	4.28	4.94	-0.299	19.6	
Rolling / Drag	5.38	5.87	-0.307	25	
Side	-1.29	2.3	-8.45	3.79	



Distance to LVDT

Smart Compare

Export Machine Learning Data

Figure 36 EMI LCM Data Reduction User Interface

Once the required LCM calibration data is entered through the first set of buttons, “Run Test” is pressed to open a file explorer window from where the LCM data file is selected, and the VBA macro runs to check if the distance recording LVDT was operational in the LCM dataset.

If it was not operational, then the macro runs the time-based reduction function, where time is on the x-axis of the force graph, and the data is clipped at the front end, where it first deviates from the baseline force reading, and then clipped on the back end when the force data returns to baseline readings. In order not to prematurely clip the back end of the data, the VBA code checks that the force data remains at baseline for at least 0.5 seconds before clipping the back end, but the clip still occurs at the start of the 0.5-second check. After running the test button, the Excel main page shows an LCM data graph.

The “Smart Compute” button is the next essential portion of the reduction spreadsheet that allows the user to select the corresponding Smart Pick data file (.csv) and clip the back end to match the time frame of the LCM data. Since the Smart Pick sensor automatically starts recording at the first large impact with the rock specimen, there is no need to clip the front end of the data file. The data plots from the “Smart Compute” macro are presented in Figure 38.

Finally, the “Export Machine Learning Data” button is run, which performs sample rate matching between the LCM and Smart Pick data and packages the LCM and Smart Pick data into a single, specifically formatted CSV file that is saved to the machine learning data folder. Figure 37 summarizes the data reduction pipeline.

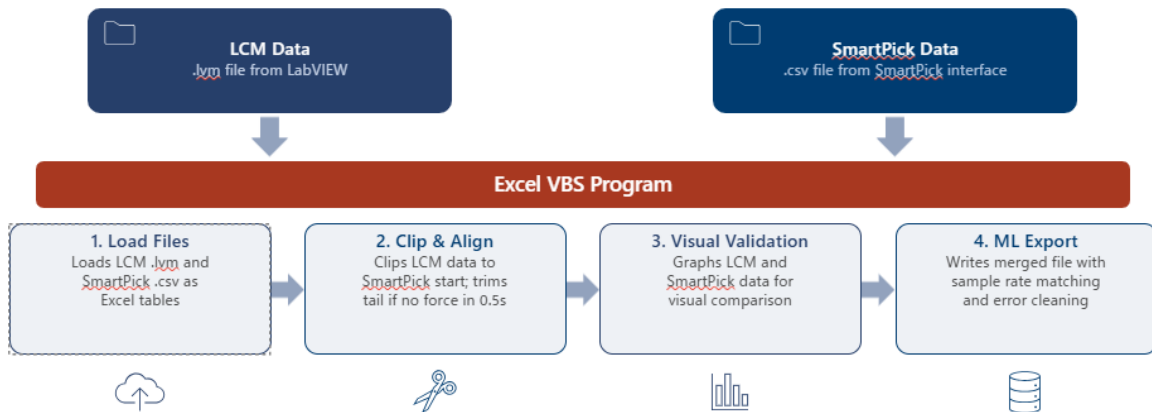


Figure 37 Data Reduction Pipeline

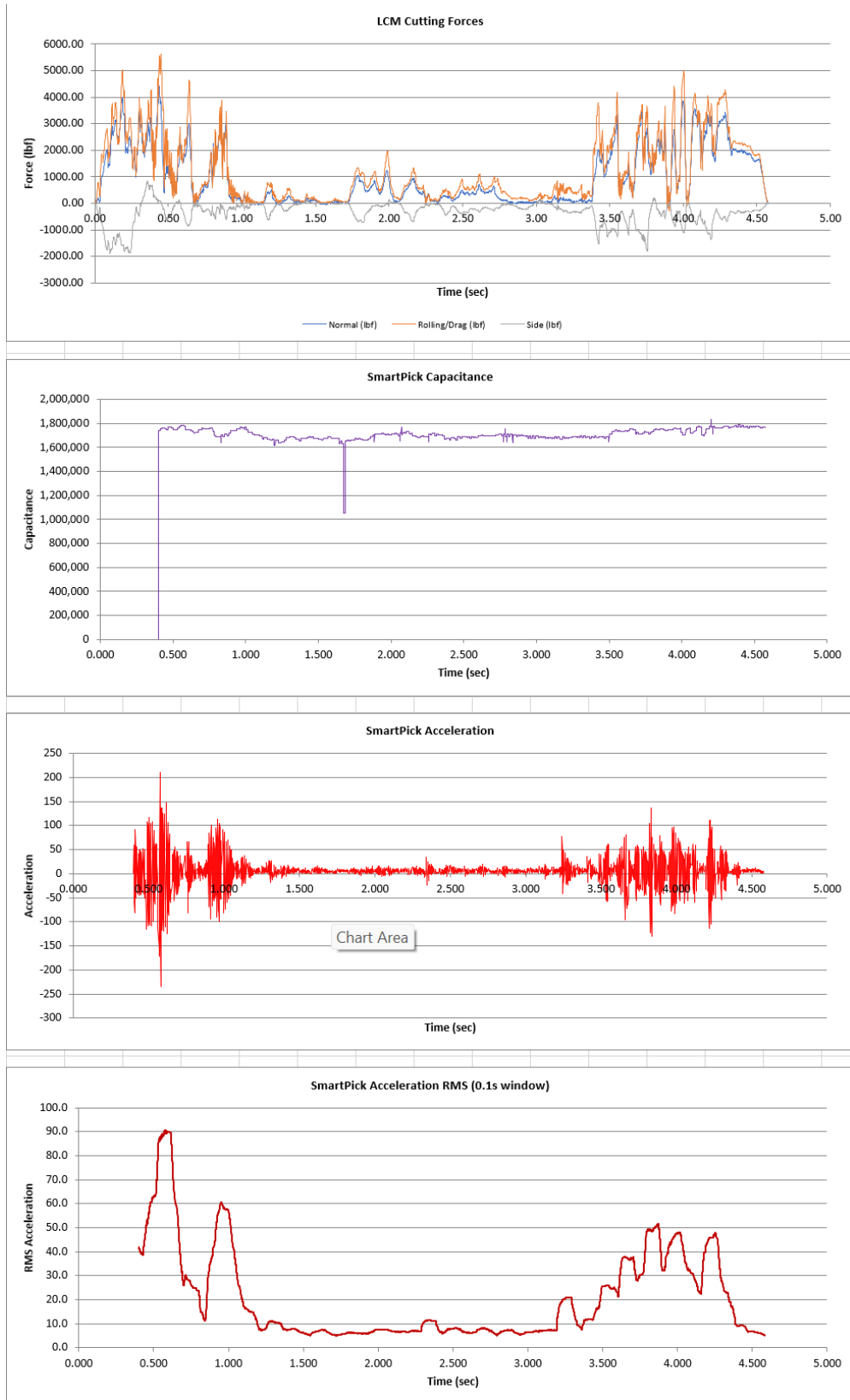


Figure 38 EMI LCM Smart Compare Graphs

3. Dataset and Feature Engineering

The training data consists of eight LCM cuts collected on April 7, 2026, each of which cuts three concrete layers in sequence: 1,200 psi mix, fake coal simulant (Hydrostone-biochar blend), and a 4,000 psi mix. All eight cuts were captured with either a New or Light Wear pick. Each cut yields the Smart Pick channels (acceleration, raw capacitance, running RMS of acceleration, and the time derivative of capacitance) sampled at 528 Hz, alongside the LCM tri-axial load cell readings in lbf. A derived channel, $sp_specific_energy = sp_capacitance / sp_acc_rms$, is added at load time as a proxy for force-per-unit-vibration that is physically analogous to specific energy in rock mechanics.

For the machine learning pipeline, time-series data are sliced into 0.10-second windows with 50% overlap, producing 679 windows across all eight cuts. To prevent the model from memorizing overlapping windows that span the train/validation boundary, the split is performed at the cut level rather than at the window level. This means that a full cut data file can either be used for training or for validation in the machine learning model. The model is specifically coded to prevent learning and validation on Windows from the same cut file. Of the weight cuts, six are held entirely for training (510 windows), and two for validation (169 windows). For each window, 43 hand-crafted statistical features are computed, summarized in Table 7 below.

Table 7 Neural Network Statistical Features

Channel(s)	Domain	Features per channel	Total
sp_acceleration, sp_capacitance, sp_specific_energy	Time-domain	mean, std, RMS, peak, peak-to-peak, skewness, kurtosis	$3 \times 7 = 21$
sp_acceleration, sp_capacitance, sp_specific_energy	Frequency-domain	spectral centroid, spectral energy, dominant frequency, band energy (0–50 Hz, 50–200 Hz, 200+ Hz)	$3 \times 6 = 18$
sp_acc_rms, sp_cap_rate	Scalar summary	mean, std	$2 \times 2 = 4$
Total feature dimension			43

The inputs are normalized with a RobustScaler, which uses medium and inter-quartile range rather than the mean and standard deviation. This is deliberate, as the rate-of-capacitance channel sp_cap_rate exhibits a single extreme spike at the moment of tool contact (on the order of 10^8 , versus a 99th-percentile value near 10^6), and the standard scaler would let that spike dominate normalization. The spike itself is represented in the peak and peak-to-peak features, so the model retains access to it without distortion of the rest of the feature space. Force targets are normalized with a StandardScaler whose parameters are saved and inverted at the evaluation time, so all reported metrics are in the original engineering units of pound force. The neural network data pipeline is presented in Figure 39 below.

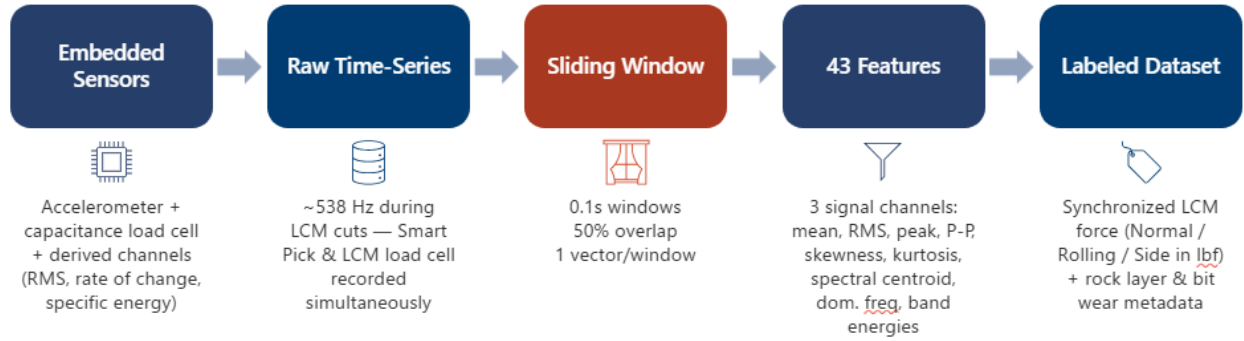


Figure 39 Neural Network Data Pipeline

4. Network Architecture

The model, SmartPickNet, is a multi-task multilayer perceptron implemented in PyTorch. A shared three-layer backbone (43-128-64-32) compresses the input feature vector into a 32-dimensional shared representation. Each hidden layer is batch-normalized with ReLU activation. The 32-dimensional shared representation then feeds three independent two-layer heads:

- Force-regression head that outputs three triaxial force components in scaled units
- A rock layer classification head with one logit per rock class
- A bit wear classification head with one logit per wear class

Sharing a backbone across the three tasks is intentional because in multi-task learning, the joint training allows the backbone to learn representations that are useful for predicting forces, rock type, and wear simultaneously, which tends to improve sample efficiency in the limited data that the model currently has to work off of. With more data collected in the future, especially across different bit wear types, the model will perform better and be more accurate. The network architecture is shown in Figure 40 and Figure 41.

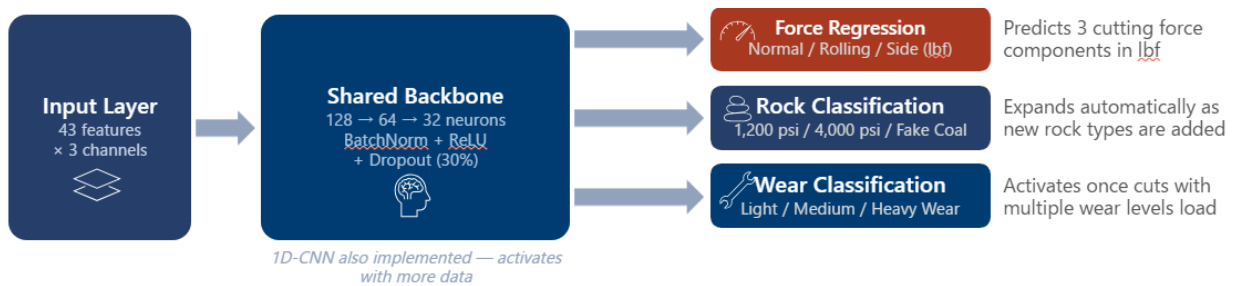


Figure 40 General Architecture (Three Heads)

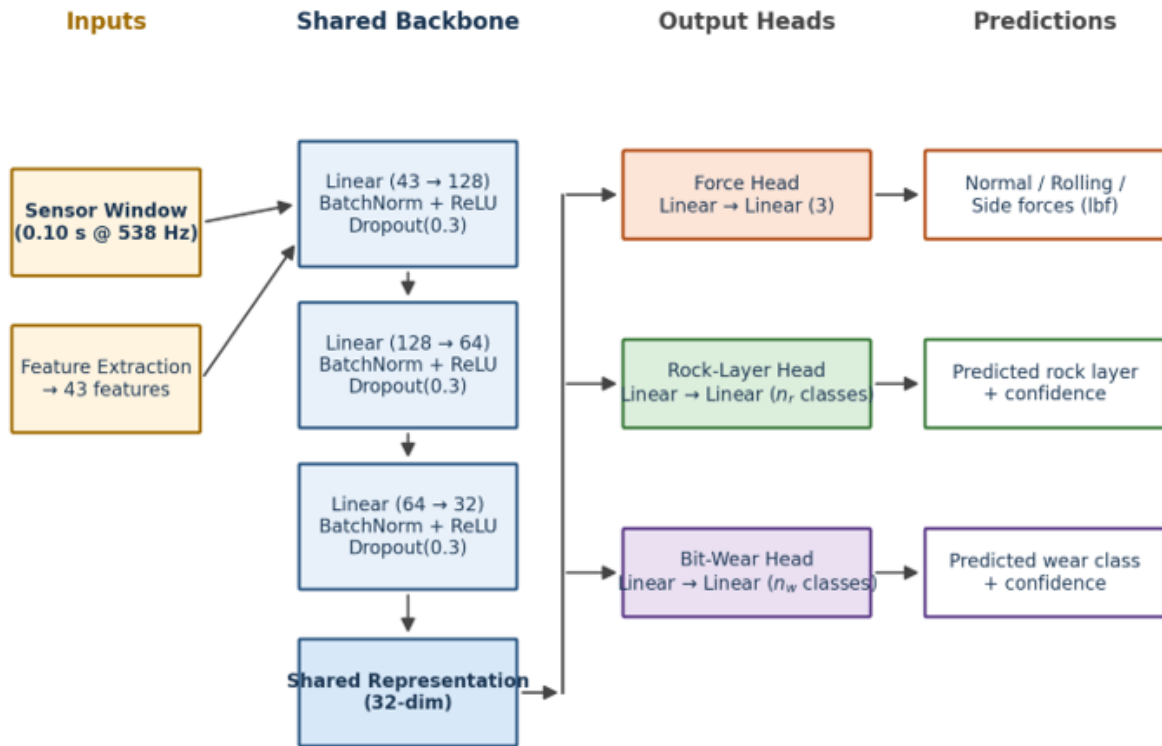


Figure 41 Smart Pick Neural Network Architecture

5. Training Methodology

The network learns all three things at once: force magnitude, rock layer, and wear state. In this way, the training loss is a weighted sum of three terms. Force prediction uses mean-squared error, while rock layer and wear state both use cross-entropy. The two classification losses are scaled down by a factor of 0.3 so that force prediction remains the primary objective.

The Multi-Layer Perception (MLP) is benchmarked alongside four other classical models to confirm it is functioning as expected, and better than the classical models. The MLP is run alongside Linear Regression, Ridge Regression, Random Forrest, and Gradient Boosting models in the correlate.py code. The five models are described in Table 8.

Table 8 Five Regression Models Via correlate.py

Model	What It Is	Why Included
Linear Regression	Fits a straight line between sensors and forces	Baseline — sets the minimum bar any model must beat
Ridge Regression	Linear regression with L2 penalty to reduce overfitting	Tests whether a regularized linear model improves on the baseline
Random Forest	Hundreds of decision trees voted together	Handles non-linear sensor-force relationships; provides feature importance
Gradient Boosting	Trees trained sequentially, each correcting the last	Often the strongest classical ML model on tabular data
Neural Network (MLP)	Same 3-layer PyTorch network used in the main pipeline	Benchmarked alongside classical models to confirm it earns its complexity

Another issue is that some rock layers appear more often than others in the test data. For example, in our test bed, the fake coal occupies over 50% of the cut length. To balance this in the model, the rock layer loss applies class weights equal to the inverse of each class's frequency. Without this correction, the model would learn to predict the most common class rather than distinguishing all layers accurately. The wear state loss is designed to activate automatically, so if there exists only one wear state class in the training data set, then the wear state loss weighting is skipped. If the training data set contains multiple wear classes, then the weighting is applied, the code is versatile for both types of training data inputs and requires no code changes for these scenarios.

The Adam algorithm with a learning rate of 10^{-3} and weight decay of 10^{-4} is used to optimize the model. A ReduceLROnPlateau scheduler monitors the validation error and halves the learning rate if no improvement is seen for 20 consecutive epochs. Training runs for a maximum of 200 epochs for a batch size of 16, and the checkpoint that achieves the lowest validation error is saved as the final model.

6. Preliminary Results

The model converges cleanly within the first 75 epochs and remains stable after this when running with the current data set of 8 cuts. The best validation checkpoint that was captured at epoch 73 achieves an average per-axis mean absolute error of 721.9-pound force. Rock layer classification accuracy peaks at 69% on the validation set, which is promising since 33% would be expected for random guessing for the three-head set. Both metrics are computed on cuts that the model has never seen during training, so they reflect generalization rather than memorization. The training and validation plots are shown in Figure 42 where the left graph shows the composite loss and its force regression and rock classification components, and the right graph shows the validation mean absolute error (MAE) per axis. The left graph proves the model is learning as the loss for the two heads decays constantly, meaning that the model is learning without instability or divergence. The right graph shows the model MAE across all 200 epochs, and it marks epoch 73 as the best checkpoint where the validation error was the lowest before the model stopped showing meaningful improvement. Overall, the left shows the model is learning and converging, while the right shows the accuracy of the predictions. The fact that the curves flatten rather than spike after the point epoch 73 indicates that the model is clean and does not overfit.

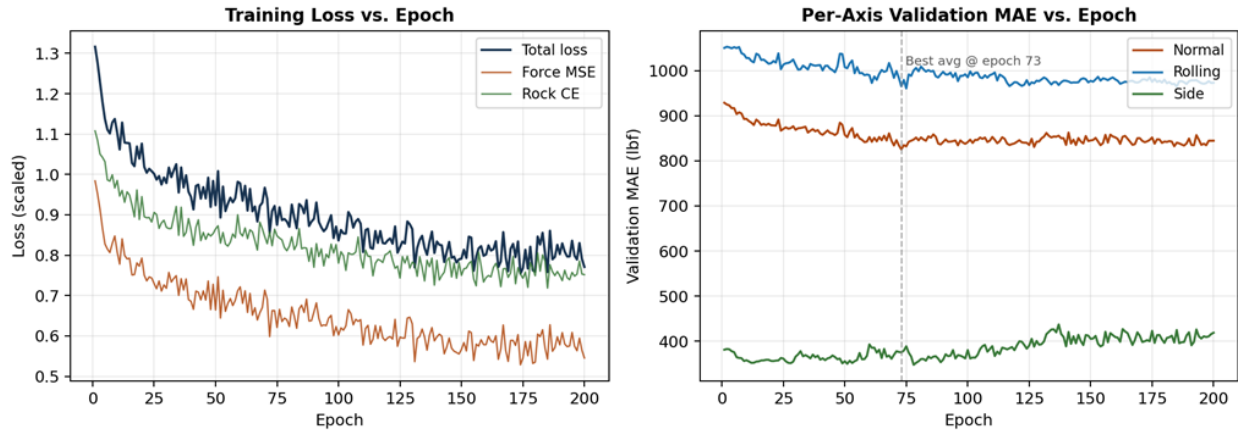


Figure 42 Training Behavior

When breaking the validation results down by rock layer, it reveals where the model is strong and where additional data is needed to improve the accuracy of the model. The fake coal layer is dominating the validation set in window count, and it is also the most reliably predicted. The fake coal is being predicted with a sub-600-pound force MAE and with 83% rock class prediction accuracy. The 1,200-psi concrete is predicted slightly worse at a 69% correct rock class prediction. Finally, the 4,000-psi concrete, by contrast, is almost always confused with the 1,200-psi concrete in the current cut data because of overlapping force ranges in the very small validation sample available currently. This problem can be resolved by performing more LCM cuts to have more data available for training the model. Table 9 shows the prediction accuracy summary by rock classification.

Table 9 Per-layer Validation Results

Rock layer (validation)	Windows	MAE Normal (lbf)	MAE Rolling (lbf)	MAE Side (lbf)	Rock accuracy
Fake Coal	101	508.2	561.3	227.4	83%
1,200 psi Concrete	26	1133.7	1505.9	754.2	69%
4,000 psi Concrete	42	1397.1	1601.4	496.6	5%
Overall (avg)	169	825.3	965.1	375.3	69% (peak)

Per-window predictions on a held-out cut illustrate how these aggregate numbers translate into time-series behavior. Figure 43 below shows predicted versus actual triaxial forces for cut 04-07_1-2-3, with the background shaded by the model’s predicted rock layer label. The neural network tracks the central tendency of the loading well, captures the disengagement events between layers, and produces rock layer transitions whose timing aligns with the actual layer boundaries.

The primary limitation visible in the plots is that the predicted forces are smoother than the actuals, which is expected behavior of a machine learning pipeline trained on aggregated window statistics rather than raw waveforms. The smoothing is inherent in the MLP network due to the MLP taking pre-computed summary statistics for each time window and predicting outputs from those numbers alone. This is the simplest form of neural network, and through this, the sharp, short-lived force spikes are averaged away during the summarization step. The model never has a chance to learn or reproduce the spikes. On the contrary, the proposed solution is switching to a larger data set (more cuts to learn from) and to a 1-Dimensional Convolutional Neural Network (1D-CNN), which operates directly on the raw time-series waveform. It slides small, learned filters across the signal to detect local patterns such as rapid force transients, vibration signatures, and layer transitions that the summary statistics do not capture. This is one of the motivations for the planned switch to a 1D-CNN backbone described in the Limitations and Path Forward section below.

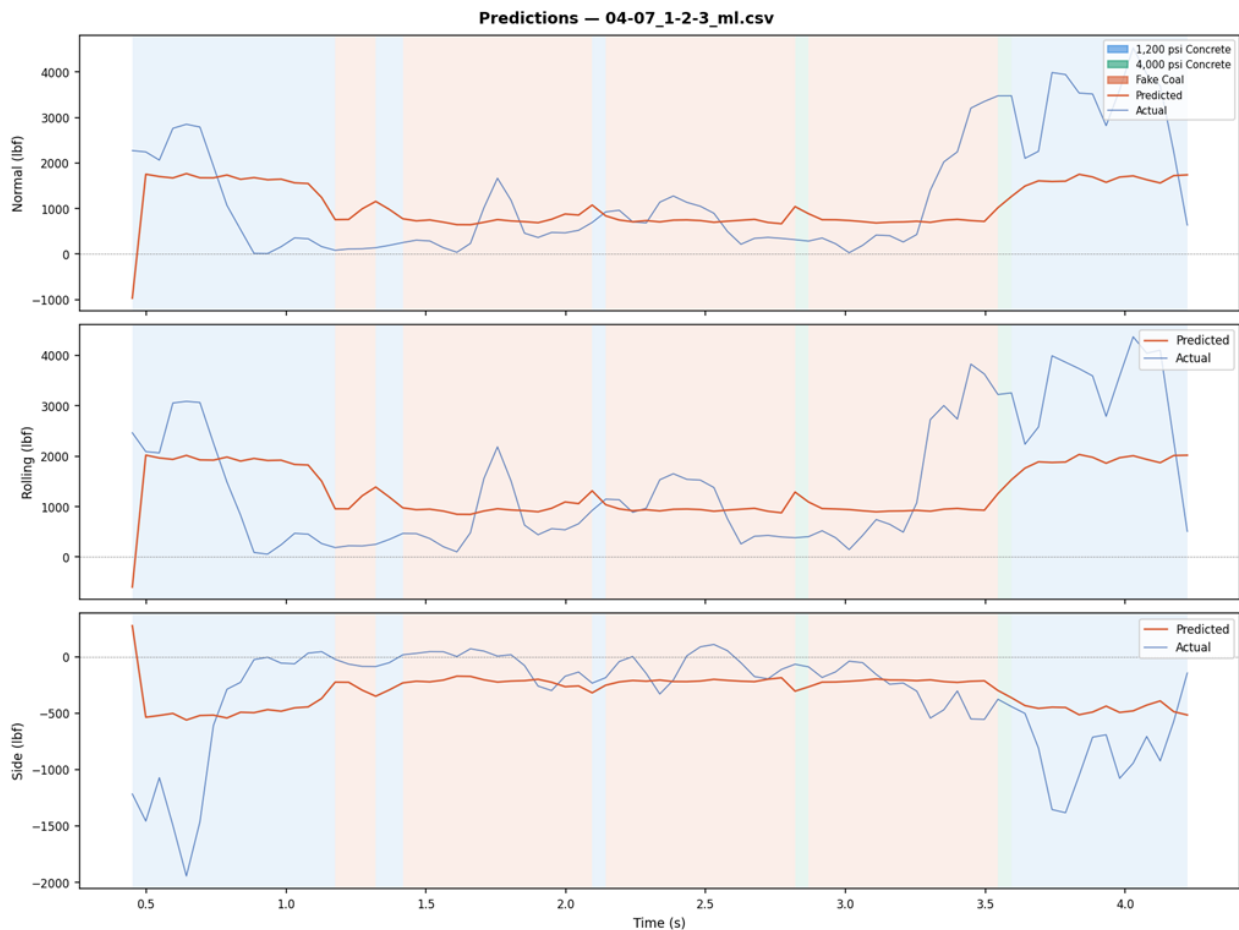


Figure 43 Predicted (red) vs Actual (blue) Force Lines on a Validation Cut with Background Shading per Predicted Rock Type

7. Limitations and Path Forward

This implementation is preliminary by design, as the priority for this semester was to demonstrate that a single trainable model can ingest the Smart Pick sensor stream end-to-end and

emit calibrated engineering-unit predictions and rock-class labels. With that demonstrated, two targeted investments will improve the performance of the model. The first is data. More data is necessary for a robust model. The current training and validation data set contains only 679 windows from eight cuts on three rock layers and a single wear state. Collecting cuts that span additional rock types and that include medium and heavy wear bits will both broaden the rock-layer vocabulary and unlock the wear head, which cannot be utilized with the current data cost, containing only a majority of light wear bits. The program is coded to automatically engage the third learning head for wear when a second wear class appears in the training data. The second is updating the model architecture. Once the data set exceeds 10 cuts available for learning, the SmartPickConvNet, a 1D-CNN sibling with the same three output heads, will run instead of the current network. This is implemented and ready to use in the code as soon as the data set is large enough. This new convolutional backbone consumes raw windowed time series rather than the handcrafted statistics. This means it learns its own temporal filters and is generally a better fit than the MLP once enough data is available to train. This is particularly beneficial for capturing the high-frequency force peaks that current MLPs smooth over.

Beyond model improvements, two engineering steps can be made to move the pipeline toward field deployment. The first is dedicated to bench calibration of the Smart Pick load cell to get a linear static capacitance to force curve. This calibration data will give the regression head a stronger physical anchor and reduce the burden on the network to learn that mapping from scratch. The second is on-device inference. The trained model is small and can run comfortably on a CPU, which makes deployment to the ESP32 microcontroller on the PCB traceable through ONNX export and a lightweight inference runtime. Together, these steps transform this preliminary implementation into a real-time, on-pick measurement system rather than an offline analysis tool.

V. Project Management

A. Overview

Project management began as the responsibility of the Scrum Lead but became team responsibility over the duration of the project. On a high level, a Gantt chart entailing project milestones and week-to-week responsibilities of the team was created. This was enforced on the low level with the use of the Scrum Sprint Cycle system to keep the team on track with the project.

B. Work Breakdown Structure

A Gantt chart was used to detail the work breakdown structure of the project. An updated version of this chart can be found in *Appendix **Error! Reference source not found.***. This chart outlines sprint deadlines, working windows for project milestones, and large project deadlines such as the PDR, CDR, and FDR. At the outset, the Team Rock Solid Solutions designed the work breakdown schedule to be front-heavy to clear up time later in semesters for other responsibilities and possible setbacks.

C. Management with Scrum

Team Rock Solid Solutions implemented the [Scrum](#) framework to manage the project. The Scrum framework breaks down large, month and year-long projects into two-week sprints. To track progress items during sprints, the team implemented a [Trello Board](#). Here, the Scrum Master and team members could add tasks, assign them to team members, and mark them complete for the team to see.

D. Next Steps

The project has been completed to a great degree of success. Rock Solid Solutions has provided a fully modular system capable of monitoring loads exerted on rock picks during normal cutting operations, measuring system acceleration, and aligning the data with ground truth reference data from a fully calibrated linear cutting machine. Across several metrics, the system performed successfully, and premature implementation of a machine learning neural network was implemented with a limited number of data sets, which was able to, with 86 percent accuracy, correctly classify when the smart pick was cutting a coal simulant in real time. Although this system serves as a strong proof of concept and undoubtedly reaches the goals outlined at the beginning of the semester, there are necessary engineering steps to ensure the system is mine-ready and supplies data that is essential to real-time characterization of rock type and wear status that is intuitive for a mine operator. The team has identified five important areas that must be addressed to ensure the smart pick for rock mining makes it to the mines.

1. Environmental Hardening

A crucial next step to bring the smart pick into the mines is ensuring that it is resilient against water and dust which is a mining guarantee. The next team of engineer that work on this project need to investigate methods for shielding the smart pick solution from the elements while mandating the possibility of wireless communication. Some methods that have been discussed include confine the smart pick to a space embedded in the block of the rock mining assembly. One thought governing this decision is selling “smart blocks” with necessary components and waterproof and dust proof cable connections for power and load cell. The advantage of this type of solution is the extended lifespan of the block relative to the pick. The maintenance interval of the block will be very close to that of the electronics inside.

2. Distributed Power and Solution

Distributed power is incredibly important. How can we take advantage of power already available on the target mining machinery. A team would need to create a way to supply 3.3V to 5V to a smart pick solution on every rock pick on the machine. This is a very complex task involving careful attention to detail when it comes to routing wires to be mine admissible and maintainable by mine operators.

3. Multi-node Optimized Data Acquisition solution

The solution delivered by Rock Solid Solutions solution is confined to a single rock pick. There are hundreds of rock picks per machine so a multi node system with one central processing unit that routes data to a wireless communication hub to transmit to the main cab for real time data analytics is strictly necessary. The team would like to note that with 100s sensors also comes bandwidth constraints. The advantage of the interrupt driven software is the ability to collect and send data only when it is available. Since only a handful of conical rock picks are in rock at a single time, we only need to collect data for those rock picks which lightens the bandwidth required to monitor rock picks wear status in real time. The data should be tagged based on the location of each pick, so that operators can identify which picks to replace.

4. Wireless Communication

The conclusion of Silje Ostrem's master's thesis was the development of a conformal circular antenna array capable of high-throughput data transfer, providing a viable means for a wireless link. Future work on this project involves packaging the data and transmitting it using this antenna with a modulation scheme suitable for high-fidelity communications in mining environments. Several engineering decisions remain, including how data will be transferred to the central cab, whether preprocessing will be performed, which modulation scheme will be implemented, what the bandwidth limitations are, and the importance of forward error correction and detection, and how data will be routed from the central processing unit to the antenna

5. Acquire a vast data set

Within section IV the discussion of preliminary implementation of a machine learning neural network described a key challenge: data. To train a model to be accurate across three output heads: force characterization, rock characterization, and wear status, data sets cutting into known rock specimens ranging from coal to sandstone, to granite, with different wear status is strictly necessary to train a model that can, in real time, predict each category. The team suggests that extensive data sets be collected, cutting different rock specimens with 3 different wear status rock picks and properly labeling each data set. The same procedure should be followed where ground truth data is collected alongside the measurements attained from the smart pick solution.

E. Budget Management

The team was allotted \$500 at the beginning of capstone design, with additional funds provided by the client if deemed necessary. The initial estimate was around \$400 with the goal of leaving around \$100 to spare for any unforeseen costs. This estimate was based on the intended \$100/unit cost with room for prototyping. Major costs included load cell materials and electronics. Load cell material costs were underestimated. While it consisted of relatively cheap sheets of HDPE, copper, and rubber bought from McMaster Carr, the team did multiple iterations of prototypes, requiring many orders of material. The electrical components, including the PCBs, were cheaper than expected with the team purchasing only one of each component

required. By only purchasing items after careful consideration, the budget was kept in check with the final purchasing total equaling \$460.52, putting us under budget.

Bill of materials (not including shipping) and budget tracker spreadsheets are linked below, and images are included in appendix C.

[Team F85 Budget Form 25-26.xlsx](#)

[Parts Order Form.xlsx](#)

VI. Lessons Learned

Throughout the development of the Smart Pick system, the team approached each task with the “measure twice, cut once” mindset—both literally and figuratively. When determining ideal materials, their thicknesses, and designing the printed circuit board, the team considered worst-case scenarios and avoided relying on optimistic assumptions. This approach proved valuable during testing; for example, the added circuitry for improved signal integrity allowed the system to produce clear, readable results with minimal pre- and post-processing. Through this process, the team developed a stronger understanding of what constitutes good engineering design: careful planning, conservative assumptions, and validation through testing.

Additionally, the team recognized the importance of iterative design. Initial calculations suggested using thicker dielectric materials for the load cell; however, testing across different rock types, bit wear levels, and load cell configurations showed that a thinner dielectric produced more useful and responsive data. Being open to revisiting earlier assumptions allowed the team to refine the system and ultimately produce more compelling results. This experience reinforced that early analytical models are valuable starting points, but real-world experimentation is often necessary to reach the best design solution.

This project also reinforced the importance of modular design and effective teamwork. As the project progressed, the system naturally divided into mechanical, electrical, and software subsystems, including the load cell assembly, printed circuit board, microcontroller architecture, and sensing interfaces. Organizing the project in this way helped isolate problems during debugging and allowed multiple components to be developed in parallel. Because the Smart Pick integrates mechanical design, electronics, embedded software, and data analysis, collaboration across disciplines was essential. Documenting design decisions and testing procedures helped the team coordinate integration and resolve issues efficiently.

Overall, the Smart Pick project demonstrated that successful engineering design requires iterative refinement, strong communication, and structured validation of both hardware and software systems. These lessons will help guide future improvements to the Smart Pick platform and support continued development of sensing technologies for mining applications.

VII. References

[1] K. G. Hurt and K. M. MacAndrew, “Cutting efficiency and life of rock-cutting picks,” *Min. Sci. Technol.*, vol. 2, no. 2, pp. 139-151, Apr. 1985. doi: 10.1016/S0167-9031(85)90357-3.

[2] An Underground Miner, “Top 5 Underground Continuous Miners,” An Underground Miner blog, 13 Mar. 2021. [Online]. Available: <https://anundergroundminer.com/blog/top-underground-continuous-miners> [Accessed: Nov. 2, 2025].

[3] Empire CAT, “EL300 Longwall Shearer,” Caterpillar, Inc, 2013. [Online]. Available: <https://www.empire-cat.com/sites/default/files/products/documents/C841082.pdf>. [Accessed: Nov. 2, 2025].

[4] K. H. Mitterndorfer, “Roadheaders in Tunneling,” TBM: Tunnel Business Magazine, 30 Jul. 2013. [Online]. Available: <https://tunnelingonline.com/roadheaders-tunneling/> [Accessed: Nov. 2, 2025].

[5] S. Prokopenko and A. Vorobiev, ‘Recovery of worn-out picks in rock breaking’, Eurasian Mining, pp.27-30, 07 2018.

[6] U.S. Department of Labor, MSHA, “Program Policy Manual, Volume IV—Electro-Mechanical Equipment, Intrinsically Safe and Permissible Circuits,” Washington, DC, USA. [Online]. Available: <https://www.msha.gov>

[7] RoboticWorx, “Build Custom ESP32 Boards From Scratch! | The Complete Guide to Designing Your Own ESP32-S3 and C3,” *Instructables*, Feb. 24, 2024. [Online]. Available: <https://www.instructables.com/Build-Custom-ESP32-Boards-From-Scratch-the-Comple/>. Accessed: Apr. 25, 2026.

[8] MAINFRAME, “Setting up ESP32 with Arduino IDE,” YouTube, [Online video]. Available: <https://youtu.be/CD8VJl27n94>

[9] Espressif Systems, “ESP32-S3-WROOM-1 & ESP32-S3-WROOM-1U Datasheet,” Technical Documentation, Rev. 1.8, 2023. [Online]. Available: https://documentation.espressif.com/esp32-s3-wroom-1_wroom-1u_datasheet_en.pdf

[10] Espressif Systems, ESP32-S3-DevKitC-1 V1.1 Schematic, Nov. 30, 2022. [Online]. Available: https://dl.espressif.com/dl/schematics/SCH_ESP32-S3-DevKitC-1_V1.1_20221130.pdf

[11] Analog Devices “AD7745/AD7746: 24-Bit Capacitance-to-Digital Converter with Temperature Sensor,” data Sheet (Rev 0), 2005. [Online]. Available: https://www.analog.com/media/en/technical-documentation/data-sheets/ad7745_7746.pdf

[12] Analog Devices “CN-0552: Capacitance to Digital Converter with Extended Range,” Circuits from the Lab, Rev. 0, Nov. 2021. [Online]. Available: <https://www.analog.com/media/en/reference-design-documentation/reference-designs/cn-0552.pdf>

[13] Analog Devices, “ADXL375: 3-Axis, ± 200 g Digital MEMS Accelerometer Data Sheet (Rev. B),” 2013. [Online]. Available: <https://www.analog.com/media/en/technical-documentation/data-sheets/adxl375.pdf>

[14] Microchip Technology Inc., “MCP73871 Stand-Alone System Load Sharing and Li-Ion/Li-Polymer Battery Charge Management Controller Data Sheet,” DS20002090E, 2019. [Online]. Available: <https://ww1.microchip.com/downloads/en/DeviceDoc/MCP73871-Data-Sheet-20002090E.pdf>

[15] Infineon Technologies AG, “S25FL256 / S25FL128L 256-Mbit (32 Mbyte) / 128-Mbit (16 Mbyte) 3.0 V FL-L Flash Memory Data Sheet,” Data Sheet, Rev. L, 2024.[Online]. Available: https://www.mouser.com/datasheet/2/196/Infineon_S25FL256L_S25FL128L_256_MB__32_MB__128_MB-3003228.pdf?srsltid=AfmBOorojTLaESIOLyVowyo0tG2z9PfWZNgvWes_2hBGOGyUu-2rghJX2

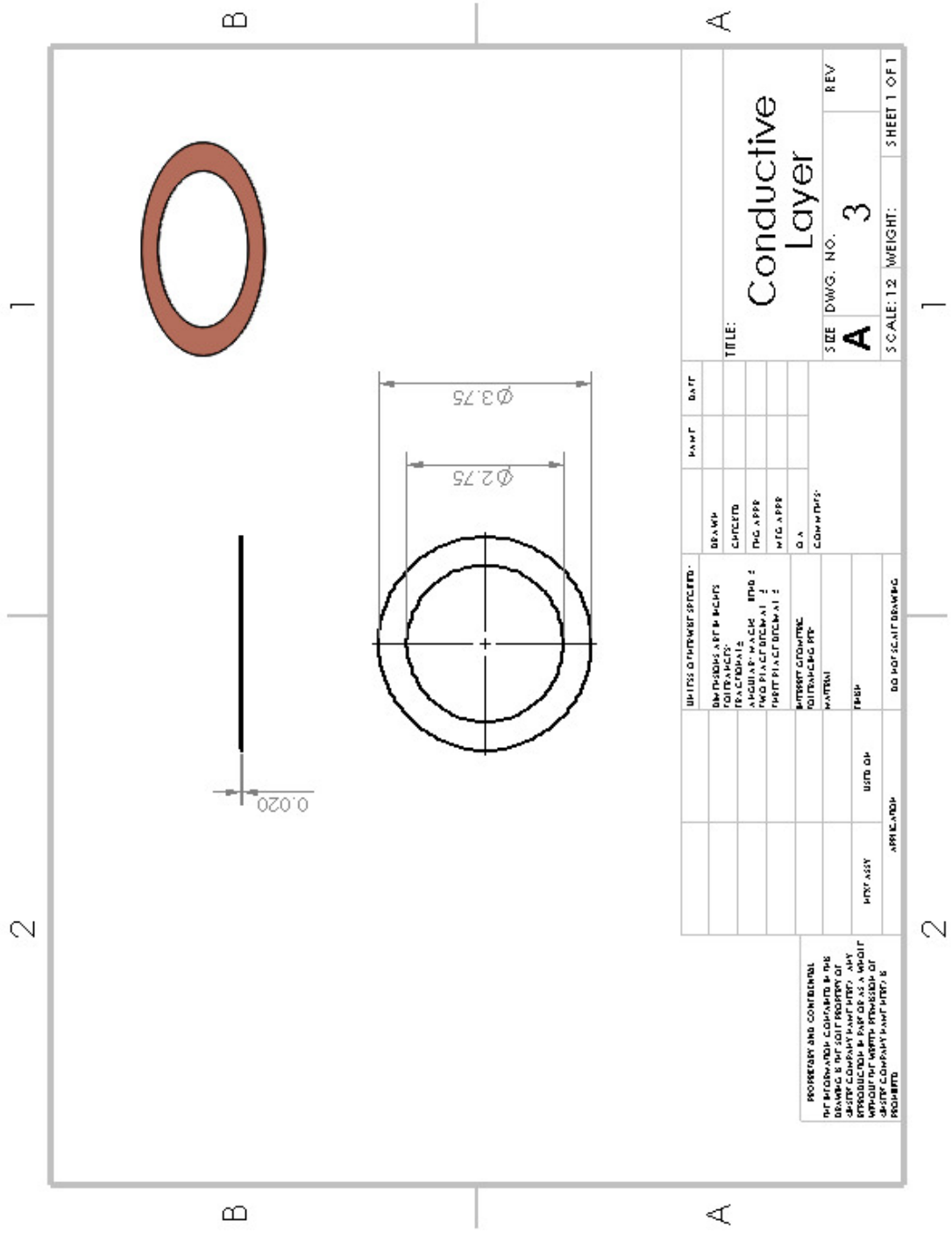
[16] Z. Peterson, “What Are Differential Pairs and Differential Signals?,” *Altium Resources*, Oct. 2, 2021. [Online]. Available: <https://resources.altium.com/p/what-are-differential-pairs-and-differential-signals>

[17] J. Inglis, “Why Object Oriented Programming,” Medium, May 31, 2020. [Online]. Available: <https://medium.com/@jinglis12/why-object-oriented-programming-556d025f1838>

VIII. Appendix

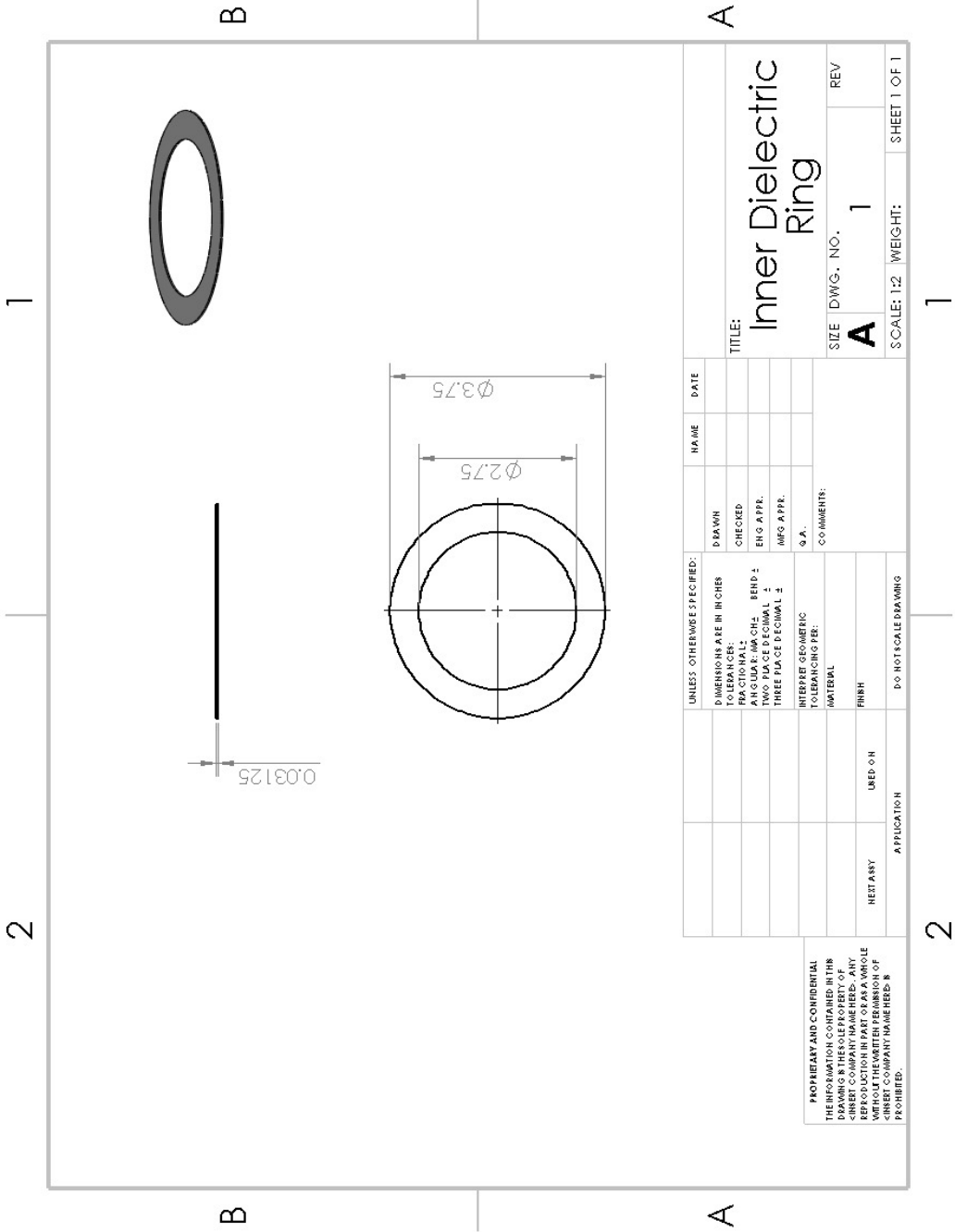
A. Technical Drawings

Technical drawings of the donut are shown below, including outer protective dielectric ring, copper conductive layer, and inner dielectric ring respectively.



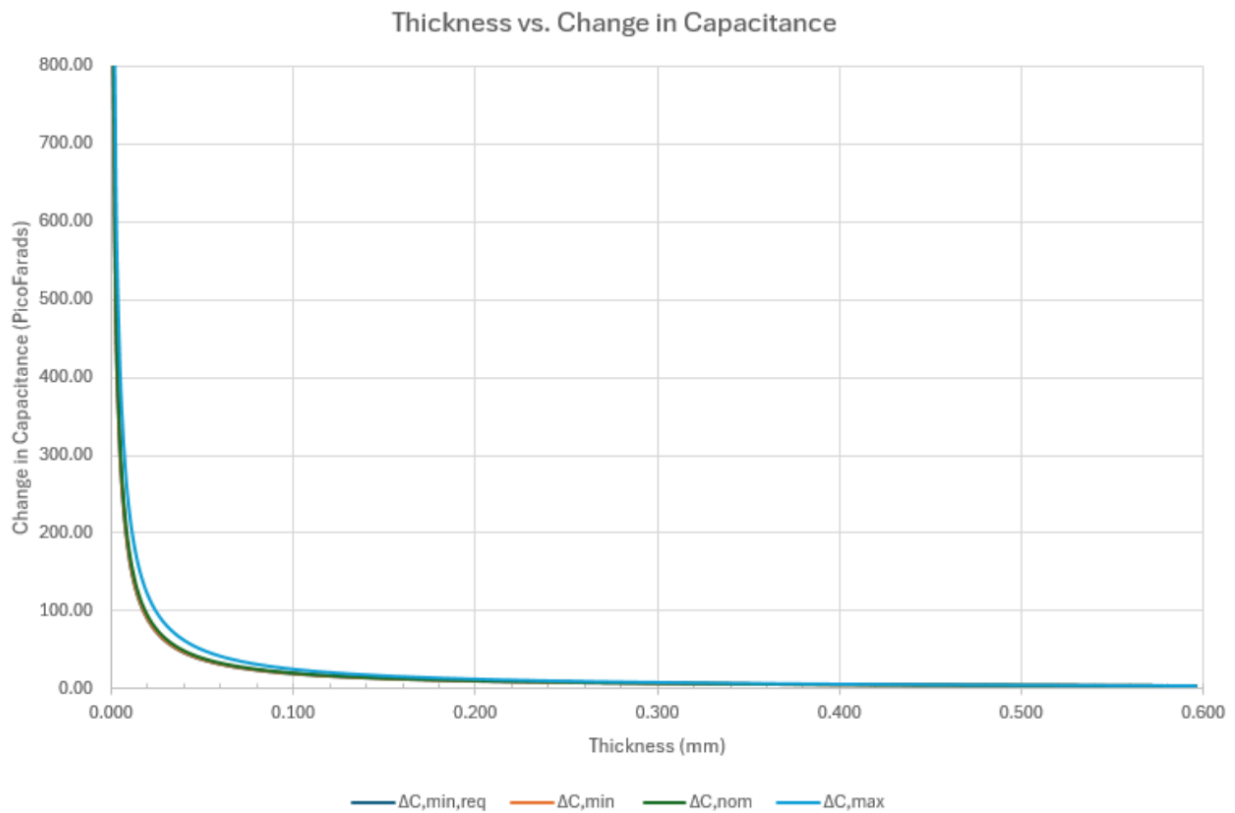
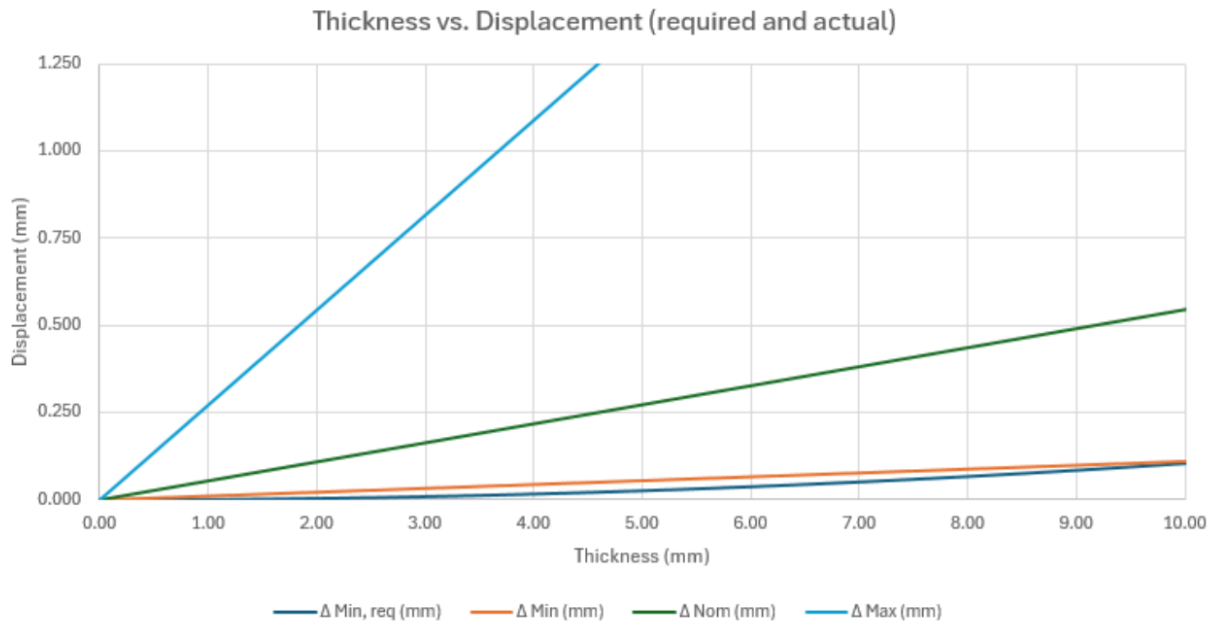
PROPERTIES AND COMMENTS: THE INFORMATION CONTAINED IN THIS DRAWING IS THE PROPERTY OF ROCK SOLID SOLUTIONS. ANY REPRODUCTION OR USE OF THIS DRAWING WITHOUT THE WRITTEN PERMISSION OF ROCK SOLID SOLUTIONS IS STRICTLY PROHIBITED.		UNITS: Q THROUGH SPECIFIED.		DRAWN:	DATE:
DIMENSIONS NOT TO SCALE UNLESS SPECIFIED OTHERWISE	CHECKED:	DATE:	TITLE:	SIZE:	DWG. NO.:
APPROVED:	DATE:	TITLE:	CONDUCTIVE LAYER	A	3
MATERIAL:	PART NUMBER:	DATE:	SCALE:	1:2	WEIGHT:
FINISH:	DATE:	TITLE:	SHEET 1 OF 1	1	1

Inner Dielectric Ring Technical Drawing:



UNLESS OTHERWISE SPECIFIED: DIMENSIONS ARE IN INCHES DECIMALS TO THIRDS FRACTIONS: ANGULAR: MM CHG BEND ± TWO PLACE DECIMAL ± THREE PLACE DECIMAL ± MFG APPR. Q.A. INTERPRET GEOMETRIC TOLERANCING PER: MATERIAL FINISH		DRAWN CHECKED ENG APPR. MFG APPR. Q.A. COMMENTS:	NAME DATE
PROPRIETARY AND CONFIDENTIAL THE INFORMATION CONTAINED IN THIS DRAWING IS THE SOLE PROPERTY OF INHERIT COMPANY NAME HERE. ANY REPRODUCTION OR TRANSMISSION OF THIS INFORMATION WITHOUT THE WRITTEN PERMISSION OF INHERIT COMPANY NAME HERE IS PROHIBITED.		TITLE: Inner Dielectric Ring	SIZE DWG. NO. REV A 1
NEXT ASY USED ON	APPLICATION	SCALE: 1:2 WEIGHT:	SHEET 1 OF 1

B. HDPE Optimization Graphs



C. Team Budget

Team Budget Tracker: [Team F85 Budget Form 25-26.xlsx](#)



Financial Summary
Fall 2025/Spring 2026
Date 4/28/2026

Team Number	85
Team Name	Smart Pick
CFO Name	Graham Walter
CFO e-mail	gwalter@mines.edu
PA Name	Roxann Hayes

Funding	Source	Date	Total
Starting Budget	Capstone	8/25/2025	\$500.00
Additional funds			
Additional funds			
Total Budget			\$500.00
Total Capstone Spend			\$460.52
Total Refunds			\$0.00
Capstone Balance			\$39.48

Total Client Spend \$ -

Instructions:

Enter date, vendor, items, select the purchase method, item cost, and if needed return date and refund amount; formulas will populate other cells

Purchases: enter each receipt as one purchase line item - cost in Column F

Reimbursement: each line should contain the items & total for each reimbursement submission, this can include multiple receipts

Update all costs to match receipts - column F

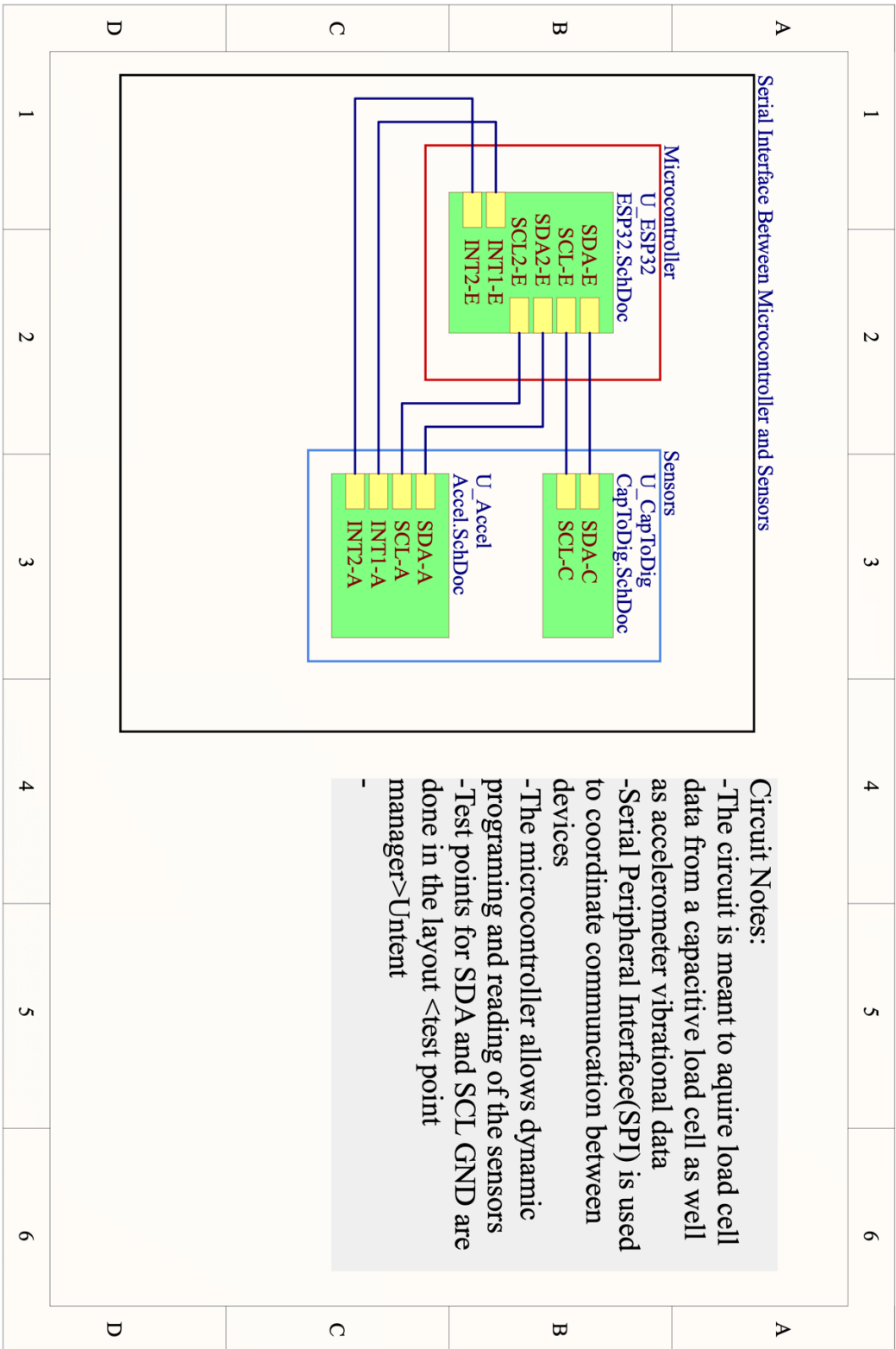
Use Client Purchased when your client provides any materials, enter the estimated cost - column G

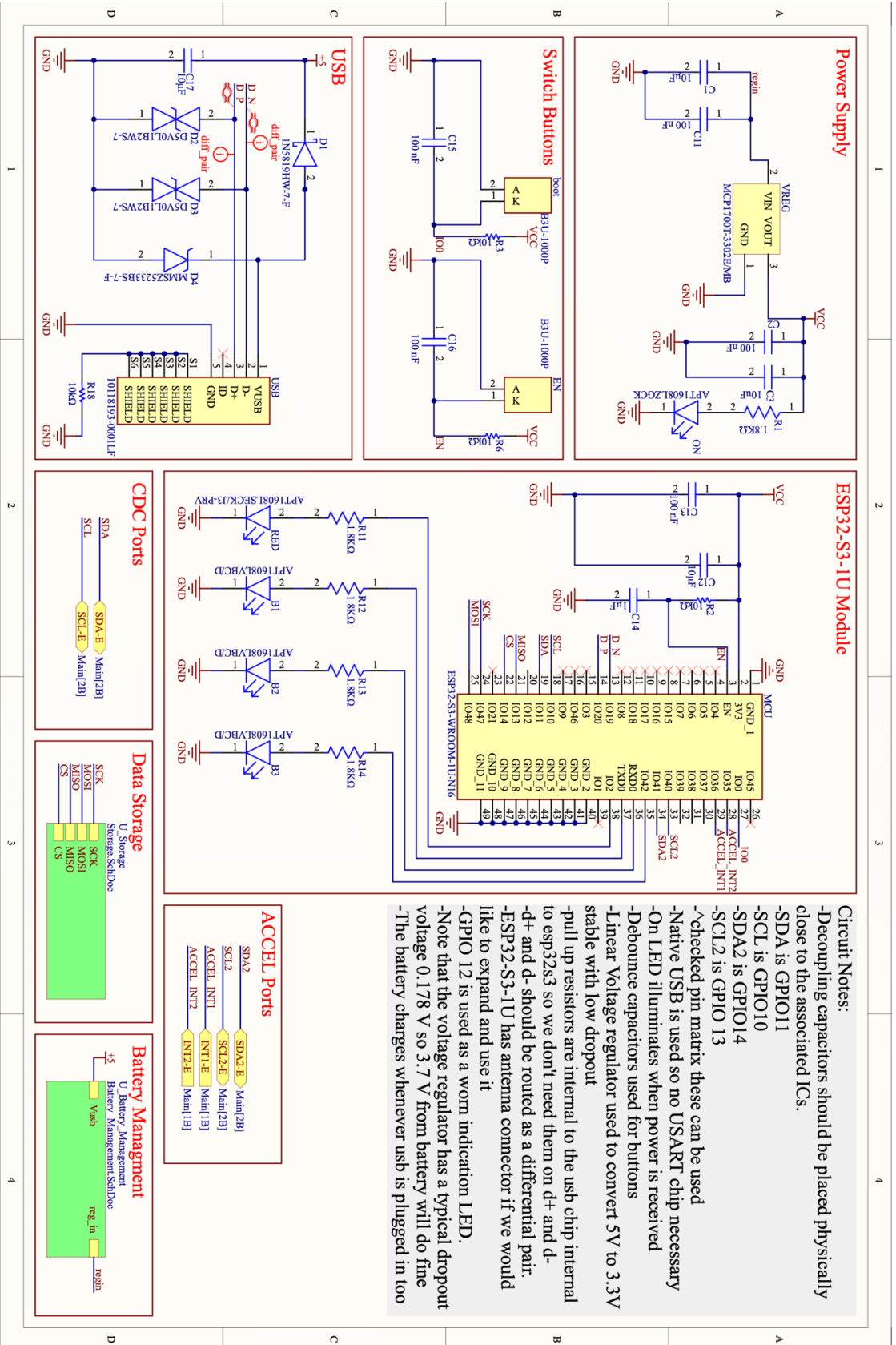
If you need more rows insert rows as needed within the given month, add pull the formula down

September									
Date	Vendor	Items	Purchase Method	Item cost	Client purchases	Capstone purchases	Return Date	Refund Amount	Notes:
					\$ -	\$ -			
					\$ -	\$ -			
					\$ -	\$ -			
					\$ -	\$ -			
September Total Spend:					\$ -	\$ -	September Refunds:	\$0.00	
October									
10/20/2025	McMaster Carr	1/8" HDPE, 1/4" HDPE, 1/8" rubber, 1/4" rubber	Capstone Purchasing	\$ 69.37	\$ -	\$ 69.37			
10/20/2025	DigiKey	CDC Converter, UBS Cable, ESP 32	Capstone Purchasing	\$ 67.66	\$ -	\$ 67.66			
10/30/2025	Home Depot	Copper, Steel, RTV Adhesive	Capstone Purchasing	\$ 63.61	\$ -	\$ 63.61			
					\$ -	\$ -			
					\$ -	\$ -			
					\$ -	\$ -			
					\$ -	\$ -			
October Total Spend:					\$ -	\$ 200.64	October Refund:	\$0.00	

November									
11/13/2025	Amazon	Copper Tape	Capstone Purchasing	\$ 29.88	\$ -	\$ 29.88			
					\$ -	\$ -			
					\$ -	\$ -			
					\$ -	\$ -			
November Total Spend:					\$ -	\$ 29.88	November Refunds:	\$0.00	
December									
					\$ -	\$ -			
					\$ -	\$ -			
					\$ -	\$ -			
					\$ -	\$ -			
December Total Spend:					\$ -	\$ -	December Refunds:	\$0.00	
January									
1/26/2026	Amazon	Electronic Connector	Capstone Purchasing	\$ 9.97	\$ -	\$ 9.97			
					\$ -	\$ -			
					\$ -	\$ -			
					\$ -	\$ -			
January Total Spend:					\$ -	\$ 9.97	January Refunds:	\$0.00	
February									
2/15/2026	PCBWay	Custom Printed Circuit Board	Reimbursement	\$67.71	\$ -	\$ 67.71			
2/13/2026	Amazon	LiPo Battery	Capstone Purchasing	\$ 14.18	\$ -	\$ 14.18			
					\$ -	\$ -			
					\$ -	\$ -			
February Total Spend:					\$ -	\$ 81.89	February Refunds:	\$0.00	
March									
3/5/2026	Amazon	LiPo Battery 4 Pack	Capstone Purchasing	\$ 24.99	\$ -	\$ 24.99			
3/12/2026	Amazon	PEBA Crimping tool and JST connector kit	Capstone Purchasing	\$ 41.79	\$ -	\$ 41.79			
3/12/2026	McMaster Carr	Various thickness HDPE sheets (x4)	Capstone Purchasing	\$ 34.36	\$ -	\$ 34.36			
					\$ -	\$ -			
March Total Spend:					\$ -	\$ 101.14	March Refunds:	\$0.00	
April									
4/28/2026	1Stop Printing	Expo Poster	Capstone Purchasing	\$ 37.00	\$ -	\$ 37.00			

D. Printed Circuit Board Design





Power Supply

ESP32-S3-1U Module

Switch Buttons

CDC Ports

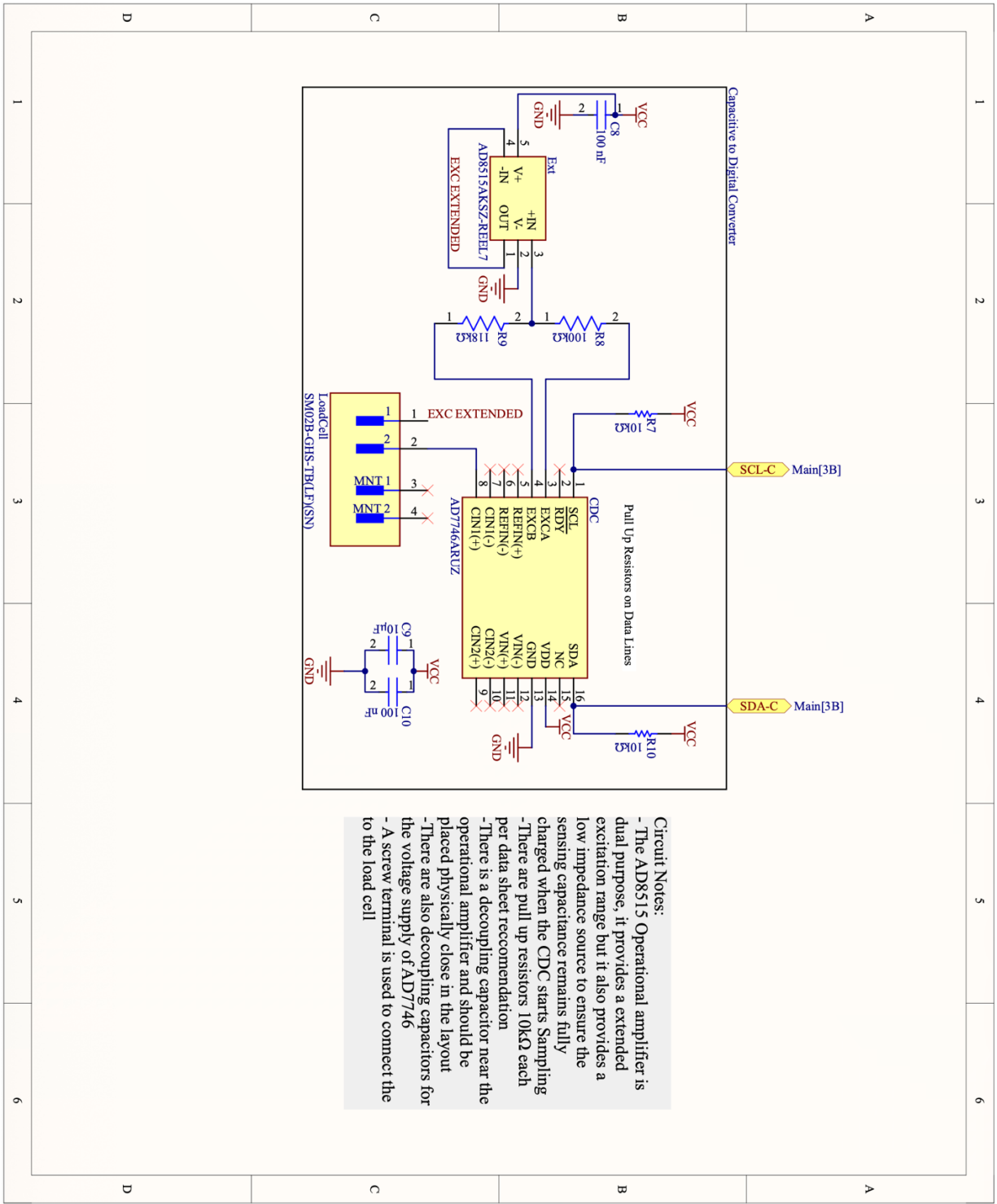
USB

Data Storage

USB

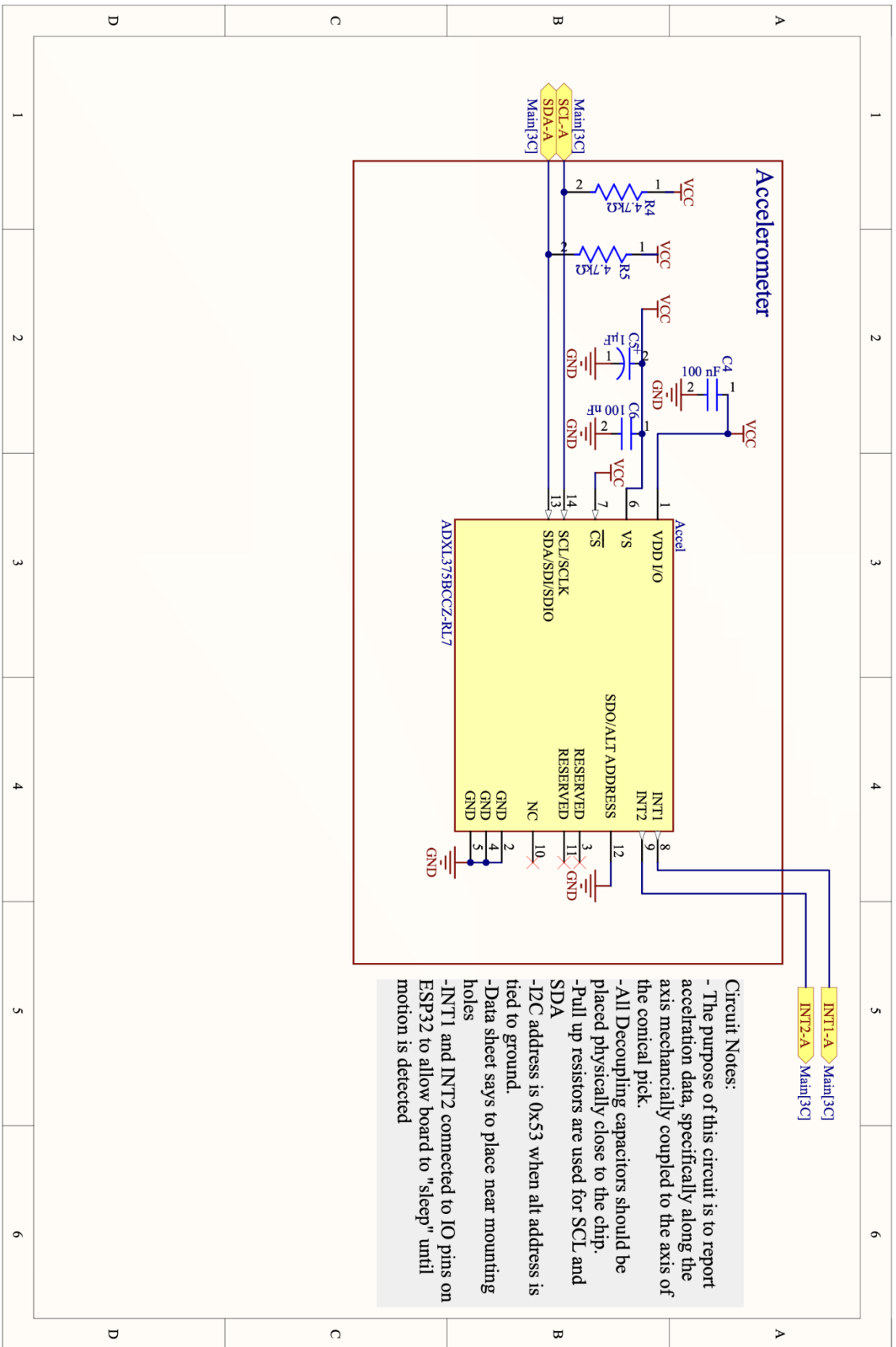
Battery Management

Circuit Notes:
 -Decoupling capacitors should be placed physically close to the associated ICs.
 -SDA is GPIO11
 -SCL is GPIO10
 -SDA2 is GPIO14
 -SCL2 is GPIO13
 -checked pin matrix these can be used
 -Native USB is used so no USART chip necessary
 -On LED illuminates when power is received
 -Debounce capacitors used for buttons
 -Linear Voltage regulator used to convert 5V to 3.3V stable with low dropout
 -pull up resistors are internal to the usb chip internal to esp32s3 so we don't need them on d+ and d- and d- should be routed as a differential pair.
 -ESP32-S3-1U has antenna connector if we would like to expand and use it
 -GPIO 12 is used as a worn indication LED.
 -Note that the voltage regulator has a typical dropout voltage 0.178 V so 3.7 V from battery will do fine
 -The battery charges whenever usb is plugged in too

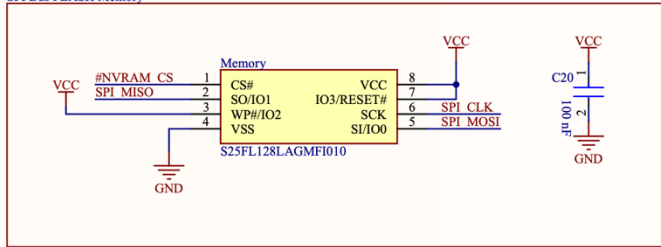


Circuit Notes:

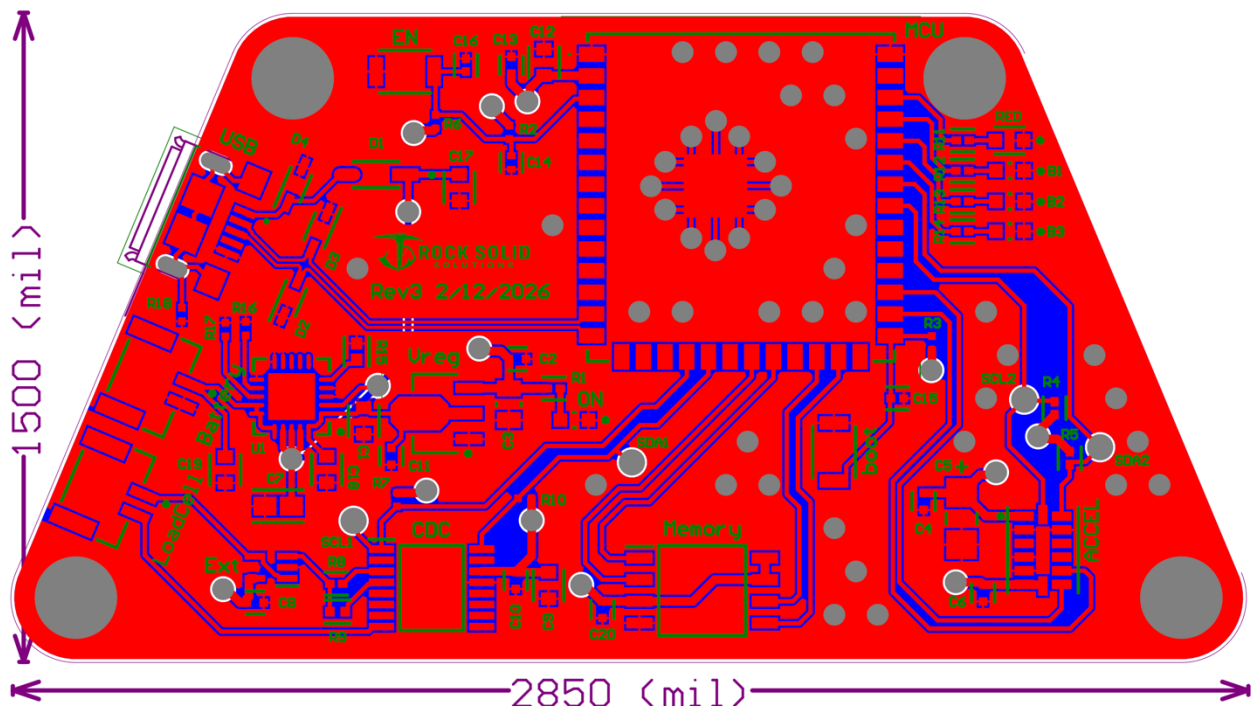
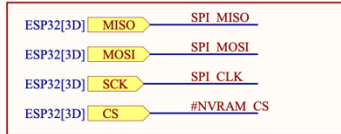
- The AD8515 Operational amplifier is dual purpose, it provides a extended excitation range but it also provides a low impedance source to ensure the sensing capacitance remains fully charged when the CDC starts Sampling
- There are pull up resistors 10kΩ each per data sheet recommendation
- There is a decoupling capacitor near the operational amplifier and should be placed physically close in the layout
- There are also decoupling capacitors for the voltage supply of AD7746
- A screw terminal is used to connect the to the load cell



SPI Bus FLASH Memory



Circuit Notes:
 -16Mbytes = 2.5 hours memory collection capacity @ 1600 bytes/s (800Hz)
 -Place capacitor physically close to the chip



E. Operational/Service Manual

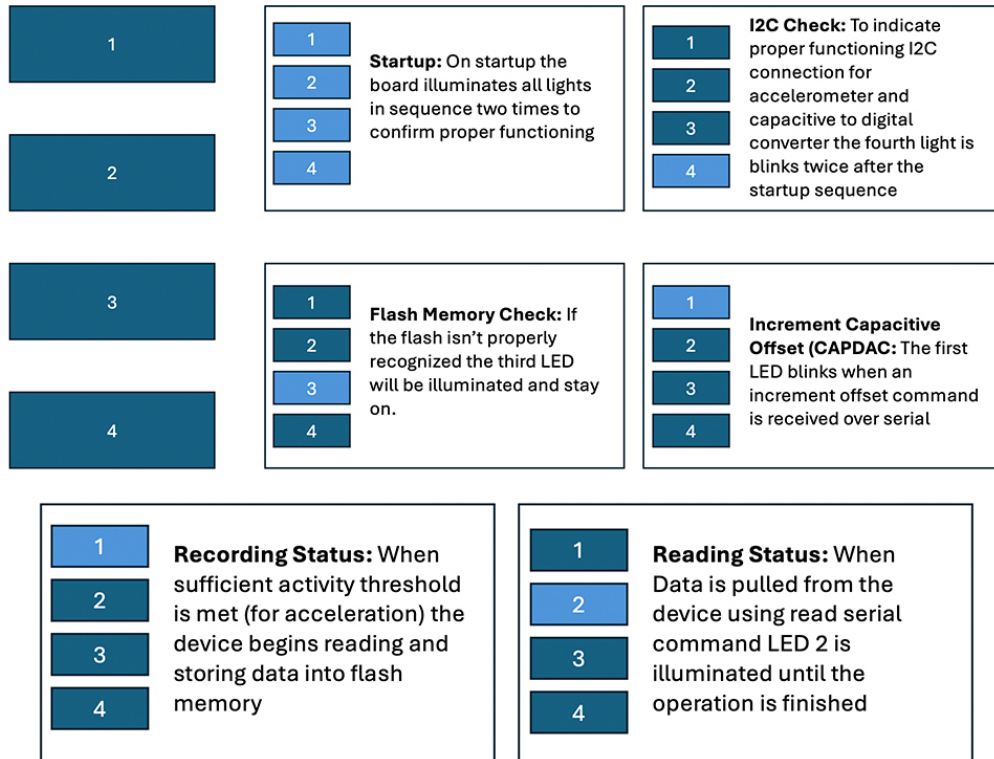
The manual is a separate document entitled “Smart Pick for Rock Mining: Operations and Maintenance Manual.” And is attached to the assignment submission, and a link is provided:

[Operations_Manual.docx](#)

F. LED Interface Guide

The printed circuit board has a limited user interface when operating without a serial connection. To deliver real-time insights about what the board is doing during its operations, an LED interface is designed and illustrated below.

LED Interface Guide

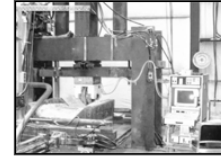


G. LMC & Smartpick Data
 1. Cut 04-7_1-2-8



Earth Mechanics Institute

Mining Engineering Department, CSM

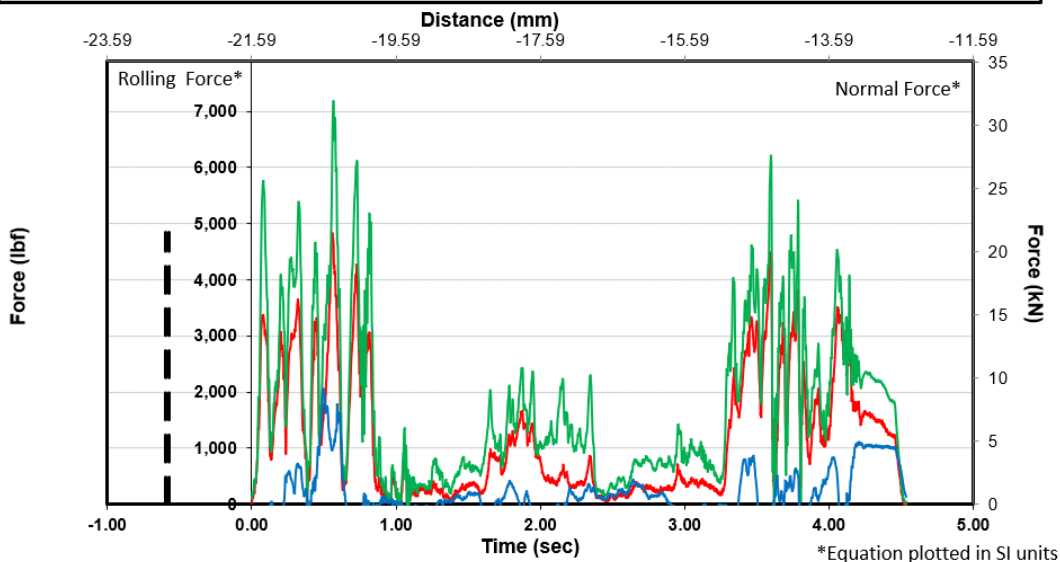
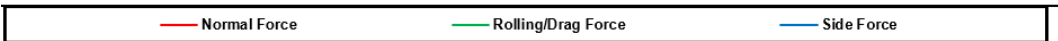


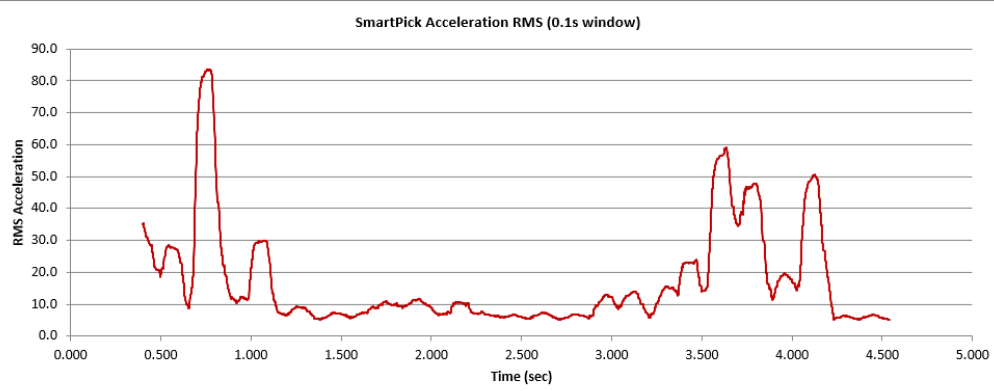
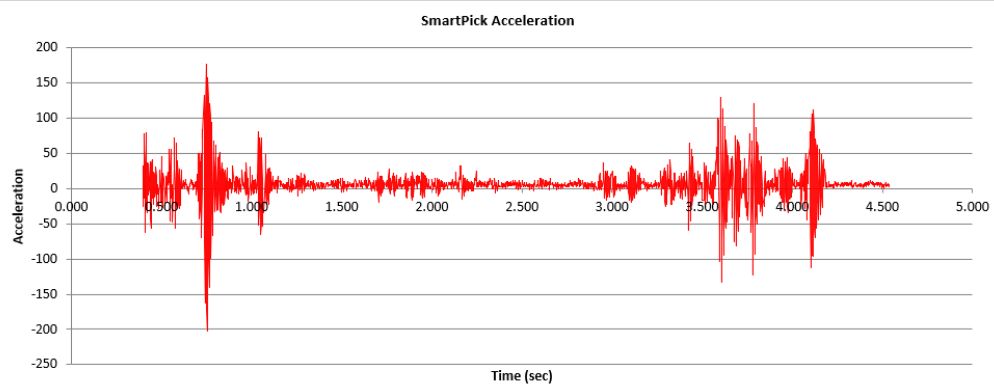
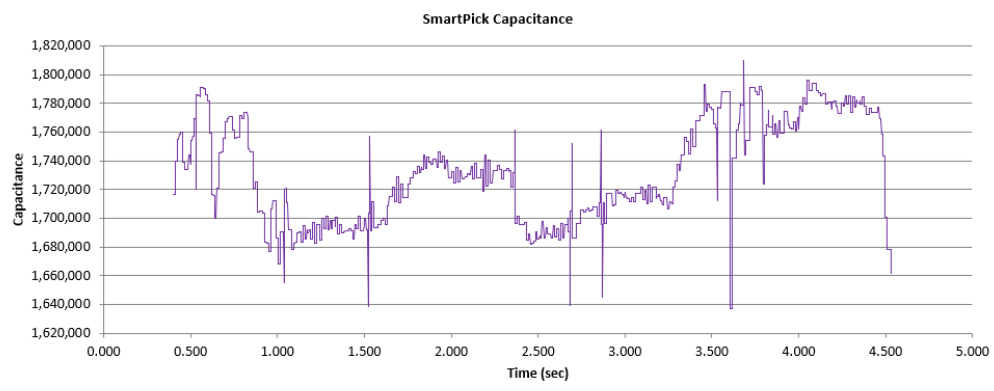
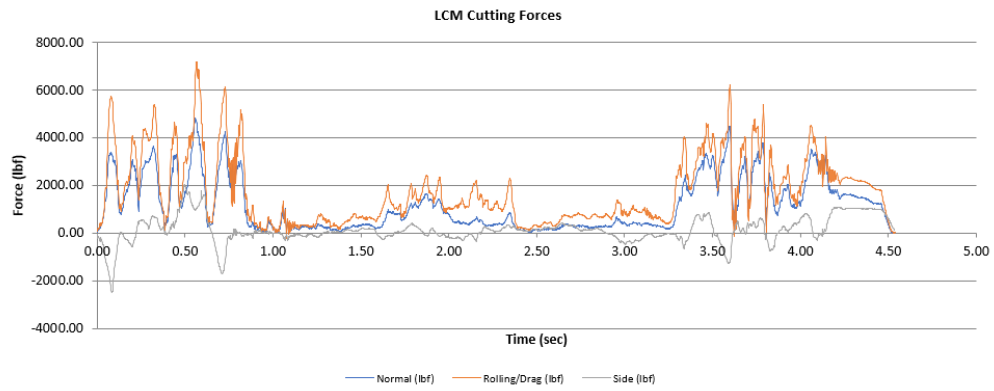
LCM Reduction Program (V 3.1)

Client :	EMI	Date Tested :	04/07/2026
Project :	Smart Pick	Date Reduced :	04/12/2026
Project Location :	Colorado School of Mines	Tested by :	MJ, BB, JR, GW, KP, SM
Calibration File :	Manual Reduction_01_1/7/2021	Reduced by :	MJ

Test Series :	A15	Saddle :	Red Radial
Book No :	1	Target Cutting Speed :	10.0 in/sec
File Name :	04-07_1-2-8.lm.txt	Actual Cutting Speed :	0.0 in/sec
Rock Sample :	Conc-Biochar-Conc		
Rock Source :	CSM	Line Spacing :	4.00 in 102 mm
Cutting Tool :	U92	Penetration :	1.000 in 25.40 mm
Cutting Tool Source :	Kenametal	S/P Ratio :	4.0

		US System (in lbf)	Average	Std. Dev.	Minimum	Maximum
Force Angle:	0	Normal	1250	1230	-9.02	4841
Cutting Coefficient	1.446	Rolling / Drag	1800	1730	-213	7191
Specific	0.885 hp-hr/yd ³	Side	46	644	-2480	2061
Energy	0.868 kWh/m ³					
		SI System (in kN)	Average	Std. Dev.	Minimum	Maximum
Comments :		Normal	5.56	5.47	-0.0401	21.4
		Rolling / Drag	8.01	7.7	-0.947	31.4
		Side	0.205	2.86	-11	9.11





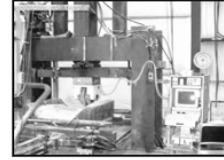
2. Cut 04-7_1-2-7



Earth Mechanics Institute

Mining Engineering Department, CSM

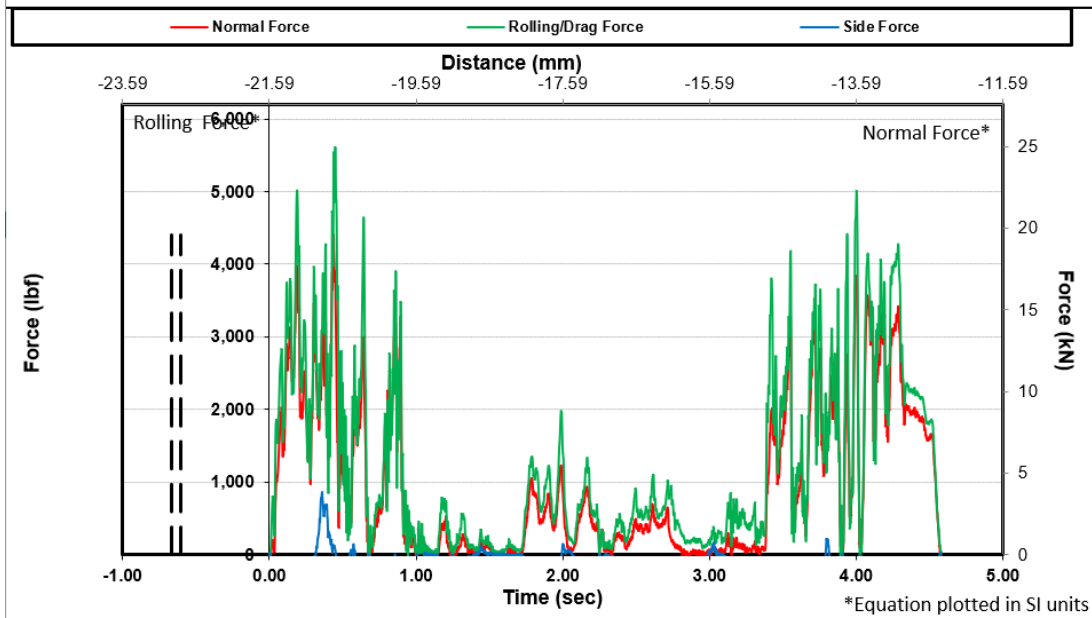
LCM Reduction Program (V 3.1)

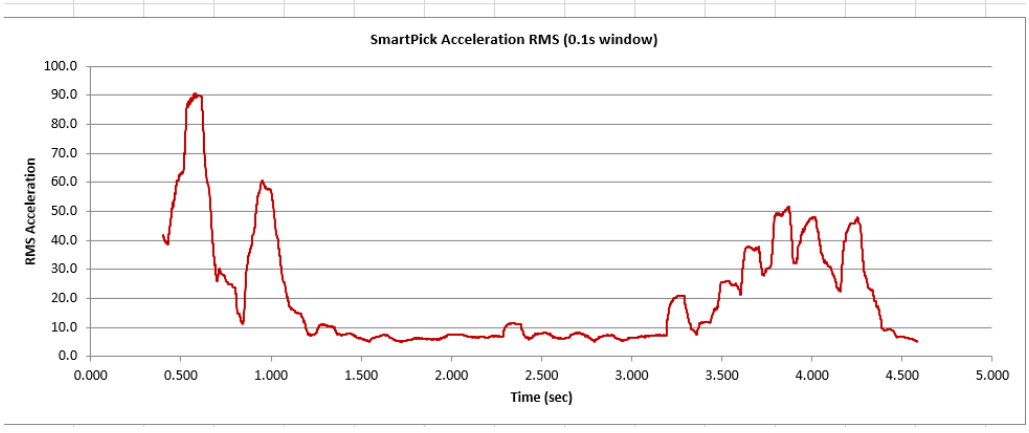
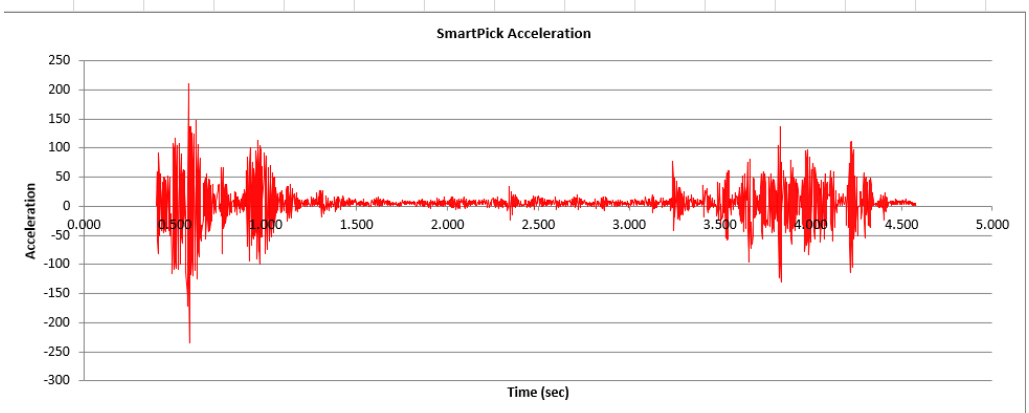
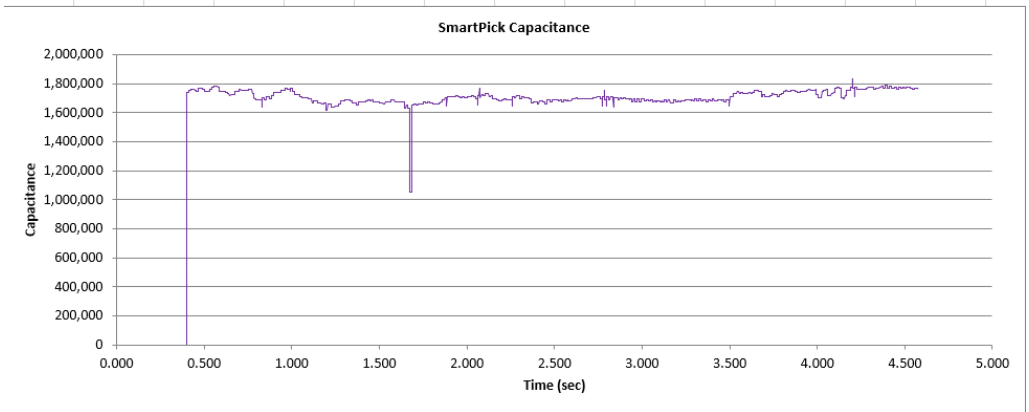
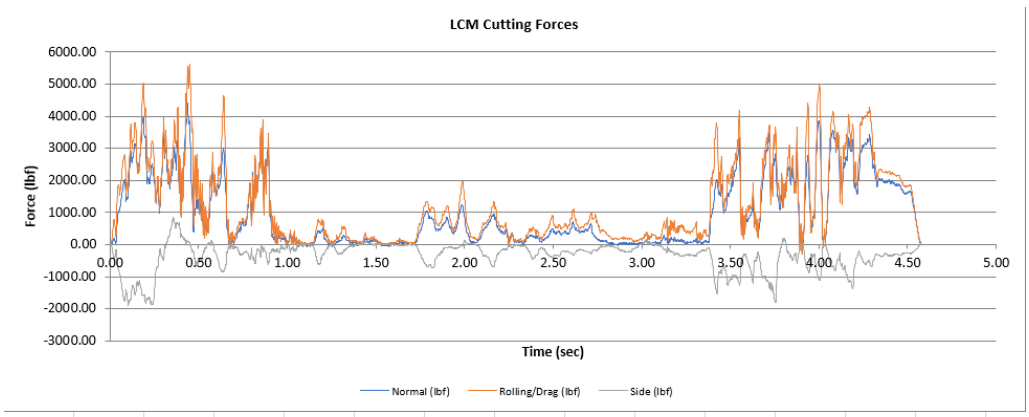


Client : EMI	Date Tested : 04/07/2026
Project : Smart Pick	Date Reduced : 04/12/2026
Project Location : Colorado School of Mines	Tested by : MJ, BB, JR, GW, KP, SM
Calibration File : Manual Reduction_01_1/7/2021	Reduced by : MJ

Test Series : A15	Saddle : Red Radial
Book No : 1	Target Cutting Speed : 10.0 in/sec
File Name : 04-07_1-2-7.lvm	Actual Cutting Speed : 0.0 in/sec
Rock Sample : Conc-Biochar-Conc	
Rock Source : CSM	Line Spacing : 4.00 in 102 mm
Cutting Tool : U92	Penetration : 1.000 25.40
Cutting Tool Source : Kenametal	S/P Ratio : 4.0

		US System (in lbf)	Average	Std. Dev.	Minimum	Maximum
Force Angle:	0					
Cutting Coefficient	1.253	Normal	963	1110	-67.2	4410
Specific	0.592 $hp-hr/yd^3$	Rolling / Drag	1210	1320	-69	5610
Energy	0.581 kWh/m^3	Side	-290	517	-1900	851
		SI System (in kN)	Average	Std. Dev.	Minimum	Maximum
		Normal	4.28	4.94	-0.299	19.6
		Rolling / Drag	5.38	5.87	-0.307	25
		Side	-1.29	2.3	-8.45	3.79
Comments :						





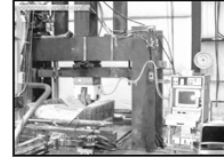
3. Cut 04-7_1-2-6



Earth Mechanics Institute

Mining Engineering Department, CSM

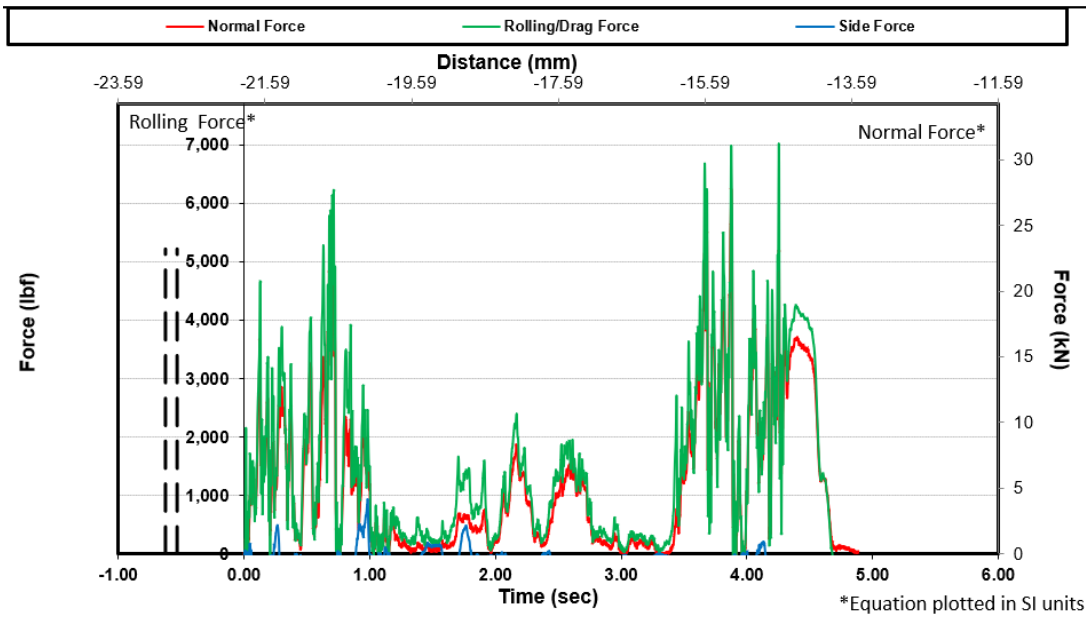
LCM Reduction Program (V 3.1)

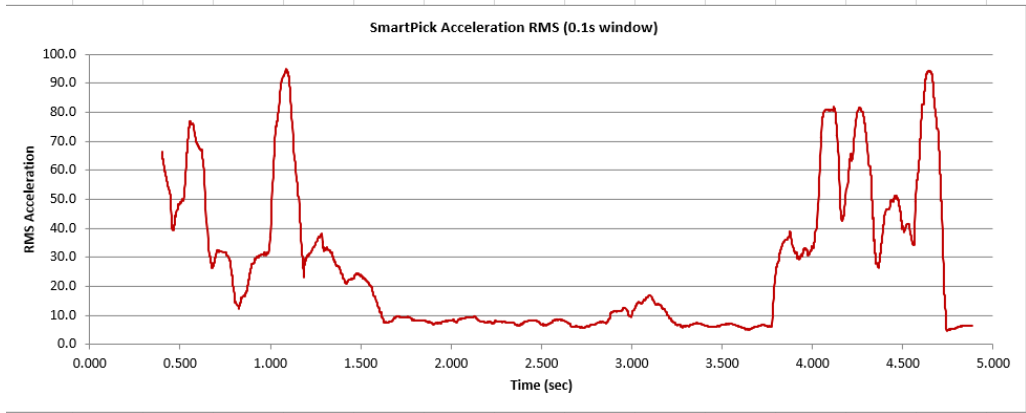
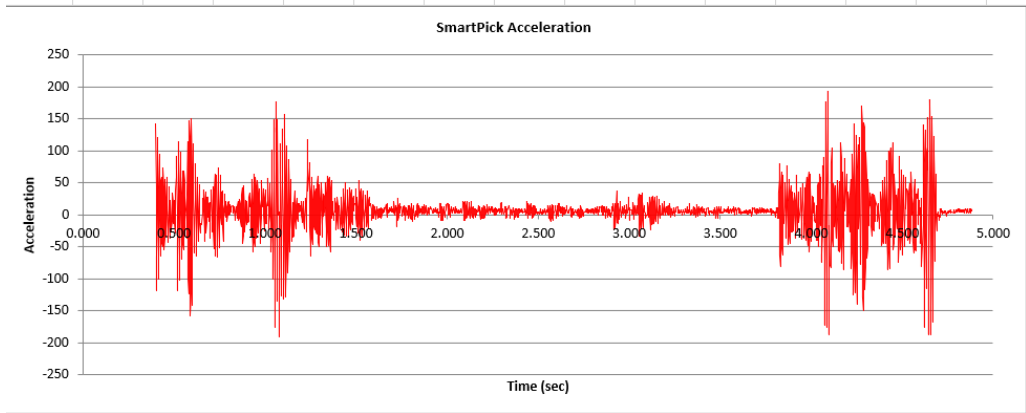
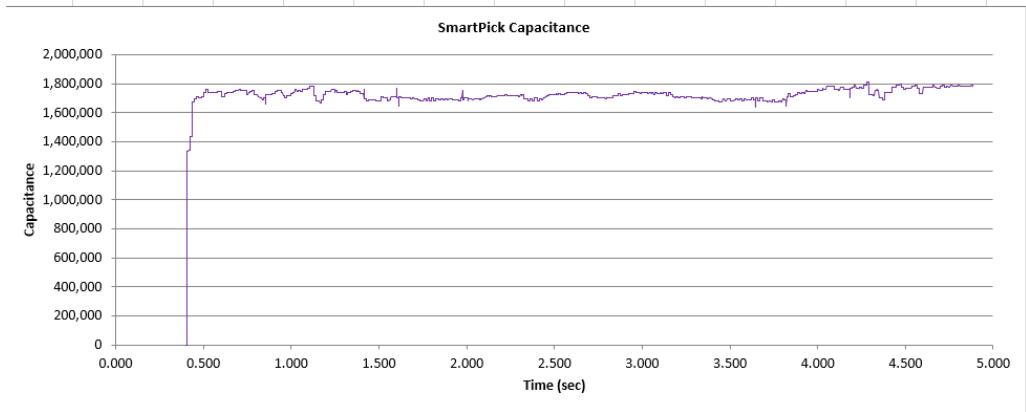
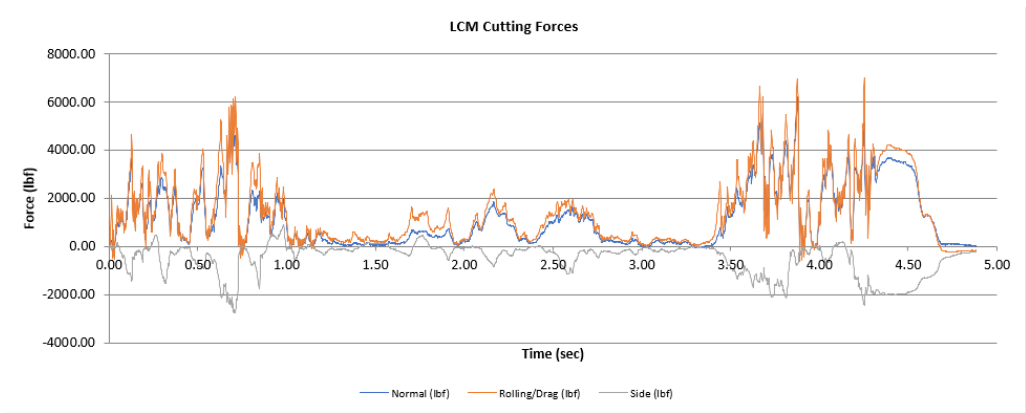


Client : EMI	Date Tested : 04/07/2026
Project : Smart Pick	Date Reduced : 04/12/2026
Project Location : Colorado School of Mines	Tested by : MJ, BB, JR, GW, KP, SM
Calibration File : Manual Reduction_01_1/7/2021	Reduced by : MJ

Test Series : A15	Saddle : Red Radial
Book No : 1	Target Cutting Speed : 10.0 in/sec
File Name : 04-07_1-2-6.lvm	Actual Cutting Speed : -0.1 in/sec
Rock Sample : Conc-Biochar-Conc	
Rock Source : CSM	Line Spacing : 4.00 in 102 mm
Cutting Tool : U92	Penetration : 1.000 25.40
Cutting Tool Source : Kenametal	S/P Ratio : 4.0

Force Angle:	0	US System (in lbf)	Average	Std. Dev.	Minimum	Maximum
Cutting Coefficient	1.313	Normal	984	1040	-200	5220
Specific	0.634 $hp-hr/yd^3$	Rolling / Drag	1290	1260	-512	6220
Energy	0.622 kWh/m^3	Side	-318	611	-2730	930
		SI System (in kN)	Average	Std. Dev.	Minimum	Maximum
Comments :		Normal	4.38	4.63	-0.89	23.2
		Rolling / Drag	5.74	5.6	-2.28	27.7
		Side	-1.41	2.72	-12.1	4.14





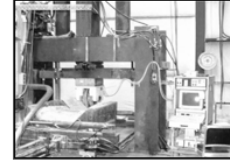
4. Cut 04-7_1-2-5



Earth Mechanics Institute

Mining Engineering Department, CSM

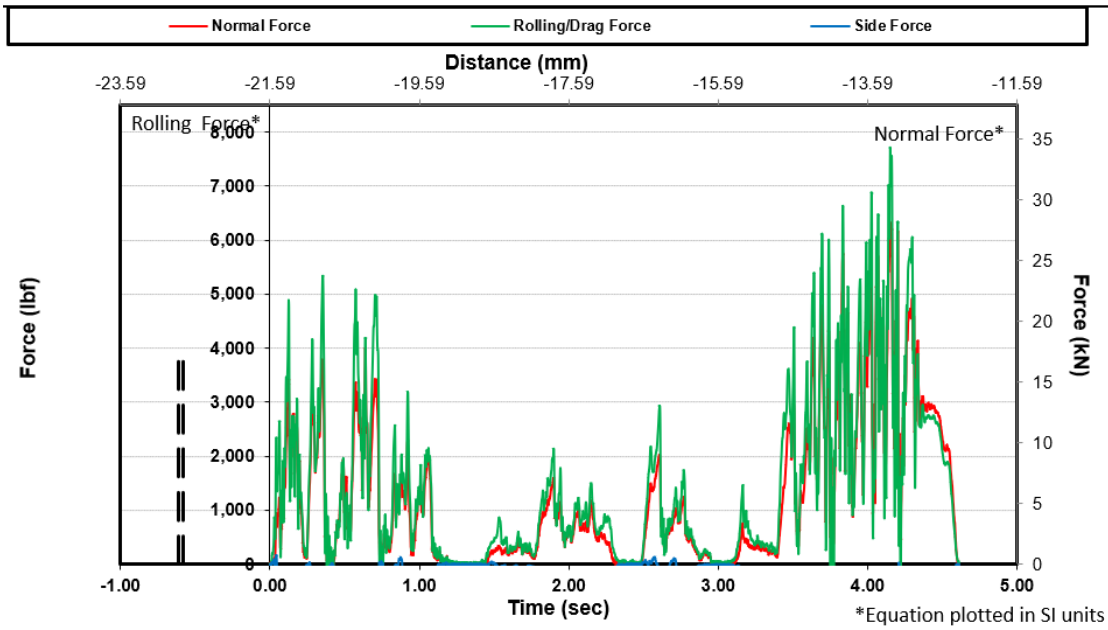
LCM Reduction Program (V 3.1)

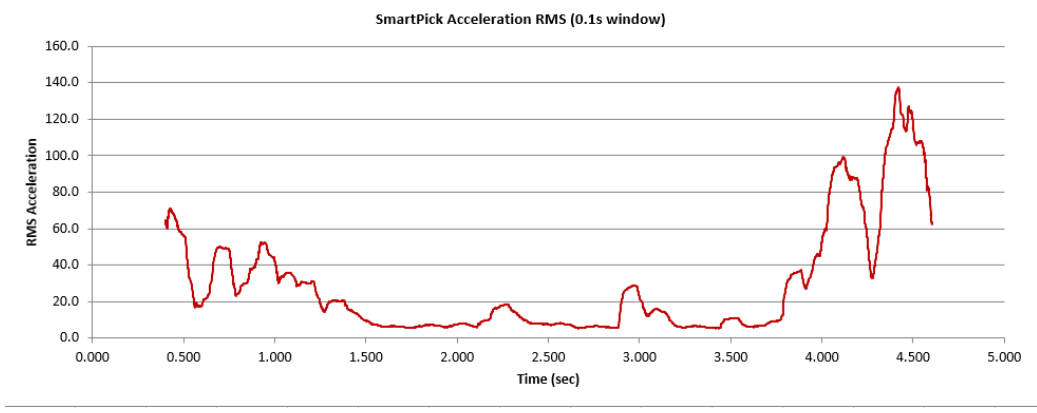
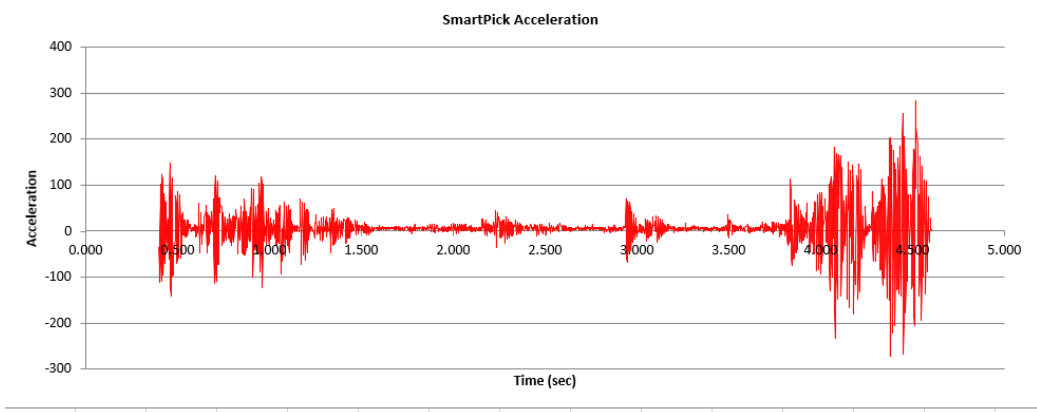
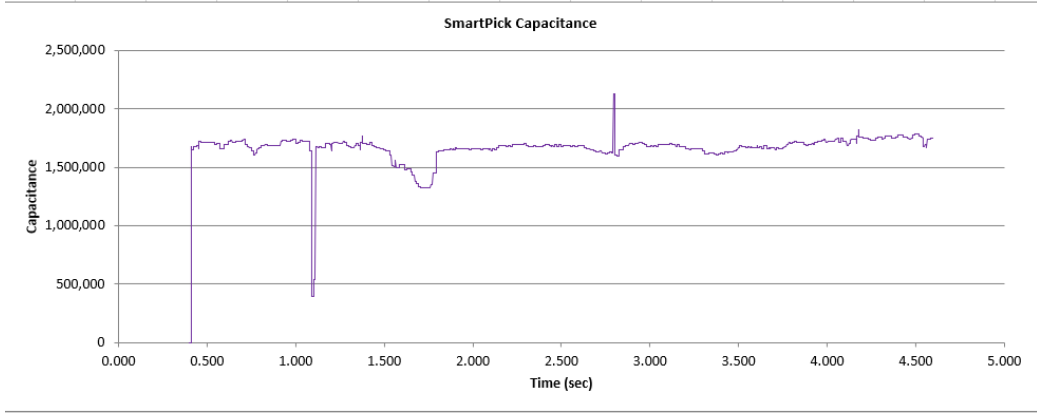
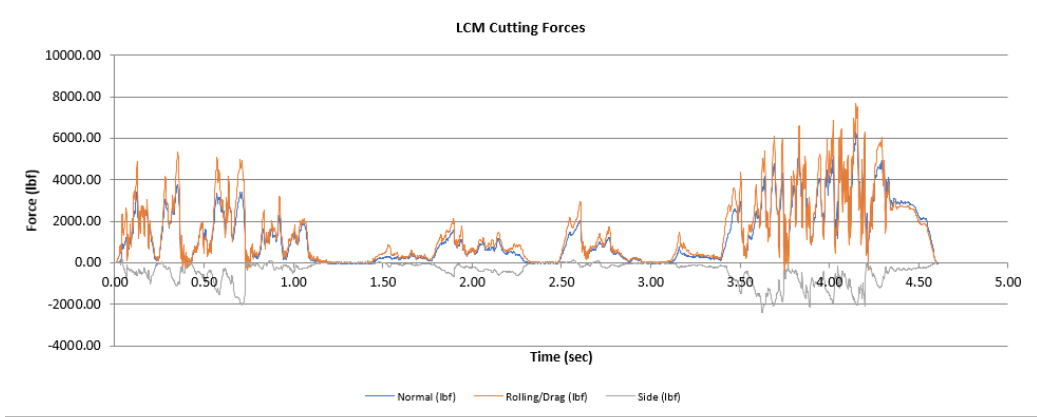


Client : EMI	Date Tested : 04/07/2026
Project : Smart Pick	Date Reduced : 04/12/2026
Project Location : Colorado School of Mines	Tested by : MJ, BB, JR, GW, KP, SM
Calibration File : Manual Reduction_01_1/7/2021	Reduced by : MJ

Test Series : A15	Saddle : Red Radial
Book No : 1	Target Cutting Speed : 10.0 in/sec
File Name : 04-07_1-2-5.lvm	Actual Cutting Speed : 0.0 in/sec
Rock Sample : Conc-Biochar-Conc	Line Spacing : 4.00 in 102 mm
Rock Source : CSM	Penetration : 1.000 25.40
Cutting Tool : U92	S/P Ratio : 4.0
Cutting Tool Source : Kenametal	

Force Angle:	0	US System (in lbf)	Average	Std. Dev.	Minimum	Maximum
Cutting Coefficient	1.253	Normal	906	994	-73.4	4000
Specific	0.557 $hp-hr/yd^3$	Rolling / Drag	1140	1240	-335	5330
Energy	0.547 kWh/m^3	Side	-286	414	-2040	168
		SI System (in kN)	Average	Std. Dev.	Minimum	Maximum
Comments :		Normal	4.03	4.42	-0.326	17.8
		Rolling / Drag	5.07	5.52	-1.49	23.7
		Side	-1.27	1.84	-9.07	0.747





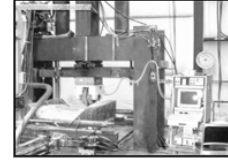
5. Cut 04-7_1-2-4



Earth Mechanics Institute

Mining Engineering Department, CSM

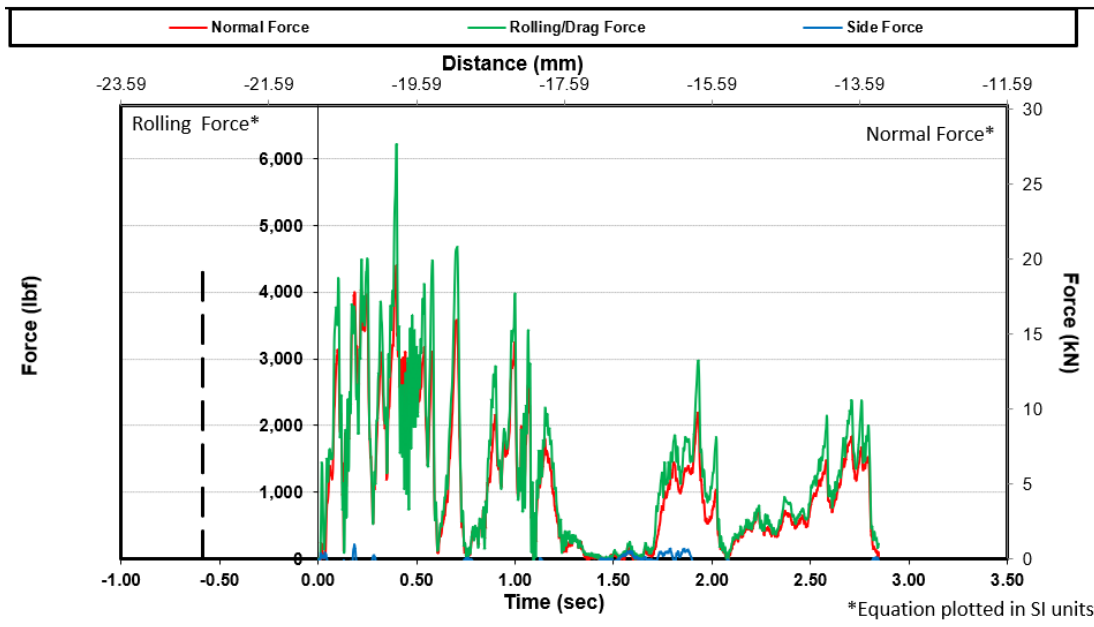
LCM Reduction Program (V 3.1)

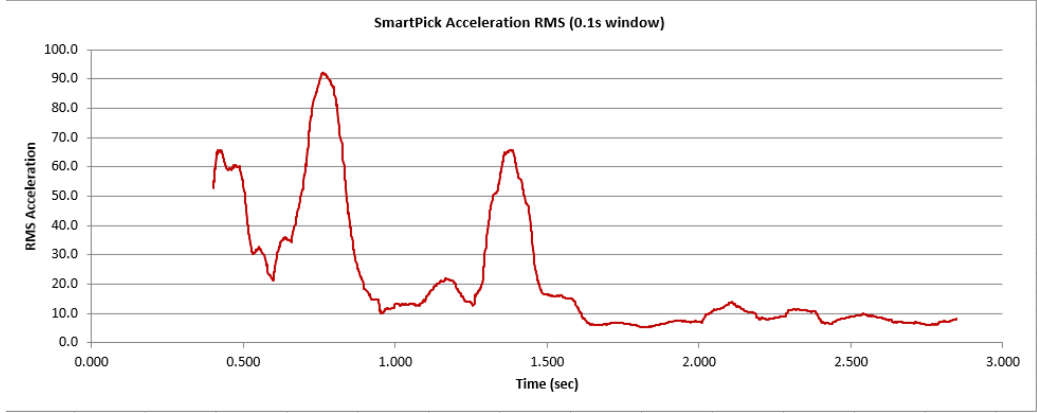
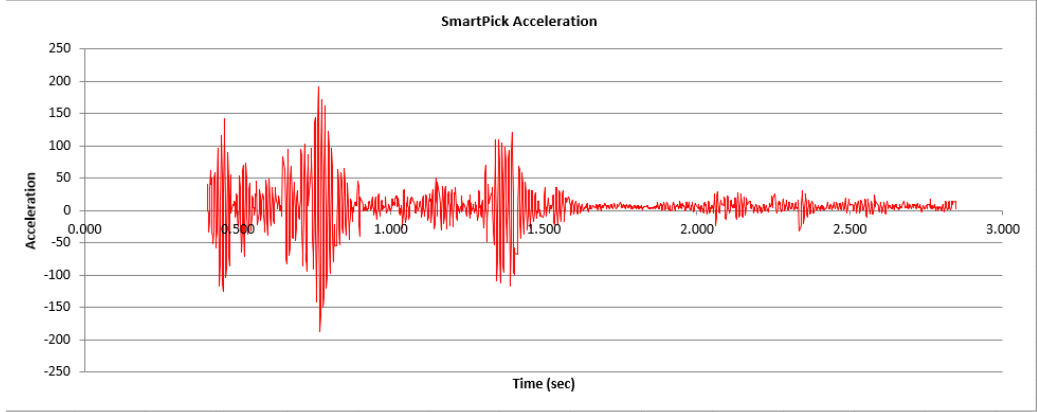
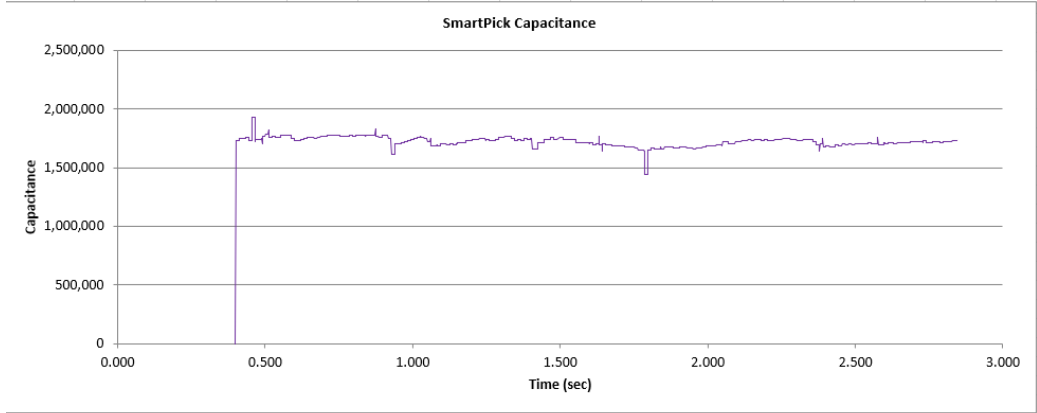
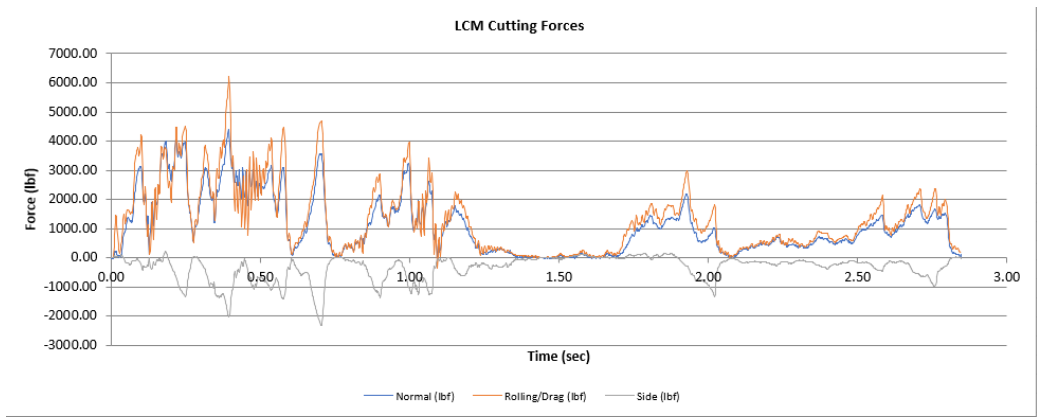


Client : EMI	Date Tested : 04/07/2026
Project : Smart Pick	Date Reduced : 04/12/2026
Project Location : Colorado School of Mines	Tested by : MJ, BB, JR, GW, KP, SM
Calibration File : Manual Reduction_01_1/7/2021	Reduced by : MJ

Test Series : A15	Saddle : Red Radial
Book No : 1	Target Cutting Speed : 10.0 in/sec
File Name : 04-07_1-2-4.lvm	Actual Cutting Speed : 0.0 in/sec
Rock Sample : Conc-Biochar-Conc	Line Spacing : 4.00 in 102 mm
Rock Source : CSM	Penetration : 1.000 25.40
Cutting Tool : U92	S/P Ratio : 4.0
Cutting Tool Source : Kenametal	

		US System (in lbf)	Average	Std. Dev.	Minimum	Maximum
Force Angle:	0	Normal	1250	1160	-37.9	4400
Cutting Coefficient	1.161	Rolling / Drag	1450	1350	-357	6210
Specific	0.713 hp-hr/yd ³	Side	-401	482	-2330	224
Energy	0.699 kWh/m ³					
		SI System (in kN)	Average	Std. Dev.	Minimum	Maximum
Comments :		Normal	5.56	5.16	-0.169	19.6
		Rolling / Drag	6.45	6.01	-1.59	27.6
		Side	-1.78	2.14	-10.4	0.996





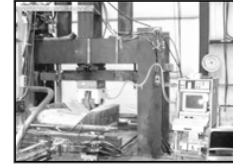
6. Cut 04-7_1-2-3



Earth Mechanics Institute

Mining Engineering Department, CSM

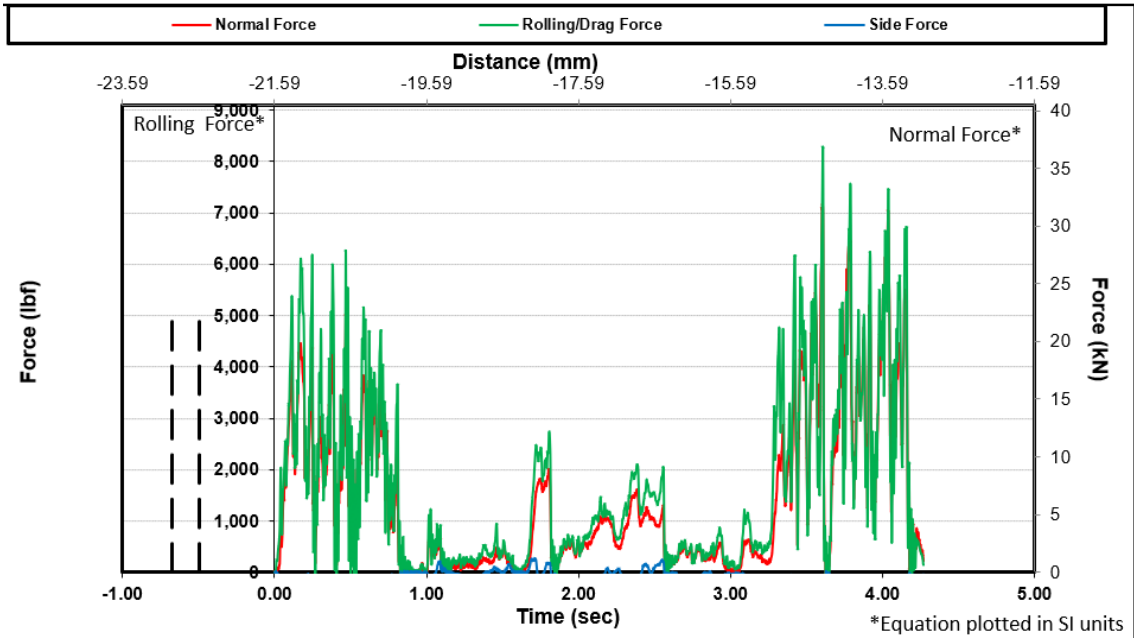
LCM Reduction Program (V 3.1)

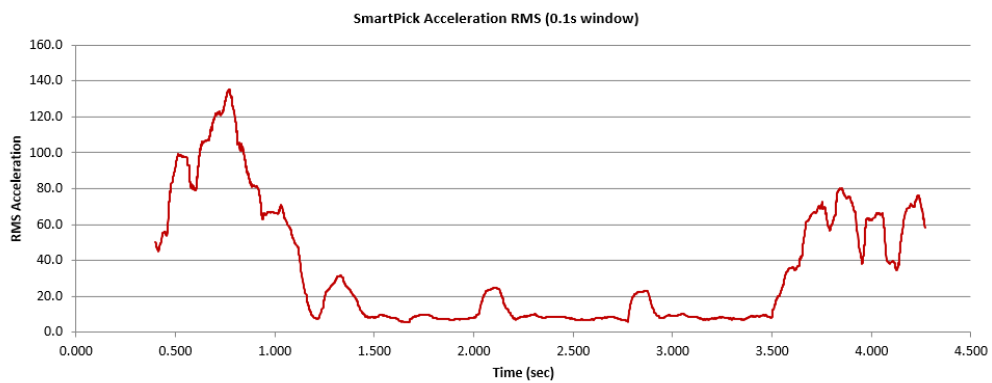
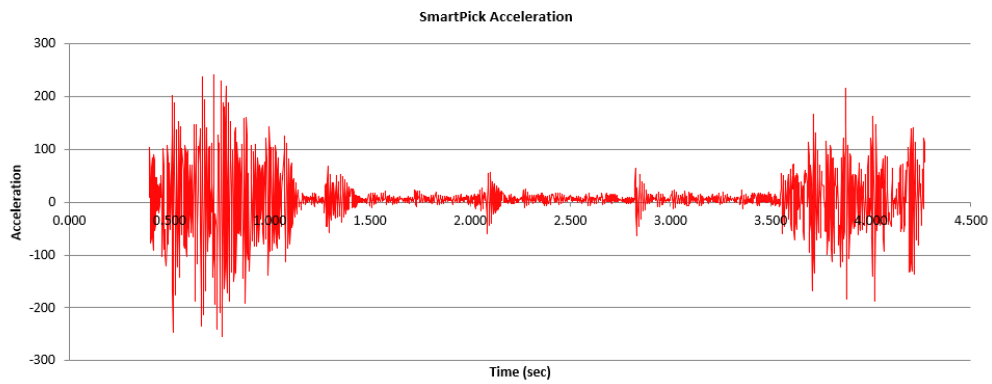
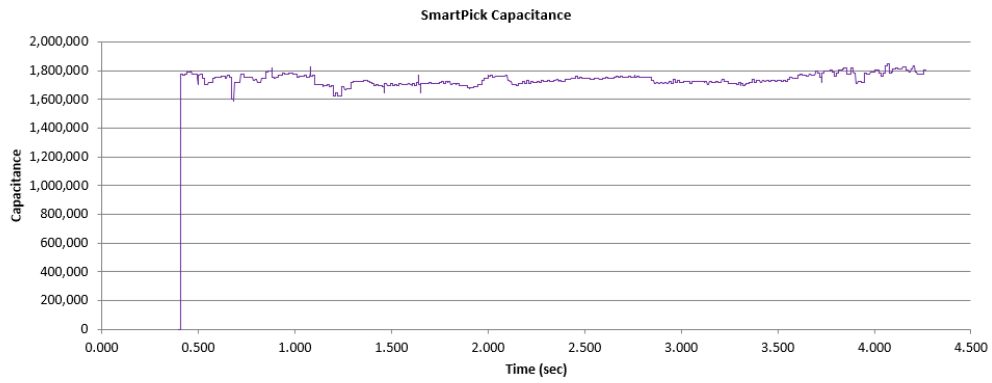
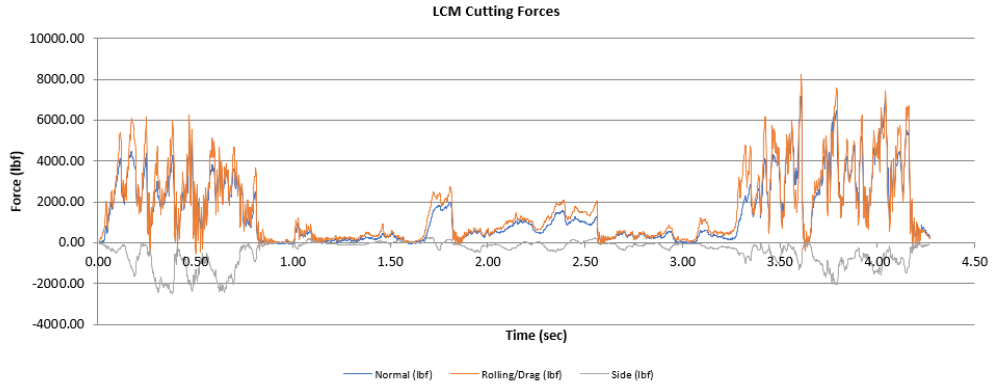


Client :	EMI	Date Tested :	04/07/2026
Project :	Smart Pick	Date Reduced :	04/12/2026
Project Location :	Colorado School of Mines	Tested by :	MJ,BB,JR,GW,KP,SM
Calibration File :	Mannual Reduction_01_1/7/2021	Reduced by :	MJ

Test Series :	A15	Saddle :	Red Radial
Book No :	1	Target Cutting Speed :	10.0 in/sec
File Name :	04-07_1-2-3.lvm	Actual Cutting Speed :	-0.1 in/sec
Rock Sample :	Conc-Biochar-Conc	Line Spacing :	4.00 in 102 mm
Rock Source :	CSM	Penetration :	1.000 25.40
Cutting Tool :	U92	S/P Ratio :	4.0
Cutting Tool Source :	Kenametal		

Force Angle :	0	US System (in lbf)	Average	Std. Dev.	Minimum	Maximum
Cutting Coefficient	1.214	Normal	1190	1290	-80.9	4990
Specific	0.707 <i>hp-hr/yd³</i>	Rolling / Drag	1440	1570	-653	6260
Energy	0.694 <i>kWh/m³</i>	Side	-490	738	-2460	271
		SI System (in kN)	Average	Std. Dev.	Minimum	Maximum
Comments :		Normal	5.29	5.74	-0.36	22.2
		Rolling / Drag	6.41	6.98	-2.9	27.8
		Side	-2.18	3.28	-10.9	1.21





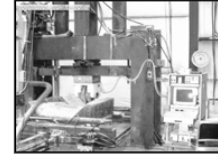
7. Cut 04-7_1-1-3



Earth Mechanics Institute

Mining Engineering Department, CSM

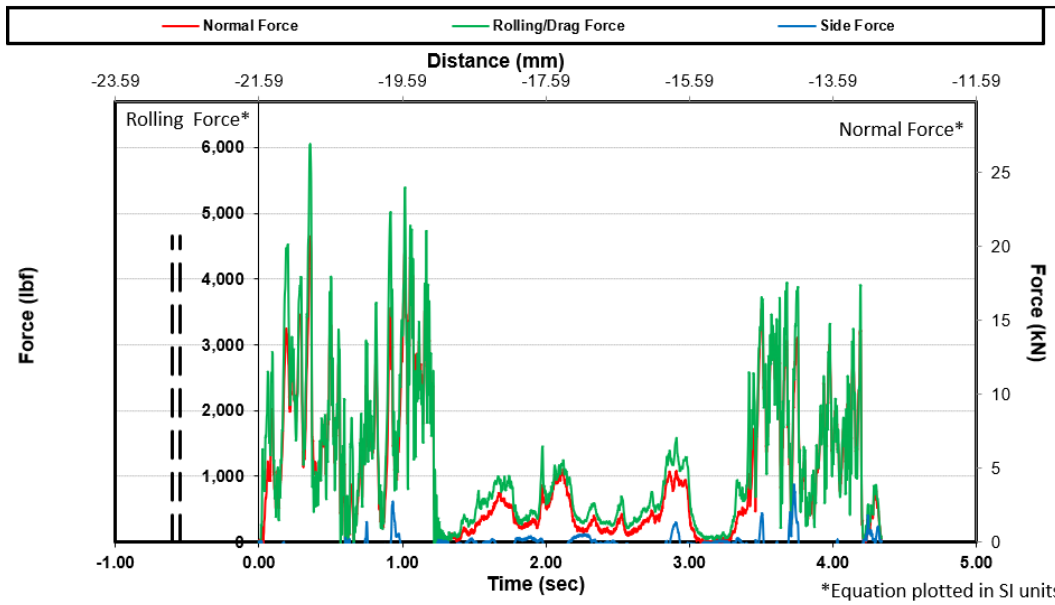
LCM Reduction Program (V 3.1)

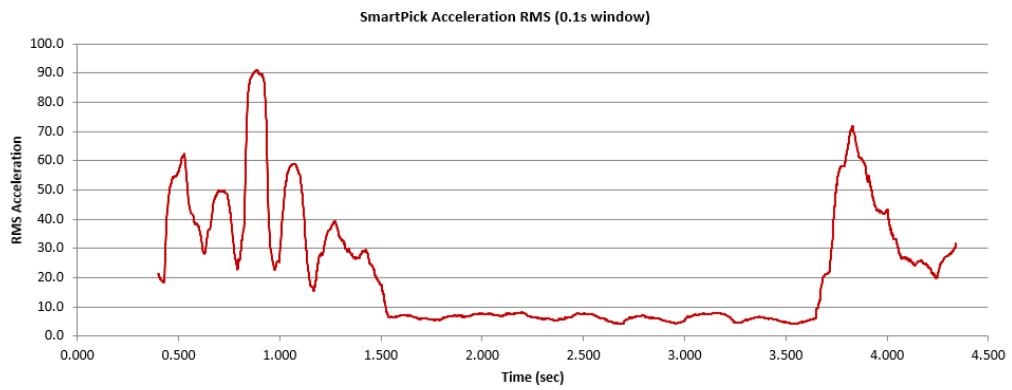
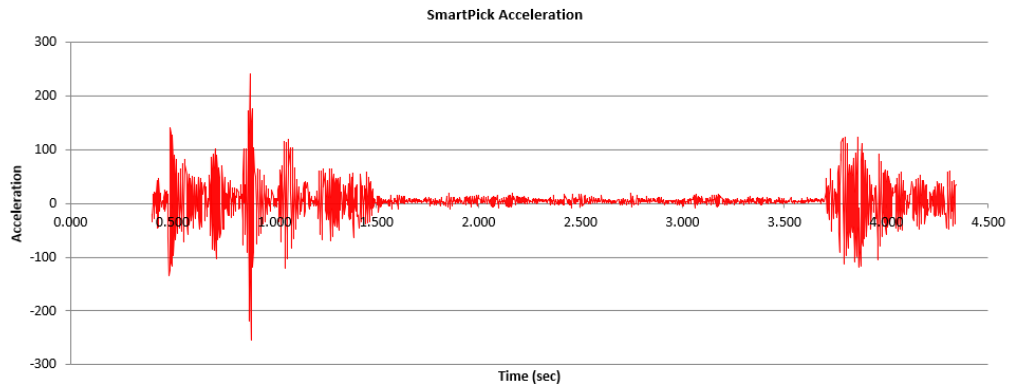
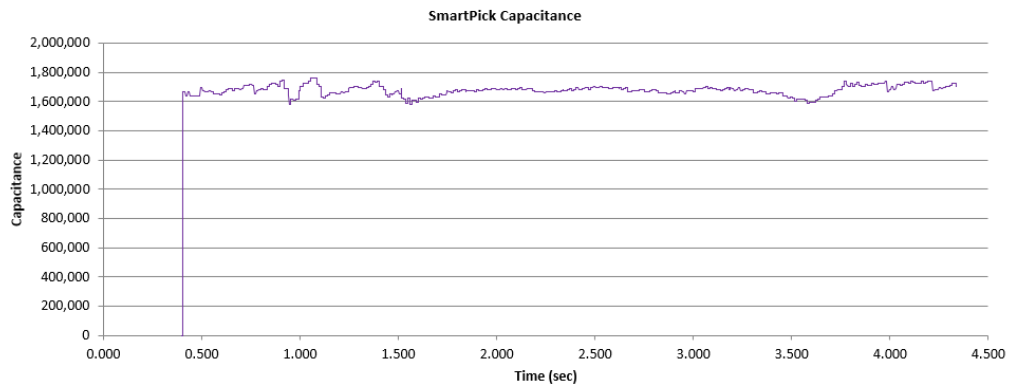
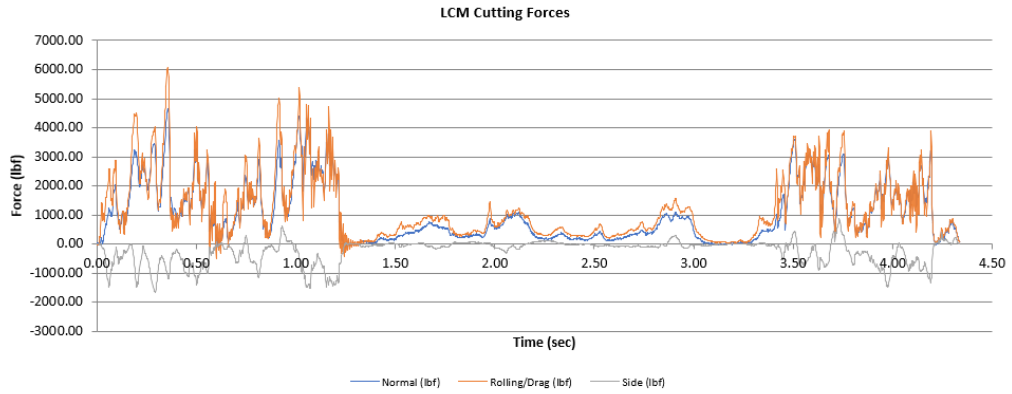


Client : EMI	Date Tested : 04/07/2026
Project : Smart Pick	Date Reduced : 04/12/2026
Project Location : Colorado School of Mines	Tested by : MJ,BB,JR,GW,KP,SM
Calibration File : Manual Reduction_01_1/7/2021	Reduced by : MJ

Test Series : A15	Saddle : Red Radial
Book No : 1	Target Cutting Speed : 10.0 in/sec
File Name : Test_1-1-3.lm	Actual Cutting Speed : 0.0 in/sec
Rock Sample : Conc-Biochar-Conc	in mm
Rock Source : CSM	Line Spacing : 4.00 102
Cutting Tool : U92	Penetration : 1.000 25.40
Cutting Tool Source : Kenametal	S/P Ratio : 4.0

Force Angle:	0	US System (in lbf)	Average	Std. Dev.	Minimum	Maximum
Cutting Coefficient	1.162	Normal	1330	1150	-136	4650
Specific	0.761 hp-hr/yd ³	Rolling / Drag	1550	1300	-488	6060
Energy	0.747 kWh/m ³	Side	-399	462	-1680	620
Comments :		SI System (in kN)	Average	Std. Dev.	Minimum	Maximum
		Normal	5.92	5.12	-0.605	20.7
		Rolling / Drag	6.89	5.78	-2.17	27
		Side	-1.77	2.06	-7.47	2.76





8. Cut 04-7_1-1-2



Earth Mechanics Institute

Mining Engineering Department, CSM

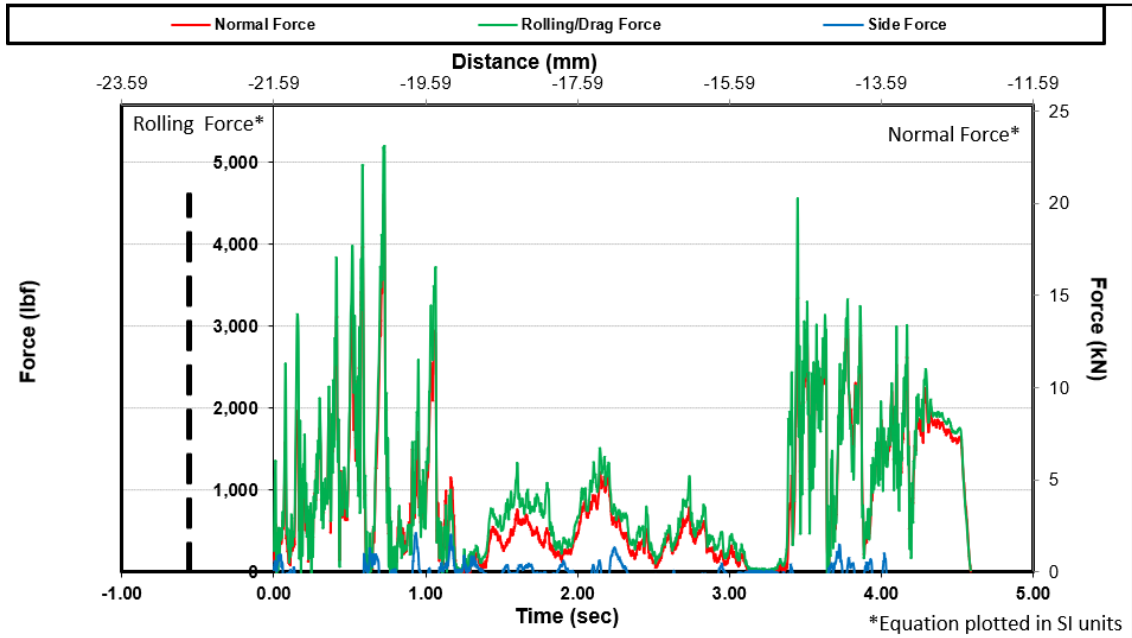
LCM Reduction Program (V 3.1)

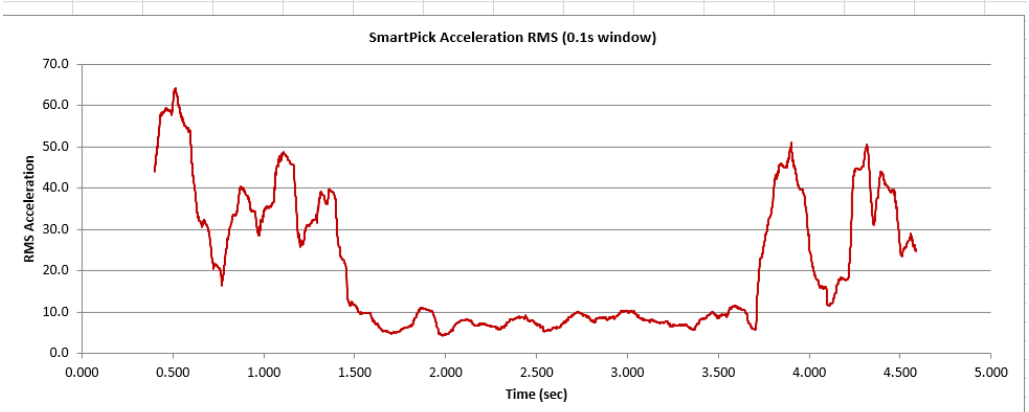
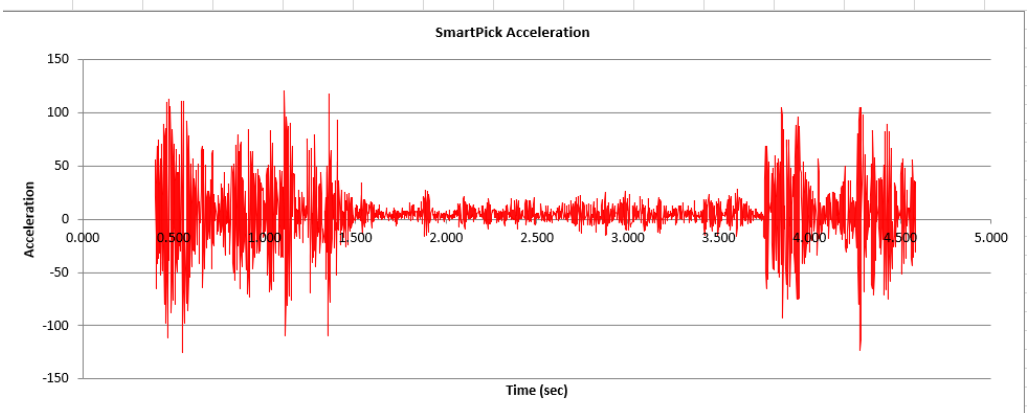
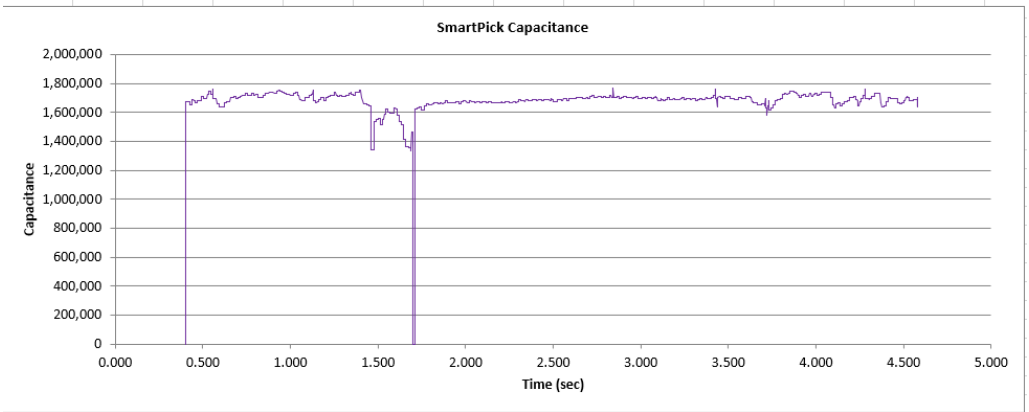
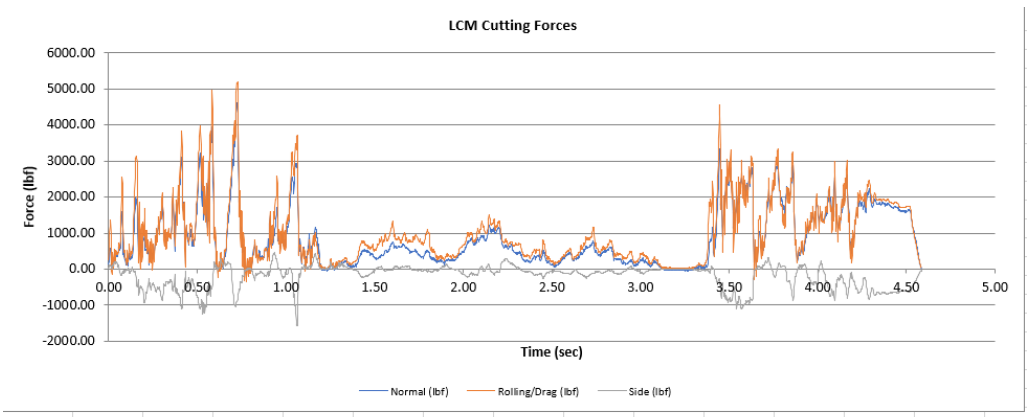


Client : EMI	Date Tested : 04/07/2026
Project : Smart Pick	Date Reduced : 04/12/2026
Project Location : Colorado School of Mines	Tested by : MJ, BB, JR, GW, KP, SM
Calibration File : Manual Reduction_01_1/7/2021	Reduced by : MJ

Test Series : A15	Saddle : Red Radial
Book No : 1	Target Cutting Speed : 10.0 in/sec
File Name : Test_1-1-2.lvm	Actual Cutting Speed : 0.0 in/sec
Rock Sample : Conc-Biochar-Conc	Line Spacing : 4.00 in 102 mm
Rock Source : CSM	Penetration : 1.000 25.40
Cutting Tool : U92	S/P Ratio : 4.0
Cutting Tool Source : Kenametal	

Force Angle: 0		US System (in lbf)	Average	Std. Dev.	Minimum	Maximum
Cutting Coefficient 1.204		Normal	830	832	-121	4610
Specific 0.491 <i>hp-hr/yd³</i>		Rolling / Drag	999	971	-343	5200
Energy 0.481 <i>kWh/m³</i>		Side	-184	346	-1580	468
		SI System (in kN)	Average	Std. Dev.	Minimum	Maximum
		Normal	3.69	3.7	-0.538	20.5
		Rolling / Drag	4.44	4.32	-1.53	23.1
Comments :		Side	-0.818	1.54	-7.03	2.08

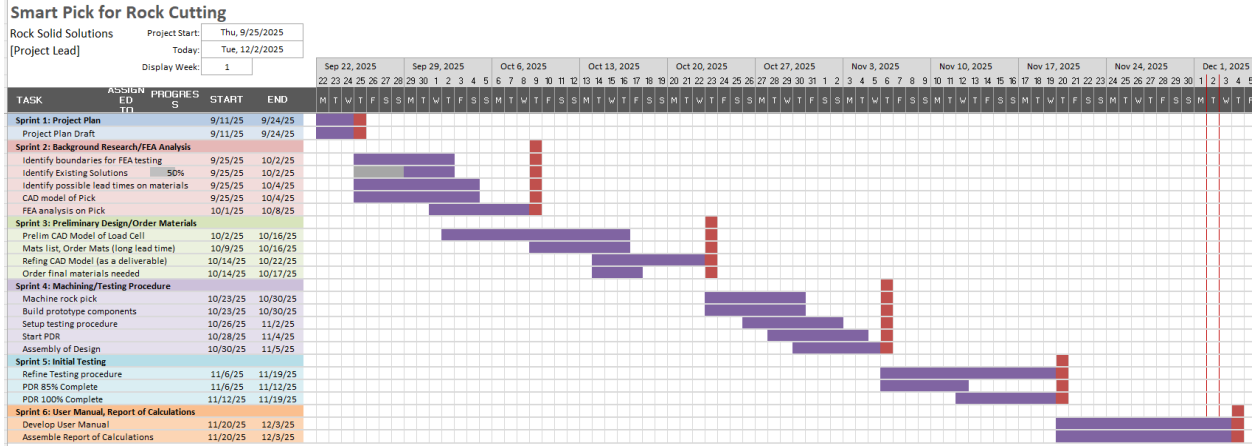




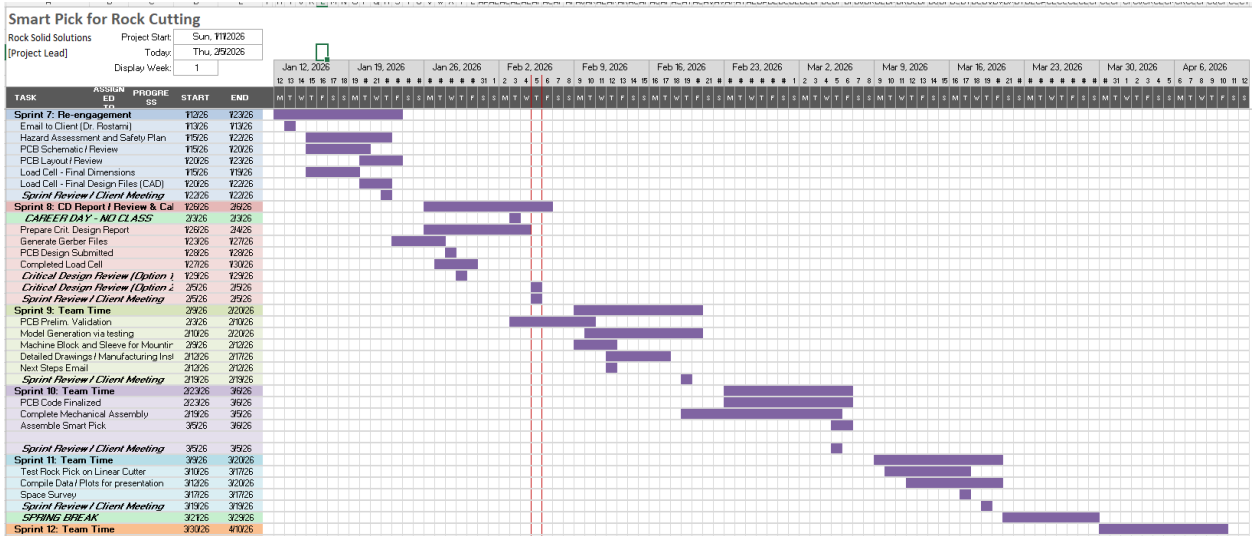
H. Team Schedule

See links for full Gantt Charts.

Fall 2025: [Rock_Solid_gantt_chart_F25.xlsx](#)



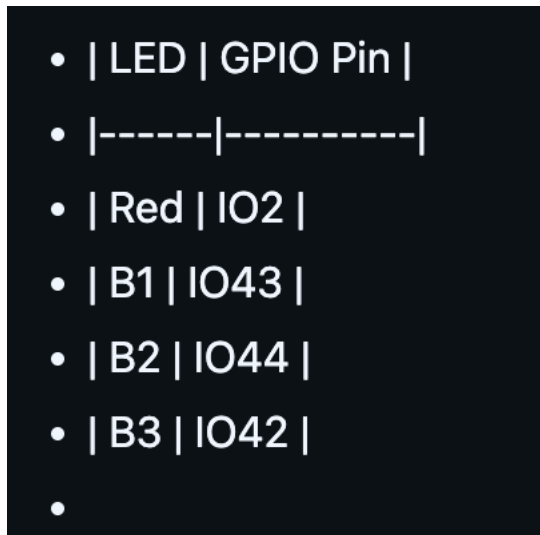
Spring 2026: [Schedule_SP26.xlsx](#)



I. Code and Documentation

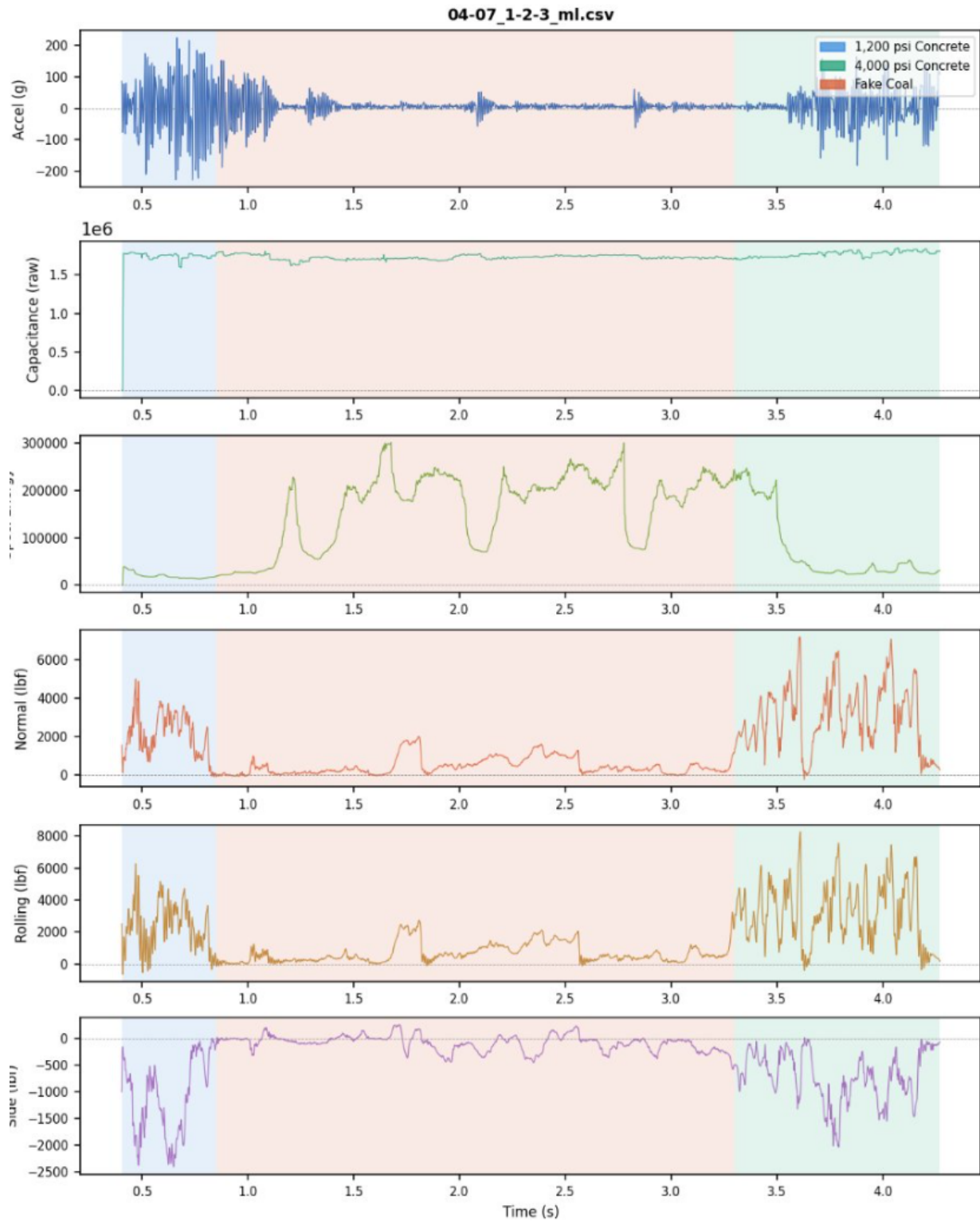
The code for this project is completely open source and available for download on GitHub via the following link: https://github.com/kobeprior99/Smart_Pick

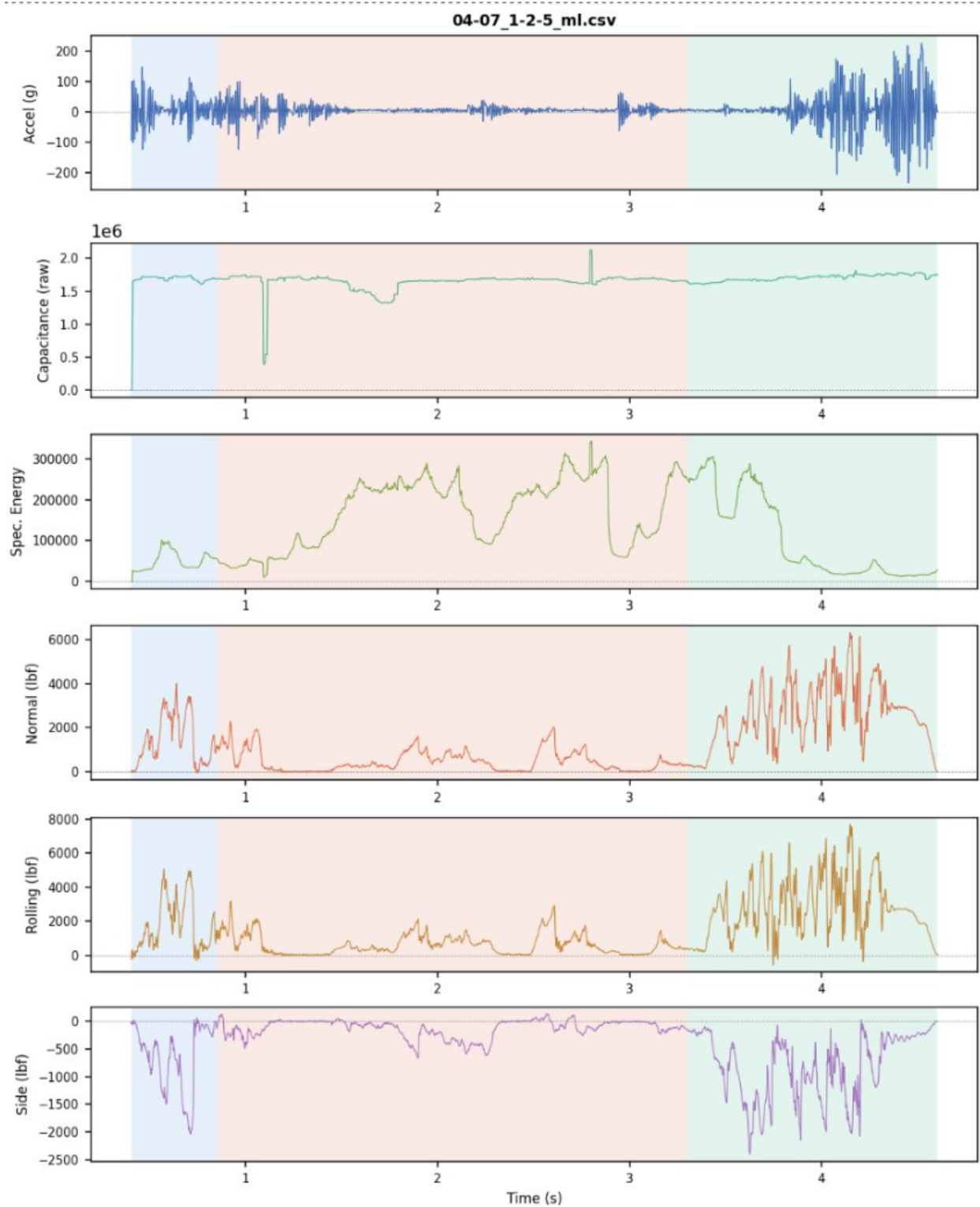
The overall structure of the code is separated into two directories named “Arduino_Files” and “Python_Files”. There is a “README.md” file in each directory explaining what is contained in the directory, which involves describing in detail the functionality of each program, how to flash hardware to devices, how to install necessary dependencies, and how to run code. The “Arduino_Files” folder contains all code flashed onto the ESP32 microcontroller on the custom printed circuit board. Specifically, “Smart_Pick.ino” is a file that implements classes for each subsystem included in that directory; namely, accelerometer, capacitive to digital converter, flash memory, and the LED subsystem. Within the “Python_Files” directory, there is a file named “main.py” that can be run using the terminal command “python3 main.py,” and it initiates a local, web-based graphical user interface built on the NiceGui framework. All library dependencies and installation instructions are provided in README.md files along with hardware definitions. For example, in the LED subsystem, the readme file contains which pins on the microcontroller are connected to which LEDs (see figure below).

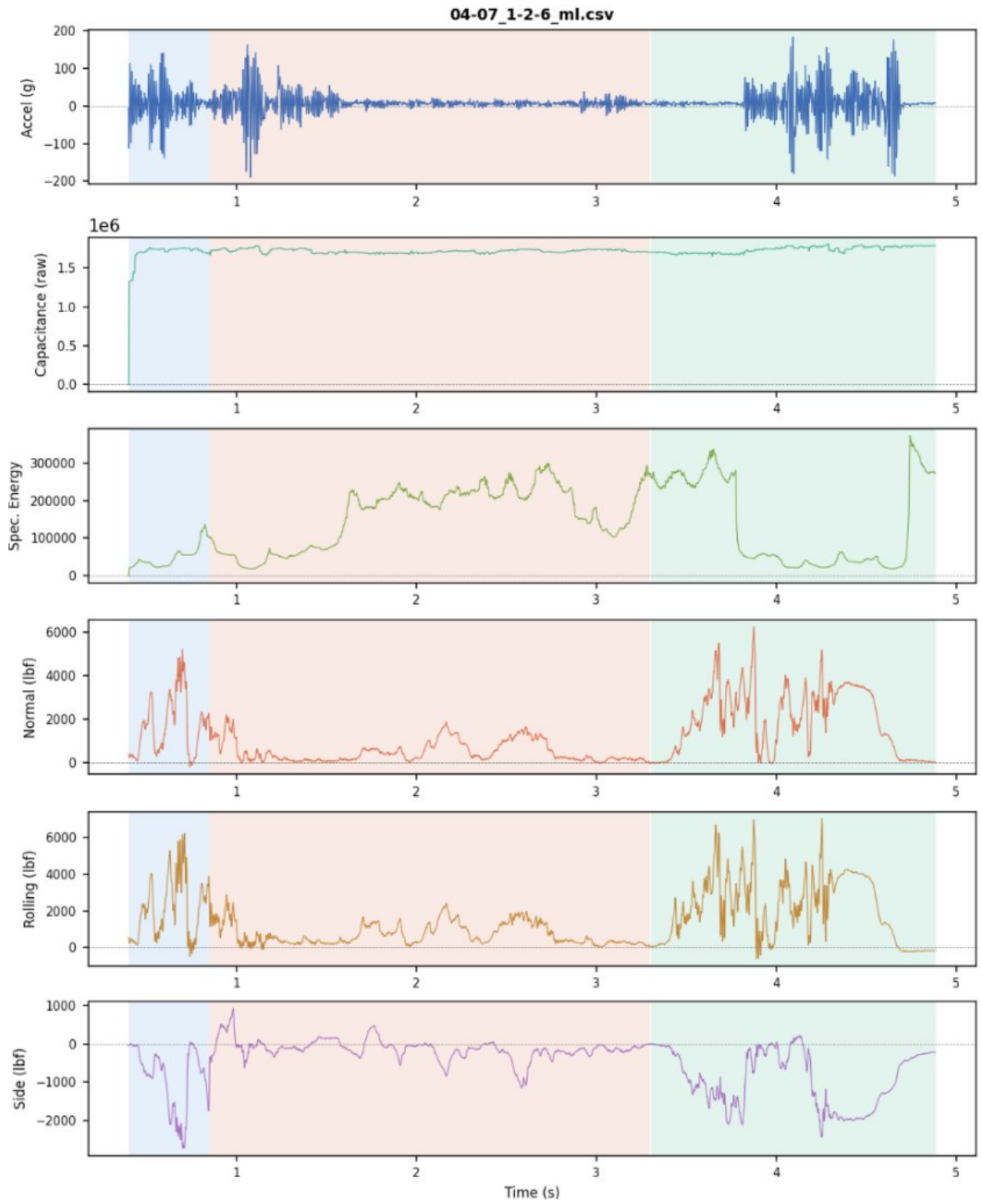


By being very intentional about documentation in “ReadMe.md” files and with inline comments of code, Rock Solid Solutions has set up the next team of engineers who will take this project on very well for success. Although lines of code are not a direct measure of the technical impressiveness of software, it serves as a metric for the amount of work poured into this project. In total, **1,043,716** lines of code were written.

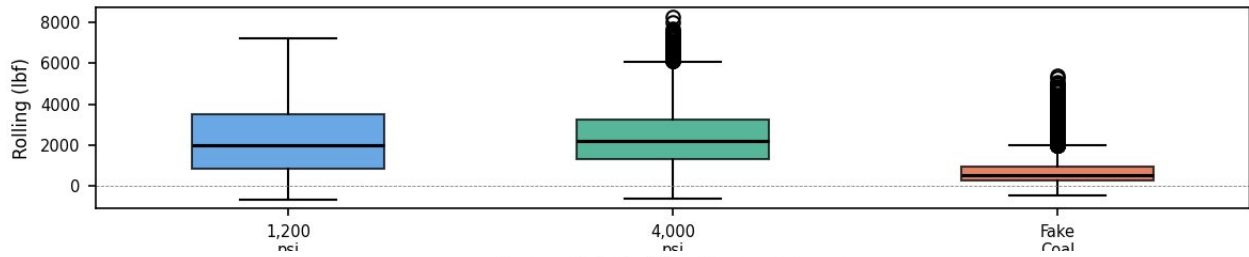
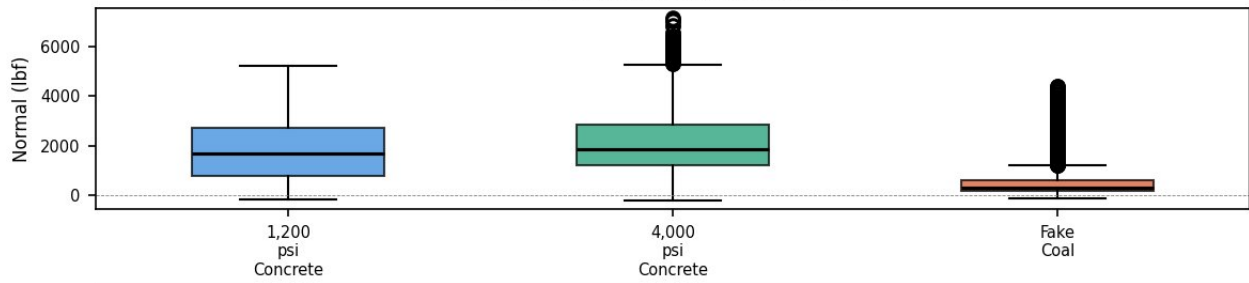
J. Machine Learning Graphs



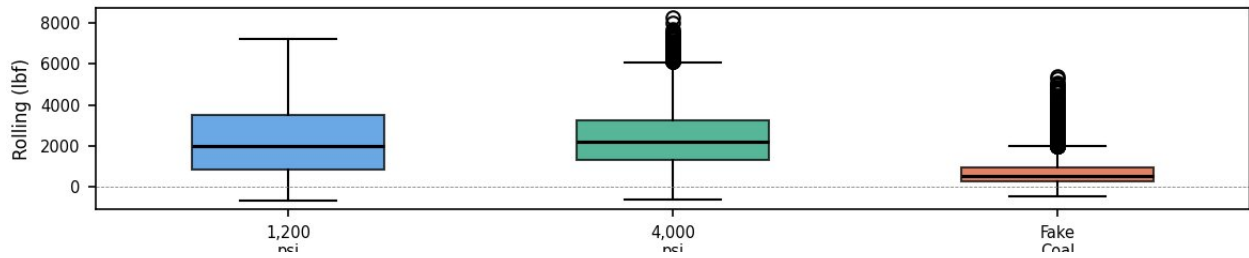
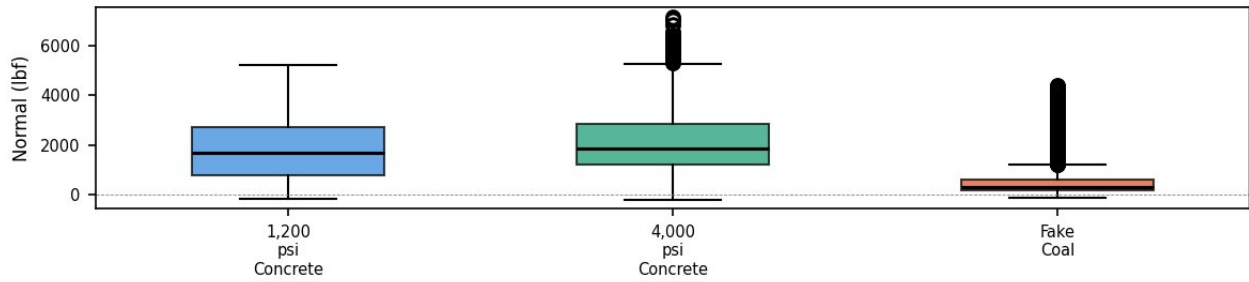




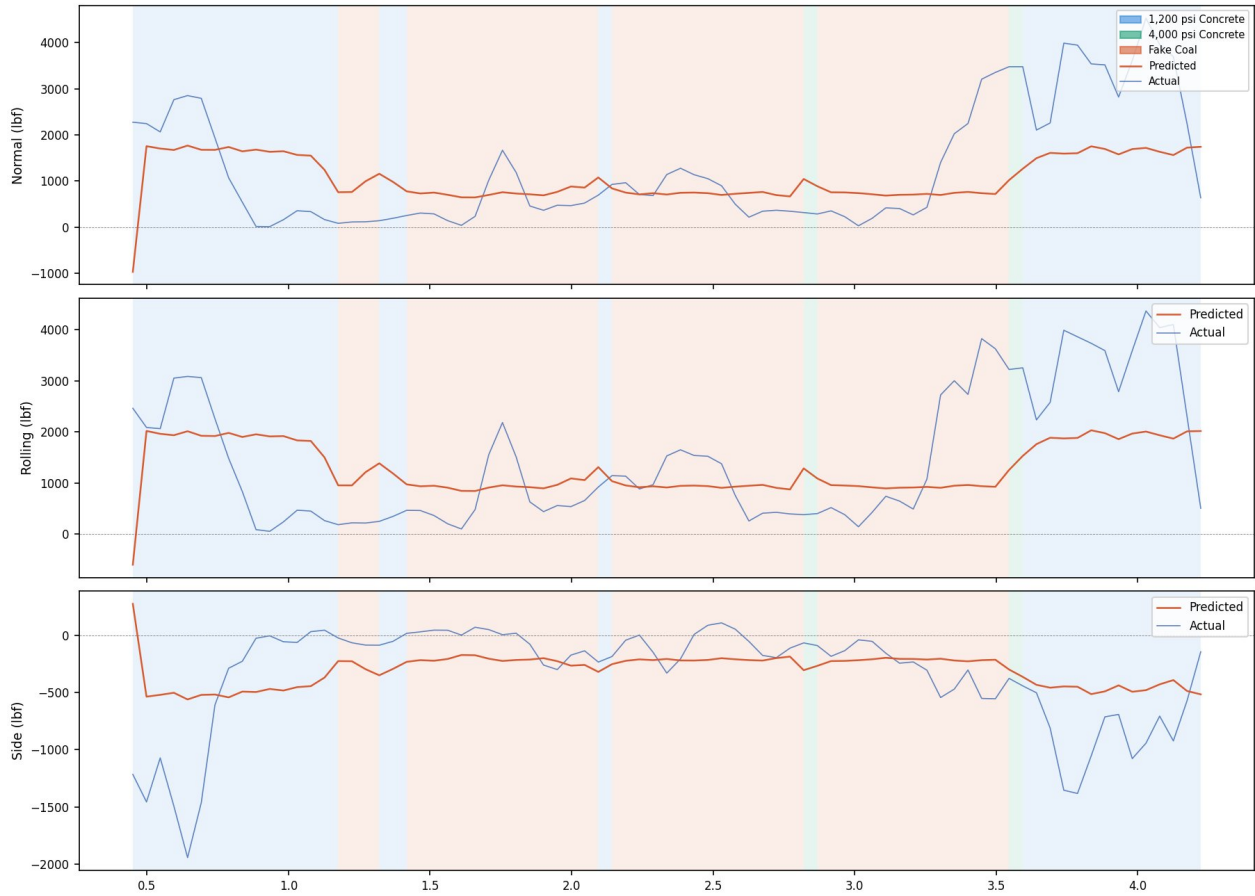
Force distribution by rock layer



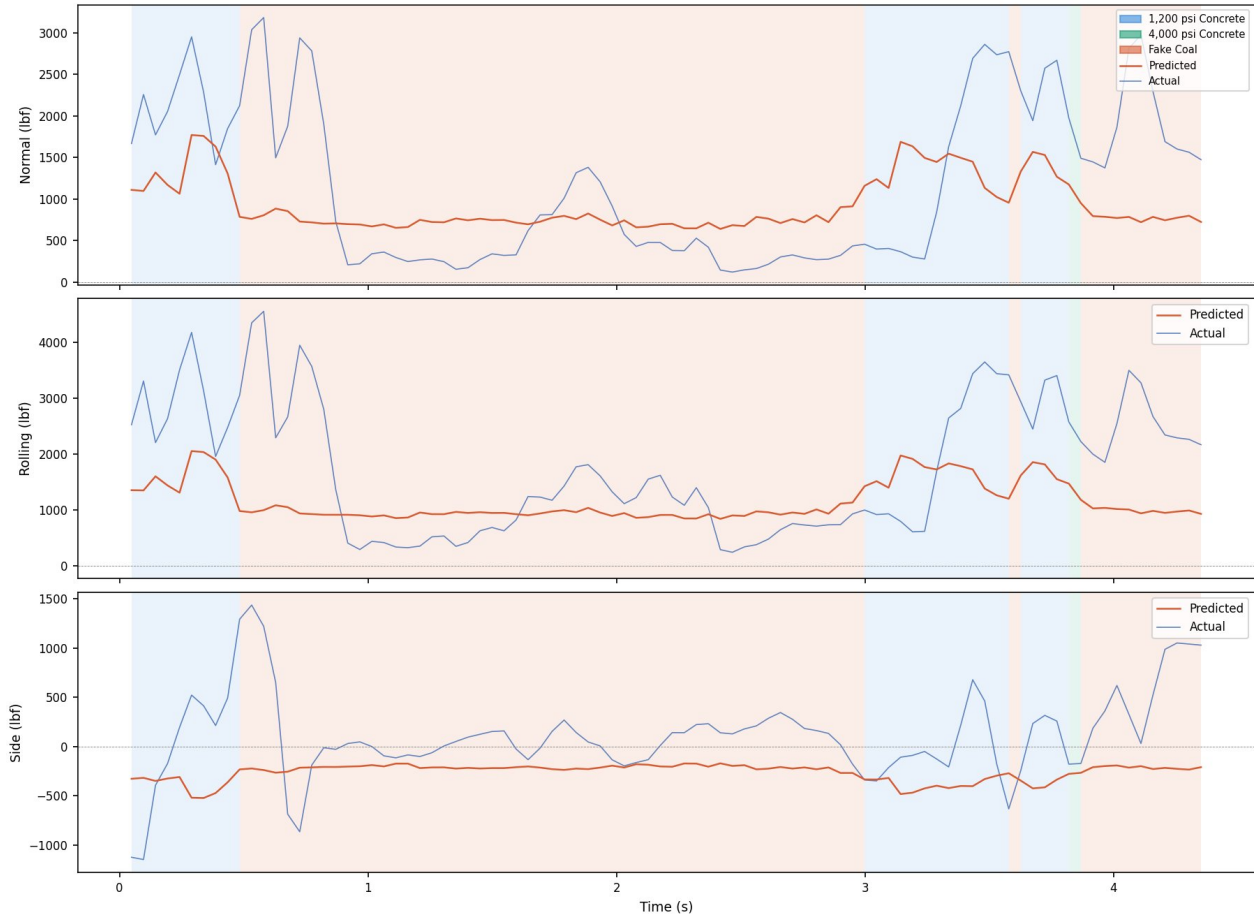
Force distribution by rock layer




Predictions — 04-07_1-2-3_ml.csv



Predictions — 04-07_1-2-8_ml.csv



K. Team Members

Picture	Name	Relevant Skills	Contact
	Ben Bergeron	Structural/Static force Analysis, CAD design	bbergeron@mines.edu
	Milos Jankovic	Autodesk FEA, CAD, Rock Fragmentation, Machine Learning	mjankovic@mines.edu
	Sophia Mimlitz	Embedded Code, Circuit Design, Wireless Communication & Controls	sophiamimlitz@mines.edu
	Kobe Prior	Digital Signal Processing, Circuit Design, Coding	kdprior@mines.edu
	Jared Richel	CAD design and analysis, Welding/Fabricating, Machining	jrichel@mines.edu
	Graham Walter	SolidWorks CAD and FEA, Machining, Instrumentation	gwalter@mines.edu